Development and optimization of receptor fusion proteins for the inhibition of IL-6-type cytokines *in vivo*

Von der Fakultät für Mathematik, Informatik und Naturwissenschaften der RWTH Aachen University zur Erlangung des akademischen Grades eines Doktors der Naturwissenschaften genehmigte Dissertation

vorgelegt von

Diplom-Biologe

Dieter Görtz geb. Schwache

aus Heinsberg

Berichter: Prof. Dr. rer. nat. Gerhard Müller-Newen

Univ.-Prof. Dr. rer. nat. Bernhard Lüscher

Tag der mündlichen Prüfung: 17.12.2015

Für Christina,

Hanna & Peter.

Kurzzusammenfassung

Zytokine sind kleine, sezernierte Proteine mit regulatorischen Funktionen in vielen biologischen Prozessen, einschließlich der Immunantwort. Eine Dysregulation der Zytokin-Signaltransduktion spielt oft eine maßgebliche Rolle bei der Entstehung und Aufrechterhaltung von akuten und chronischen Entzündungen. Aktuelle Anti-Zytokin-Therapien haben wesentlich dazu beigetragen die Behandlung entzündlicher Erkrankungen zu verbessern. Medikamente gegen Zytokine gehören in der Regel zur Gruppe der Biologika, wie zum Beispiel neutralisierende Antikörper oder auch lösliche Rezeptoren.

Zur Inhibition von Zytokinen, die über heteromere Rezeptorkomplexe signalisieren, entwickelten wir eine Strategie, welche auf der Fusion der Ligandenbindungsdomänen der beteiligten Rezeptoruntereinheiten basiert. Diese Rezeptor-Fusions-Proteine (RFP) sind höchst effektiv, hochspezifisch, monogen, und eignen sich daher besonders für gentherapeutische Ansätze.

Der erste Teil dieser Arbeit befasst sich mit der Entwicklung eines neuartigen RFP gegen murines Interleukin-31 (IL-31). IL-31 wird hauptsächlich mit entzündlichen Hauterkrankungen in Verbindung gebracht, und signalisiert über einen heterodimeren Rezeptorkomplex bestehend aus dem Interleukin-31-Rezeptor (IL-31R) und dem Oncostatin M-Rezeptor (OSMR). Die Fusion der Domänen D1-D4 des murinen OSMR und der Domänen D1-D2 des murinen IL-31R verbunden durch einen flexiblen Linker führt zu einem effektiven Inhibitor von murinem IL-31 (mIL-31-RFP). Um das inhibitorische Potential des mIL-31-RFP zu untersuchen, entwickelten und charakterisierten wir ein Zell-basiertes System zur Analyse der murinen IL-31- und OSM-abhängigen Signaltransduktion. mIL-31-RFP inhibiert spezifisch die IL-31-induzierte Signaltransduktion und hemmt nicht die Aktivität von murinem OSM.

Im zweiten Teil dieser Arbeit, untersuchten wir, auch als Machbarkeitsnachweis für weitere monogene RFPs, die Verwendung des zuvor beschriebenen mIL-6-RFP zur

Inhibition von Interleukin-6 (IL-6) *in vivo*. Dazu wurden transgene Mäuse, die mIL-6-RFP induzierbar und gewebespezifisch exprimieren, generiert und charakterisiert.

In einem parallelen Ansatz, wurde mIL-6-RFP weiterentwickelt, um zum einen die inhibitorische Aktivität über die Fusion mit dem Fc-Anteil von murinem IgG2a (mIL-6-RFP-Fc) zu erhöhen, und zum anderen über eine Codon-Optimierung der mIL-6-RFP-Fc cDNA eine Steigerung der Protein-Expression zu erreichen. Nach direkter Applikation in Mäuse hemmte rekombinantes mIL-6-RFP-Fc die IL-6-induzierte Aktivierung des Transkriptionsfaktors STAT3 und der ERK1/2-Kinasen in der Leber und Niere. Gentransfer durch hydrodynamische Plasmid-Transfektion in Mäuse führte zur hepatischen mIL-6-RFP-Fc-Expression und Sekretion in das Blut in erheblichen Mengen. mIL-6-RFP-Fc inhibierte die hepatische Akut-Phase-Protein-Synthese und verbesserte die Nierenfunktion in einem renalen Ischämie und Reperfusions-Krankheitsmodell.

Die hier beschriebene Strategie ist auf viele weitere Zytokine, die zur Entwicklung von akuten und chronisch Entzündungen und anderen Krankheiten beitragen, übertragbar.

Abstract

Cytokines are small soluble proteins with regulatory functions in many biological processes including immune responses. Dysregulated cytokine signaling is often responsible for the development and maintenance of acute and chronic inflammation. Current anti-cytokine therapies have substantially improved the treatment of inflammatory diseases. Cytokine-targeting drugs are usually biologics such as neutralizing antibodies or soluble receptors. To target cytokines that signal through heteromeric receptor complexes we developed a strategy that involves the inline fusion of the ligand binding domains of the corresponding receptor subunits. These receptor fusion proteins (RFPs) are highly potent and specific, monogenic by design, and therefore well suited for gene transfer approaches.

The first part of this project deals with the development of a novel RFP targeting murine interleukin-31 (IL-31). IL-31, mostly involved in skin diseases, signals through heterodimeric receptor complexes comprised of the interleukin-31 receptor (IL-31R) and the oncostatin M receptor (OSMR) subunits. Inline fusion of domains D1-D4 of murine OSMR and domains D1-D2 of murine IL-31R connected by a flexible linker results in a potent inhibitor for murine IL-31 (mIL-31-RFP). To assess the inhibitory potential of mIL-31-RFP we established and characterized a cell-based system for the analysis of murine IL-31 and oncostatin M (OSM) signaling. mIL-31-RFP specifically inhibits IL-31-dependent signal-transduction and does not interfere with the activity of mOSM.

In the second part of this project, we investigated, as a proof-of-principle for other monogenic RFPs, the potential of the previously described mIL-6-RFP to inhibit interleukin-6 (IL-6) *in vivo*. Therefore, transgenic mice that express mIL-6-RFP in an inducible and tissue-specific manner were generated and characterized.

In a parallel approach, we re-engineered mIL-6-RFP by fusion to the Fc of mIgG2a (mIL-6-RFP-Fc) for enhanced inhibitory activity and improved protein expression by codon optimization. Upon application in mice, recombinant mIL-6-RFP-Fc inhibited

IL-6-induced activation of the transcription factor STAT3 and ERK1/2 kinases in liver and kidney. Gene transfer through hydrodynamic plasmid delivery in mice resulted in hepatic production and secretion of mIL-6-RFP-Fc into the blood in considerable amounts, blocked hepatic acute-phase protein synthesis and improved kidney function in a renal ischemia and reperfusion injury model.

The strategy described here is applicable for many cytokines involved in inflammatory and other diseases.

Table of Contents

Table of Figures

List of Tables

Abbreviations

A_____

A2M   α-2 macroglobulin

AAV   Adeno-associated virus

ACD   Allergic contact dermatitis

AD   Atopic dermatitis

ADCC   Antibody-dependent cellular cytotoxicity

AIA   Antigen-induced arthritis

AKI   Acute kidney injury

B_____

BGH pA   Bovine growth hormone poly-adenylation signal

bilat.   Bilateral

bp   Base pairs

BSA   Bovine serum albumin

BSF-2   B-cell stimulatory factor-2

C_____

cap   Capsid proteins

CBM   Cytokine binding module

CD   Crohn's disease

CDC   Complement-dependent cytotoxicity

CD4$^+$ cluster of differentiation 4$^+$

CLC   Cardiotrophin-like cytokine

CLF-1   Cytokine like factor-1

CM   Conditioned media

CNTF   Ciliary neurotrophic factor

CT-1   Cardiotrophin-1

D_____

D   Domain

Da   Dalton

DNA   Deoxyribonucleic acid

dox   Doxycycline

E _____

EAE	Experimental auto-immune encephalo-myelitis
EBI-3	Epstein-Barr virus induced gene 3
ERK	Extracellular signal-regulated kinase

F _____

Fc	Fragment crystalliza-ble
FcRn	Neonatal Fc receptor
FCS	Fetal calf serum
FnIII-like	Fibronectin III like domain

G _____

GLM-R	gp130-like monocyte receptor
GN	Glomerulonephritis
gp80	Glycoprotein 80 (=IL-6Rα)
gp130	Glycoprotein 130 (=IL-6Rβ)
GPL	Gp130 like protein

H _____

hIL-6-RFP	Human IL-6 receptor fusion protein

I _____

I/R	Ischemia/Reperfusion
i.p.	intraperitoneally
i.v.	intravenously
IBD	Inflammatory bowel disease
IFN	Interferon
Ig	Immunoglobulin
IL	Interleukin
ITR	Inverted terminal re-peat

J _____

Jak	Janus kinase

L _____

LAP	Liver activator protein promoter
Lcn2	Lipocalin-2
LIF	Leukemia inhibitory factor

LIFR   LIF receptor

LPS   Lipopolysaccharide

M _____

MAPK   Mitogen activated

              protein kinase

MCS   Multiple cloning site

mIL-6-RFP   Murine interleukin-6
              receptor fusion protein

mIL-31-RFP   Murine interleukin-31
              receptor fusion protein

mOSM-RFP   Murine oncostatin M
              receptor fusion protein

N _____

NFAT   Nuclear factor of acti-
              vated T cells

NGAL   Neutrophil gelatinase
              associated lipocalin

NP   Neuropoetin

NTN   Nephrotoxic nephritis

O _____

ORF   Open reading frame

OSM   Oncostatin M

OSMR   Oncostatin M receptor

P _____

PBS   Phosphate buffered
              saline

PCR   Polymerase chain re-
              action

PEPCK   Phosphoenolpyruvate
              carboxykinase

PI3K   Phosphoinositide 3-
              kinase

Pod   Promoter active in
              podocytes

PPT   Preprotrypsine

R _____

R   Receptor

RA   Rheumatoid arthritis

rAAV   Recombinant AAV

rep   Replication proteins

RFP   Receptor fusion pro-
              tein

rtTA   Reverse tetracycline
              Trans-activator

S _____

s.c.	subcutaneously
SAA1	Serum amyloid A
Sc	short-chain
SEB	Staphylococcus enter-toxin B
sgp130	soluble gp130
SH2	Src-homology 2
Shc	SH2 domain containing transforming protein
SHP-2	SH2 domain containing protein tyrosine phosphatase-2
sIL-6Rα	soluble IL-6Rα
STAT	Signal transducer and activator of transcription

T_____

TGF-β	Transforming growth factor-β

Th	T helper cell
TLR	Toll-like receptor
TNF	Tumor necrosis factor-α
TR	Tet repressor protein
TRE	Tet responsive element
Treg	Regulatory T cell
Tyk2	Tyrosine kinase 2

U _____

UV	Ultraviolet

W_____

WCL	Whole cell lysate
wt	Wildtype

Publications

Essential parts of this work will be published:

Görtz D, Schmitz-Van de Leur H, Müller-Newen G: **A receptor fusion protein for the inhibition of murine interleukin-31.** *Manuscript in preparation.*

Essential parts of this work were published:

Görtz D[#], Braun GS[#], Maruta Y, Djudjaj S, van Roeyen CR, Martin IV, Küster A, Schmitz-Van de Leur H, Scheller J, Ostendorf T, Floege J & Müller-Newen G: **Anti-interleukin-6 therapy through application of a monogenic protein inhibitor *via* gene delivery.** *Scientific Reports* **2015**, 5, 14685.

Peer-reviewed:

Schumacher A, Denecke B, Braunschweig T, Stahlschmidt J, Ziegler S, Brandenburg LO, Stope MB, Martincuks A, Vogt M, **Görtz D**, Camporeale A, Poli V, Müller-Newen G, Brümmendorf TH, Ziegler P: **Angptl4 is upregulated under inflammatory conditions in the bone marrow of mice, expands myeloid progenitors, and accelerates reconstitution of platelets after myelosuppressive therapy**. *Journal of Hematology & Oncology* **2015**, 8, 64.

Nagayama Y, Braun GS, Jakobs CM, Maruta Y, van Roeyen CR, Klinkhammer BM, Boor P, Villa L, Raffetseder U, Trautwein C, **Görtz D**, Müller-Newen G, Ostendorf T, Floege J: **Gp130-dependent signaling in the podocyte.** *American journal of physiology renal physiology* **2014**, 307(3):F346-355.

Peer-reviewed (continued):

Witten KG, Ruff J, Mohr A, **Görtz D**, Recker T, Rinis N, Rech C, Elling L, Müller-Newen G, Simon U**: Cellular uptake of fluorophore-labeled glyco-DNA–gold nano-particles.** *Journal of nanoparticle research* **2013**, 15(10):1-12.

Dittrich A, Quaiser T, Khouri C, **Görtz D**, Monnigmann M, Schaper F: **Model-driven experimental analysis of the function of SHP-2 in IL-6-induced Jak/STAT signaling.** *Molecular Biosystems* **2012**, 8(8):2119-2134.

Reviews:

Schwache D, Müller-Newen G: **Receptor fusion proteins for the inhibition of cyto-kines.** *Eur J Cell Biol* **2011**, 91(6-7):428-434.

1   Introduction

1.1   Cytokines

Cytokines are small soluble proteins with regulatory functions in many biological processes including immune responses. In contrast to hormones, cytokines are generally produced *de novo* and secreted by different cell types in response to certain stimuli. Released cytokines act in autocrine or paracrine fashion and modulate pro- or anti-inflammatory responses. Cytokines are further classified according to their biological functions into the groups of interferons, interleukins, colony stimulating factors and chemokines.

1.2   Class I cytokine receptors

The family of class I cytokine receptors, also termed hematopoietic receptors were classified through common structural features (Bazan, 1990, Wells and de Vos, 1996). Their extracellular part contains a common cytokine-binding module (CBM), which is built up by two fibronectin type-III like (FnIII-like) domains with distinctive motifs. The N-terminal domain contains a set of four conserved cysteines, whereas the C-terminal (membrane-proximal) domain contains a collection of spaced aromatic residues termed WSXWS box. In contrast to receptor-tyrosine-kinases, class I cytokine receptors have no intrinsic kinase activity within their cytoplasmic parts and are instead associated with tyrosine-kinases of the Janus kinase (Jak)-family.

1.3   Interleukin-6 family of cytokines

The family of IL-6 type cytokines (Figure 1) consists of interleukin-6 (IL-6), interleukin-11 (IL-11), leukemia inhibitory factor (LIF), cardiotrophin-1 (CT-1), ciliary neurotrophic factor (CNTF), neuropoetin (NP), cardiotrophin-like cytokine (CLC), oncostatin M (OSM), interleukin-31 (IL-31), interleukin-27 (IL-27) and interleukin-35

(IL-35). Structurally IL-6 type cytokines belong to the family of four-helix bundle cytokines (Bazan, 1990). The composite cytokines IL-27 and IL-35 are heterodimeric cytokines and also members of the IL-12 family of cytokines, where they represent the negative immunoregulatory members (Vignali and Kuchroo, 2012). IL-27 (Pflanz et al., 2002) and IL-35 (Collison et al., 2012) are composed of the α-chain p28 or p35, respectively, and the β-chain Epstein-Barr virus induced gene 3 (EBI-3). Both α-chains share the four-helix bundle structure characteristic of the IL-6 type cytokines, whereas EBI-3 shares homology with class I cytokine receptors. With IL-31 being the exception, all IL-6 type cytokines share glycoprotein 130 (gp130) as a common receptor subunit. IL-31 signals instead through the interleukin-31 receptor (IL-31R) subunit, which shows high homology to gp130 as evident by its alternative name gp130 like protein (GPL).
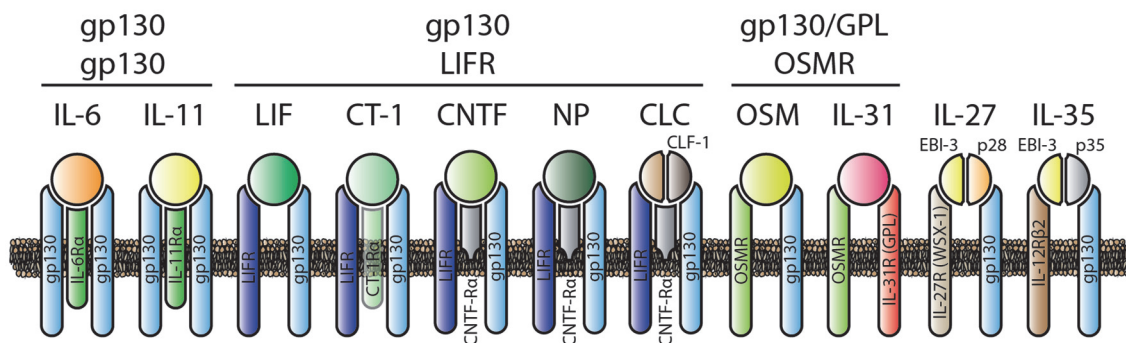
Figure 1: IL-6 type cytokines IL-6 type cytokines signal via the formation of homo- or heteromeric receptor complexes. IL-6 and IL-11 signal after binding to their corresponding α-receptors through gp130 homodimers, whereas LIF, CT-1, CNTF, NP and the composite cytokine CLC/cytokine like factor-1 (CLF-1) signal through LIF receptor (LIFR)/gp130 heterodimeric complexes. Both OSM and IL-31 signal through the OSM receptor (OSMR) in conjunction with gp130 or IL-31R, respectively. The composite cytokines IL-27 signal through IL-27 receptor (IL-27R)/gp130 complexes, whereas IL-35 signal through IL-12 receptor β2 (IL-12Rβ2)/gp130 complexes.

1.4   Interleukin-6

Before consenting on a common nomenclature (Coulie et al., 1987b), IL-6 had several other synonyms, like interferon (IFN) β2 (Weissenbach et al., 1980), hepatocyte-stimulating factor (Ritchie and Fuller, 1983), interleukin-HP1 (Van Snick et al., 1987) and 26-kDA-protein (Content et al., 1985) during its discovery phase by independent

studies, but its cDNA was originally cloned and characterized as B-cell stimulatory factor-2 (BSF-2) that drives the growth and differentiation of B-cells to immunoglobulin-producing cells (Hirano et al., 1986).

As evident by the different names given IL-6 exerts pleiotropic effects on several cell types (Figure 2). It can act as a growth factor on plasmacytoma (Nordan and Potter, 1986) or myeloma cells (Kawano et al., 1988), suppresses differentiation of osteoclast progenitors (Yoshitake et al., 2008) and induces IL-2 production, proliferation and differentiation of T cells (Garman et al., 1987, Lotz et al., 1988, Okada et al., 1988). Another T cell specific function is the ability of IL-6, in combination with transforming growth factor-β (TGF-β), to regulate the differentiation of naive cluster of differentiation 4^+ ($CD4^+$) T helper (Th) cells into Th17 cells, which produce the inflammatory cytokine IL-17 (Kimura and Kishimoto, 2010). Besides controlling proliferation and differentiation of different cell types, IL-6 plays a major role in the regulation of the acute phase protein synthesis of the liver (Gauldie et al., 1987, Andus et al., 1987). Another important role of IL-6 is the regulation of metabolic functions (Mauer et al., 2015). IL-6$^{-/-}$ mice develop mature-onset obesity (Wallenius et al., 2002). In rats IL-6 treatment leads to an increased liver catabolism of glycogen and decreased mRNA expression of phosphoenolpyruvate carboxykinase (PEPCK), a key enzyme in gluconeogenesis, leading to the depletion of glycogen stores in the liver (Lienenluke and Christ, 2007). In mice, adipocyte-derived IL-6 directly acts on hepatocytes, leading to the decreased expression of glucose-6-phosphatase (Reilly et al., 2015). Glucose-6-phosphatase catalyzes the terminal step of glycogenolysis and gluconeogenesis and therefore plays a key role in the homeostatic regulation of blood glucose levels.

Main sources for IL-6 are fibroblasts, endothelial cells, monocytes and macrophages (Kishimoto et al., 1995). Other cell types such as astrocytes, smooth muscle cells, keratinocytes, mesangial cells, T cells and B cells synthesize IL-6 after stimulation with various factors (Tanaka et al., 2014). IL-6 synthesis and secretion is induced through responses to viral infections, other cytokines, such as IL-1, tumor necrosis factor-α

(TNF) and toll-like receptor (TLR)-mediated signals like lipopolysaccharides (LPS) (Coulie et al., 1987a, Tanaka et al., 2014).

The amino acid sequence of human IL-6 consists of 212 amino acids with a signal peptide of 27 amino acids. The secreted protein has a molecular mass of 26 kDa. Mouse IL-6 shows 40% sequence homology on the protein level (Simpson et al., 1988). The serum levels of IL-6 for healthy human subjects range from 5-20 pg/ml (Kleiner et al., 2013).
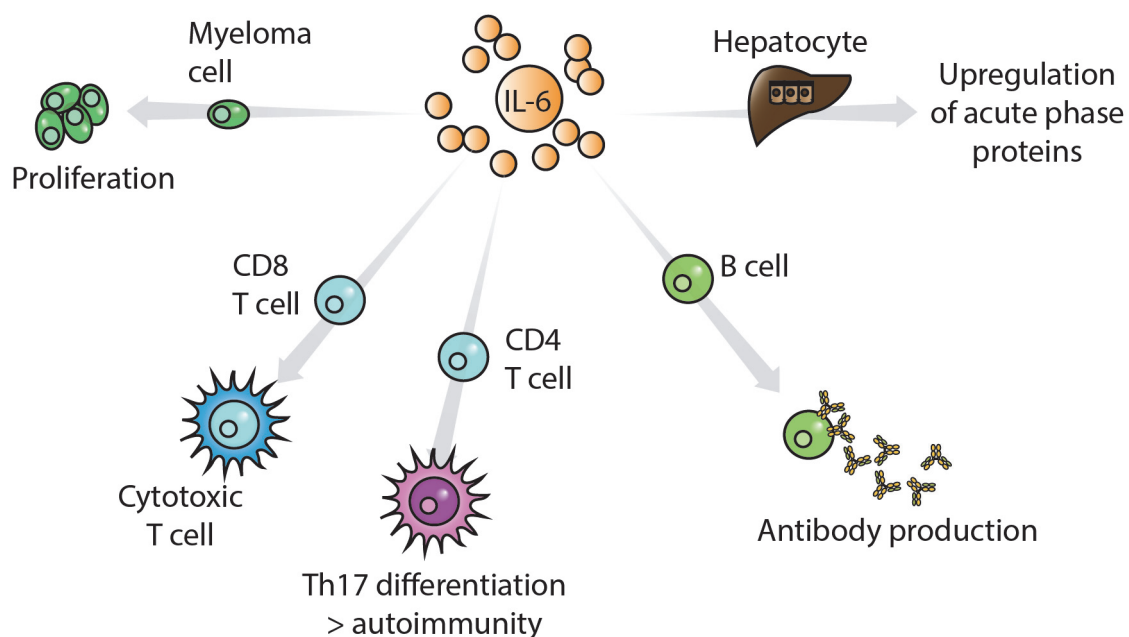
Figure 2: Pleiotropic effects of IL-6 Schematic representation of IL-6 controlled effects on a selection of cell types. Adapted from (Tanaka et al., 2012).

1.4.1   The IL-6 receptors

The signaling complex of IL-6 is composed of the signal-transducing β-receptor subunit gp130 (Taga et al., 1989) and the non-signaling IL-6 receptor α (IL-6Rα) (Yamasaki et al., 1988). The extra-cellular part of gp130 consists of a single immunoglobulin (Ig)-like domain (D1) followed by five FnIII-like domains (D2-D6) (Hibi et al., 1990). IL-6Rα consists of an Ig-like domain (D1), followed by a cytokine binding module (CBM) comprised of two FnIII-like domains (D2+D3) connected through a flexible stalk-region to its trans-membrane-domain. While gp130 is ubiquitously expressed (Saito et al., 1992), IL-6Rα expression is restricted to certain cell types like hepatocytes, intestinal epithelial

cells (Shirota et al., 1990), megakaryocytes and subsets of leukocytes and myeloid cells. IL-6 binding to its receptors is mediated by three receptor binding epitopes termed sites I, II and III. Receptor engagement starts with the formation of an IL-6/IL-6Rα complex through a low affinity interaction (K_D=1 nM) (Taga et al., 1989) between site I of IL-6 with the CBM (D2+D3) of IL-6Rα. Subsequently the IL-6/IL-6Rα complex binds to gp130 with a high affinity interaction (K_D=10 pM). Through its site II, IL-6 binds the CBM (D2+D3) of one gp130 and with its site III the Ig-like domain (D1) of another gp130 molecule. The same is true for a second IL-6 molecule leading to the formation of a highly symmetric hexameric IL-6/IL-6Rα/gp130 complex in a 2:2:2 stoichiometry stabilized by six cytokine–receptor interactions (Boulanger et al., 2003). Cells that lack IL-6Rα are not responsive to IL-6, but can be triggered to induce IL-6-dependent signal transduction by stimulation with the agonistic soluble IL-6Rα (sIL-6Rα) in complex with IL-6. The stimulation of cells with IL-6/sIL-6Rα is termed trans-signaling (Rose-John and Heinrich, 1994), while classical signaling refers to signaling through the membrane bound IL-6Rα. Generation of the soluble receptor occurs either by shedding (Mullberg et al., 1993) or alternative splicing (Müller-Newen et al., 1996). Serum concentrations of the agonistic sIL-6Rα range around 50 ng/ml (Müller-Newen et al., 1996). Soluble gp130 (sgp130) is found at a serum concentration of about 300 ng/ml, and has been found to act antagonistically on IL-6/sIL-6Rα complexes (Narazaki et al., 1993, Müller-Newen et al., 1998). Low concentrations of sgp130 specifically inhibit IL-6 trans-signaling, but sgp130 can also lead to inhibition of classical signaling depending on the ratio of IL-6 and sIL-6Rα (Jostock et al., 2001, Garbers et al., 2011, Müller-Newen et al., 1998).
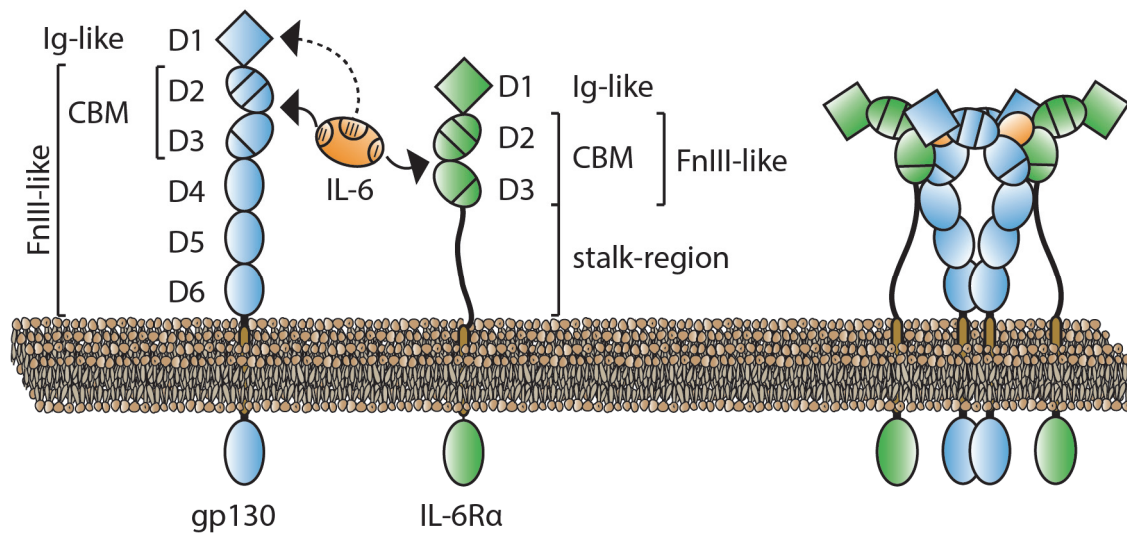
Figure 3: IL-6 receptors and their structures Schematic representation of the domain structures of IL-6 receptor subunits and formation of the hexameric IL-6 receptor complex after binding of IL-6.

1.4.2 IL-6 signal transduction

Upon assembly of the hexameric signaling complex, IL-6 induces the activation of the Janus kinase (Jak)/Signal Transducer and Activator of Transcription (STAT) signaling pathway (Heinrich et al., 2003), the mitogen activated protein kinase (MAPK) cascade, as well as the phosphoinositide 3-kinase (PI3K) cascade (Eulenfeld et al., 2012). While gp130 mediates intracellular signal transduction through Jak-activation, the cytoplasmic part of IL-6Rα has no known signal-transducing function (Taga et al., 1989). Jak1, Jak2 and Tyrosine kinase 2 (Tyk2) are the intrinsic kinases associated with gp130 through box 1 and box 2 binding motifs within the membrane-proximal cytoplasmic tail (Lupardus et al., 2011). Jak1 plays a crucial role after IL-6 dependent activation (Guschin et al., 1995). After complex assembly, Jaks are brought into close proximity to each other, allowing their auto-phosphorylation and subsequent phosphorylation of the tyrosine motifs within the cytoplasmic parts of gp130. The phosphotyrosine motifs then serve as binding sites for Src-homology 2 (SH2) domain containing proteins, including STAT transcription factors. After IL-6 dependent activation of gp130, mainly STAT3 and to a lesser extent STAT1, are recruited to the receptor. After binding STATs become tyrosine-phosphorylated, dissociate from the receptor and dimerize through intermo-

lecular phosphotyrosine/SH2-domain interactions. Phosphorylated and dimerized STAT factors then translocate to the nucleus where they bind enhancer elements on the DNA to promote induction of target genes.
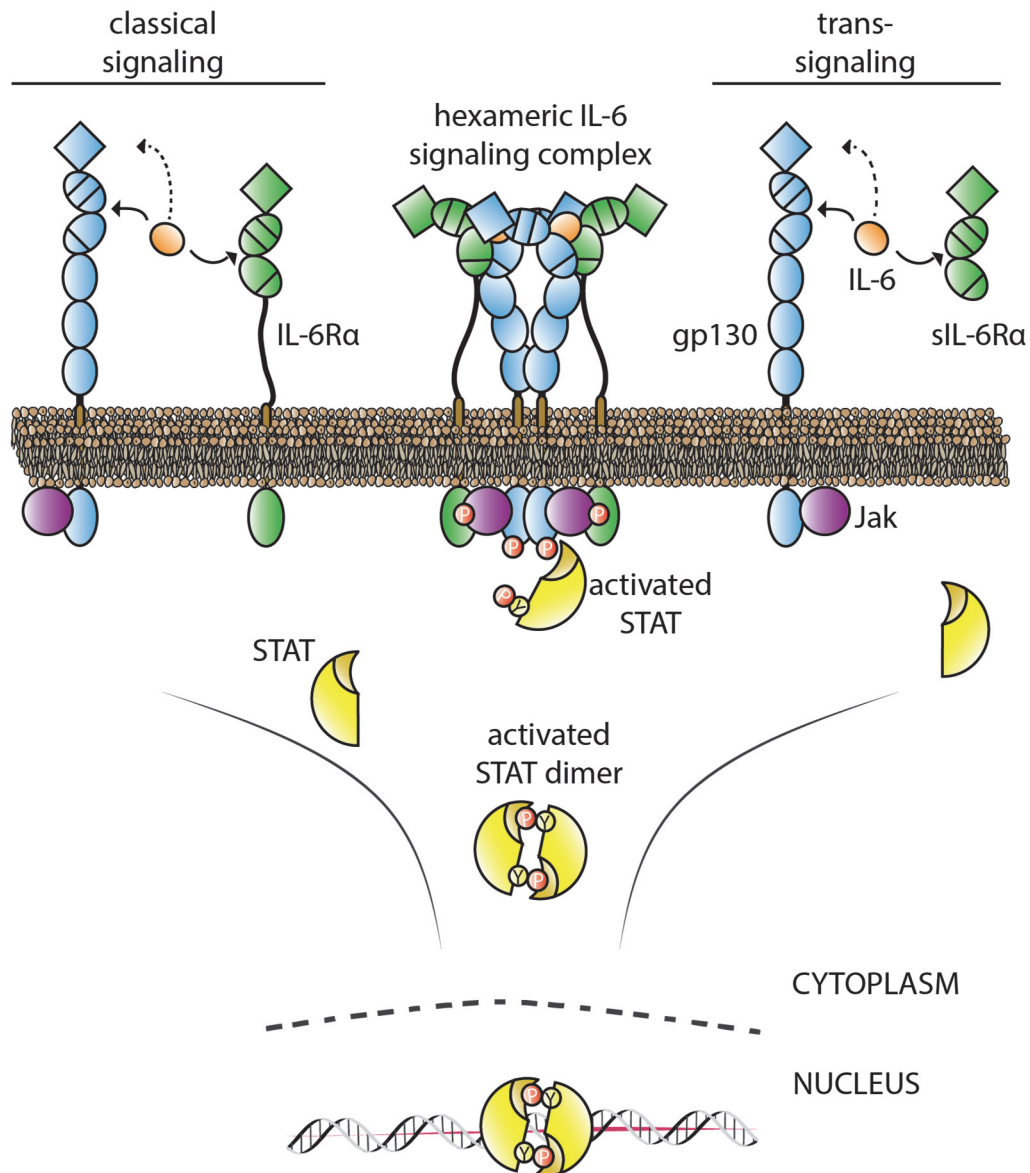
Figure 4: IL-6 dependent Jak/STAT signaling Binding of IL-6 to either membrane-bound or soluble IL-6Rα leads to the formation of the hexameric signaling complex, autophosphorylation of gp-130 associated JAKs and subsequent phosphorylation of tyrosine residues located on the cytoplasmic portion of gp130. STAT proteins are recruited to the receptor, become activated through tyrosine phosphorylation, dimerize and translocate to the nucleus where they induce target gene expression.

1.4.3   IL-6 and its role in inflammation

In the innate immune response IL-6 plays a major role by the induction of acute phase protein synthesis in hepatocytes, following IL-6-dependent activation of STAT3 (Wegenka et al., 1994). In the adaptive immune response IL-6 leads to the differentiation from B cells to antibody-producing plasma cells (Hirano et al., 1986) and together with TGF-β drives the differentiation of naïve T cells to Th17 cells (Bettelli et al., 2006). IL-6 plays a major role in maintaining the balance between regulatory T cells (Treg) and Th17 cells (Kimura and Kishimoto, 2010), by favoring Th17 cell induction while inhibiting Treg cell development. IL-6 is further able to modulate T cell differentiation of CD4$^+$ T cells in an autocrine manner towards Th2 differentiation by inducing IL-4 expression (Sofi et al., 2009).

1.4.4   Pathophysiology of IL-6

Dysregulated IL-6 expression has been implicated in the development of several diseases. The involvement of IL-6 and its contribution to the pathogenesis of disease was first discovered in cases of primary tumors of the heart, called cardiac myxoma. Increased IL-6 levels were found in myxoma culture fluid and derived tissues from patients (Hirano et al., 1987), and are responsible for the observed constitutional symptoms and immunologic abnormalities (Mendoza et al., 2001). Increased IL-6 production was also found in synovial cells of rheumatoid arthritis (RA) patients (Hirano et al., 1988), swollen lymph nodes of patients with Castleman's disease (Yoshizaki et al., 1989), and multiple myeloma cells (Kawano et al., 1988).

Inflammatory Bowel Diseases

IL-6 has further been shown to contribute to the development and inflammatory bowel diseases including both sporadic and colitis-associated colorectal cancer (Waldner et al., 2012). In colitis-associated cancer IL-6 is a critical tumor promoter during early tumorigenesis, by enhancing proliferation of tumor-initiating cells (Grivennikov et al., 2009).

Renal diseases

A role for IL-6 has also been implicated in the development of renal diseases (Jones et al., 2015). Pro-inflammatory effects have been observed in murine lupus nephritis (Kiberd, 1993). However, in the nephrotoxic nephritis (NTN) model of acute crescentic glomerulonephritis (GN) protective effects by IL-6 have been observed. There IL-6 leads to the down-regulation of pro-inflammatory macrophage proliferation (Luig et al., 2015).

Autoimmunity

IL-6 is further linked to the development of autoimmunity-related diseases through its major contributions to Th17 cell development. IL-6$^{-/-}$ mice are resistant to the induction of experimental autoimmune encephalomyelitis (EAE), partly because they expand Treg cells rather than Th17 cells (Korn et al., 2007). IL-6 upregulates the receptors for IL-23 and IL-21 in naïve T cells, both of which are at a later stage important for Th17 cell phenotype development (Ivanov et al., 2006, Zhou et al., 2007).

1.5   Interleukin-31

IL-31 was first discovered in conditioned media of activated CD4$^+$ T helper cells (Dillon et al., 2004). IL-31 shares the four-helix bundle architecture of the IL-6 family of cytokines and belongs structurally to the subgroup of short-chain (Sc) cytokines (Sprang and Fernando Bazan, 1993). The human IL-31 gene has been mapped to chromosome 12 whereas the mouse homologue is located on chromosome 5. Besides activated T-cells, other cells have been implicated as sources for IL-31. Human mast cells were shown to produce and release IL-31 after stimulation with antimicrobial peptides (Niyonsaba et al., 2010), transcriptionally regulated by nuclear factor of activated T cells (NFAT) and STAT6 (Park et al., 2012). Human eosinophils were shown to express and secrete high levels of IL-31 after stimulation with staphylococcus enterotoxin B (SEB) (Kunsleben et al., 2015). Monocytes, macrophages, immature and mature monocyte-derived dendritic cells produce IL-31 in response to ultraviolet (UV) irradiation and

hydrogen peroxide (H_2O_2) treatment (Cornelissen et al., 2011). The serum levels of IL-31 for healthy human subjects range from 6-10 ng/ml (Kim et al., 2011).

1.5.1   Interleukin-31 receptors
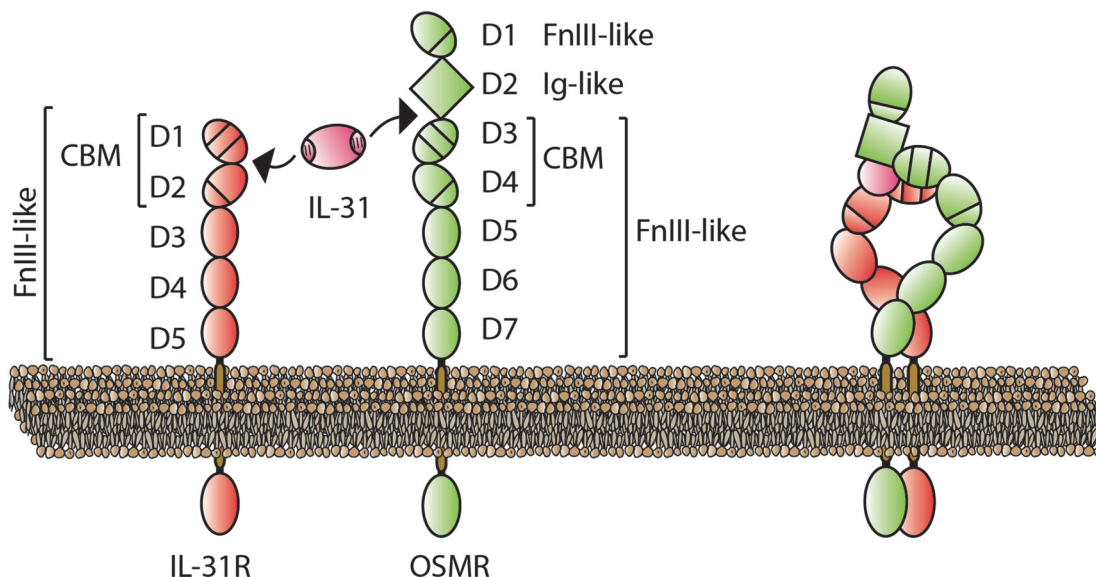

Figure 5: IL-31 receptors and their structure Schematic representation of the domain structures of IL-31 receptor subunits and formation of the trimeric IL-31 receptor complex after binding of IL-31.

IL-31 is the only cytokine of the IL-6 family that does not signal through gp130 but through a most closely related receptor originally termed gp130-like monocyte receptor (GLM-R) (Ghilardi et al., 2002) or gp130-like receptor (GPL) (Diveu et al., 2003) and is now referred to as IL-31R (Figure 5). It shares the typical architecture and structural features of type I cytokine receptors, and is found in close physical proximity to gp130 on human chromosome 5 and mouse chromosome 13. In contrast to gp130, IL-31R does not contain an N-terminal Ig-like domain. Therefore, IL-31R cannot bind to site III of IL-31 but instead binds with its CBM (D1+D2) to site II of the cytokine. Stimulation with IFN-γ leads to upregulation of IL-31R expression on monocytes (Ghilardi et al., 2002) and dendritic cells in a STAT1 dependent manner (Horejs-Hoeck et al., 2012). In murine macrophages IL-31R expression is regulated by IL-4-induced STAT6 activation (Edukulla et al., 2015). The OSMR is the second receptor component in the IL-31

receptor complex and binds with its Ig-like domain D2 to site III of IL-31 (Le Saux et al., 2010). Both receptor subunits are constitutively expressed on cells in the skin, testis, thymus and neurons of adult dorsal root ganglia (Dillon et al., 2004, Bando et al., 2006).

1.5.2 IL-31 signaling

Upon assembly of the heterotrimeric signaling complex, IL-31 induces the activation of the Jak/STAT signaling pathway (Heinrich et al., 2003) the MAPK cascade, as well as the PI3K cascade. Jak1 and Jak2 are the kinases associated with the OSMR/IL-31R signaling complex. After complex assembly, Jaks are brought into close proximity to each other, allowing their auto-phosphorylation and subsequent phosphorylation of the tyrosine motifs within the cytoplasmic parts of OSMR and IL-31R. The tyrosine motifs at position $Y652$ and $Y721$ on IL-31R serve as STAT3 and STAT5 binding sites (Ghilardi et al., 2002). Unlike OSMR, IL-31R is unable to recruit the adapter proteins SH2 domain containing protein tyrosine phosphatase-2 (SHP-2) or SH2 domain containing transforming protein (Shc), and thereby fails to mediate the phosphorylation of extracellular signal-regulated kinases (ERK)1/2 (Dreuw et al., 2004). Activation of the MAPK cascade is thereby mediated by the OSMR subunit and recruitment of Shc (Hermanns et al., 2000).

1.5.3 Pathophysiology of IL-31

In transgenic mouse models, the overexpression of IL-31 led to severe pruritus, alopecia and skin lesions (Dillon et al., 2004). In NC/Nga mice, an animal model of atopic dermatitis (Takaoka et al., 2005), expression of IL-31 mRNA was increased. Treatment with an antibody targeting the IL-31R in the same model reduced the characteristic scratching behavior, but did not influence the development of dermatitis (Grimstad et al., 2009). A recent study showed that repeated administration of IL-31 to BALB/C or NC/Nga mice leads to gradually upregulated IL-31R mRNA and protein expression in cutaneous dorsal root ganglia and correlates with increased long lasting scratching behavior (Arai et al., 2015).

IL-31 expression is increased in patients with atopic dermatitis (AD) but also in those with allergic contact dermatitis (ACD), arguing for an involvement in pruritic skin diseases (Bilsborough et al., 2006, Neis et al., 2006, Sonkoly et al., 2006). IL-31R mRNA expression is upregulated in diseased tissue from animal models of airway hyper responsiveness (Dillon et al., 2004). Sera of patients diagnosed with allergic asthma show increased levels of IL-31 (Neis et al., 2006). These findings indicate that IL-31 may contribute to the development of Th2-related diseases.

IL-31R$^{-/-}$ mice show a significant reduction in the number of immature hematopoietic progenitor cells (Broxmeyer et al., 2007). Parasitic infection of IL-31R$^{-/-}$ mice results in excessive Th2 inflammation, and therefore IL-31 may also mediate anti-inflammatory signals (Perrigoue et al., 2007, Perrigoue et al., 2009). Loss of IL-31R might lead to increased OSM signaling capacity as the shared receptor subunit is no longer occupied in the IL-31 signaling complexes and therefore alters the OSM/IL-31 signaling balance towards OSM (Bilsborough et al., 2010), resulting in a shift of the target gene expression profile.

1.6   Anti-cytokine therapies

Dysregulated cytokine signaling is of central importance in many diseases such as chronic inflammation and cancer. Therapeutic strategies aim to interfere with dysregulated cytokine signaling by specific inhibition of signaling pathways at different levels. Besides targeting of cytokine-receptor-interactions by biologics, through i.e. neutralizing antibodies or fused soluble receptors, also small molecule inhibitors targeting the intracellular signaling cascade have often been proposed as potential treatments for inflammatory diseases driven by cytokines. As there is great redundancy in the main signaling pathways already between members of the IL-6 family of cytokines, effects of small molecule inhibitors targeting i.e. kinases or transcription factors might lead to adverse side effects. Therefore it should be achieved to inhibit the pathological relevant signaling pathway already at the level of cytokine-receptor-interaction in a highly specif-

ic way. Current biological treatments are characterized by highly specific interactions with their relevant immune target.

1.6.1 Strategies targeting IL-6

As potential therapeutics for the implicated diseases and to further clarify the contribution of IL-6 several biologicals have been developed (Figure 6).
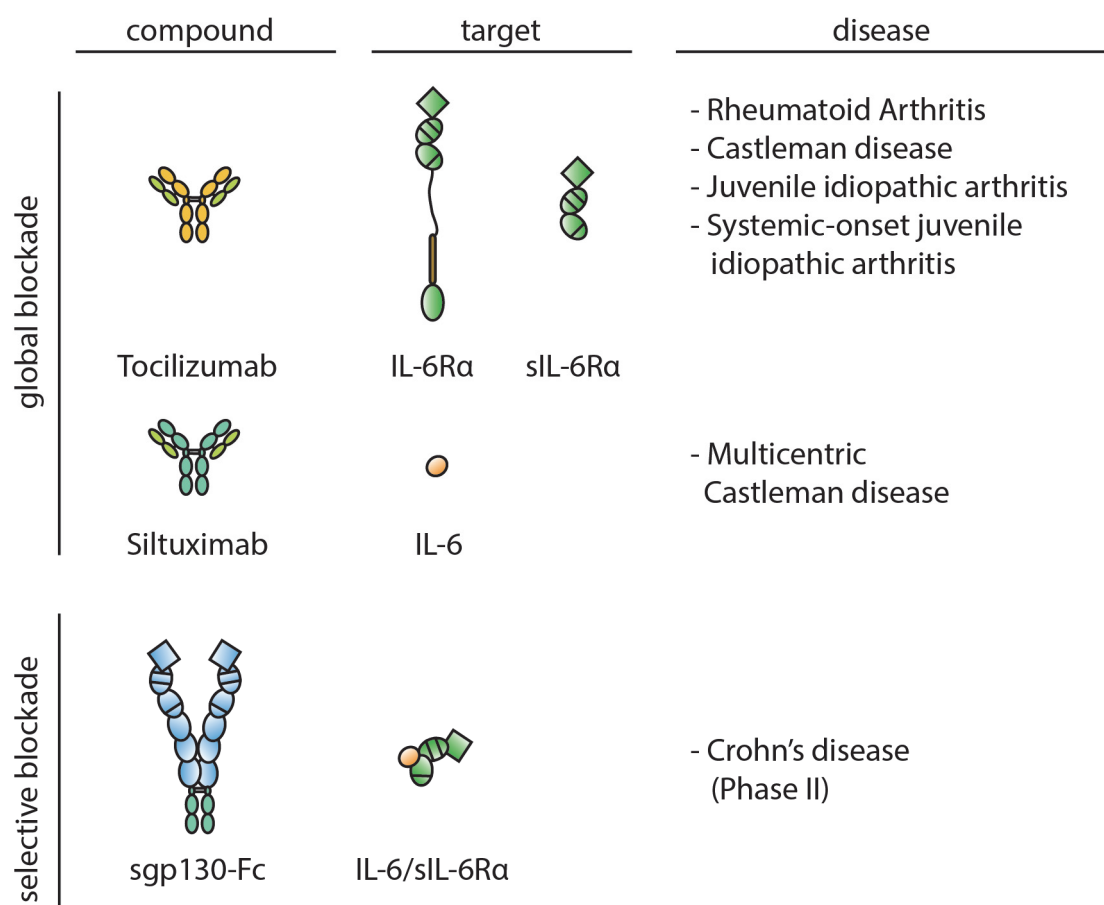
Figure 6: Anti-IL-6 therapies approved for the clinics or in clinical phases An overview about anti-IL-6 therapies that globally block IL-6 and which are approved for clinical use. Although sgp130-Fc is still in clinical phase II for the treatment of inflammatory bowel diseases, it is shown because it selectively blocks IL-6 trans-signaling.

Tocilizumab (anti-IL-6Rα antibody)

The first biological developed to target the IL-6Rα subunit is Tocilizumab, a humanized anti-IL-6Rα monoclonal IgG1 antibody. For its generation the complementarity determining regions of a mouse-anti-human IL-6Rα antibody were grafted onto human IgG1

(Sato et al., 1993). Tocilizumab blocks IL-6-mediated signal transduction by binding to either membrane-bound or soluble IL-6Rα making the receptors inaccessible for IL-6. The antibody is approved for the treatment of rheumatoid arthritis (Tanaka et al., 2013), systemic arthritis, juvenile idiopathic arthritis (Yokota et al., 2012) and Castleman's disease (Nishimoto et al., 2005) in several countries. Various results of case and pilot studies indicate that Tocilizumab may be used for the treatment of various other chronic immune-mediated diseases governed by IL-6 (Kang et al., 2015). Tocilizumab further led to a significant reduction of apolipoprotein(a) serum levels in RA patients, and could therefore be an alternative to conventional lipid apheresis as a therapeutic approach to treat elevated lipoprotein(a) serum levels, thereby reducing the risk to the development of cardiovascular disease (Schultz et al., 2010, Mueller et al., 2015).

Siltuximab (anti-IL-6 antibody)

Another biological developed is Siltuximab, a chimeric human-murine IgG1κ antibody targeting human IL-6 (van Rhee et al., 2010). Siltuximab has been approved for the treatment of multicentric Castleman's disease (Liu et al., 2014). Both Tocilizumab and Siltuximab block IL-6 signaling in a global manner, meaning inhibition of classical as well as trans-signaling.

Sgp130-Fc

A different approach is taken by another biological named sgp130-Fc. Sgp130-Fc is a fusion protein comprised of the extracellular part of gp130 (domains D1-D6) fused to the constant part (Fc) of a human IgG1 antibody. Fc-mediated dimerization of sgp130 lead to a 10-fold higher inhibition of IL-6/sIL-6Rα induced trans-signaling than the natural sgp130 monomer (Jostock et al., 2001). With the help of sgp130-Fc it is possible distinguish if IL-6 contributes to the pathogenesis of diseases either via classical signaling or trans-signaling. Inhibition of IL-6 trans-signaling has been shown to be beneficial in animal models of Crohn's disease (CD), a chronic inflammatory disease of the gastrointestinal tract (Atreya et al., 2000). Sgp130-Fc is currently undergoing clinical phase II trials for the treatment of CD and ulcerative colitis. Besides implications of IL-6 trans-

signaling in inflammatory bowel diseases (IBD), trans-signaling also seems to play a role in rheumatoid arthritis. Inhibition of IL-6 trans-signaling by sgp130-Fc effectively ameliorated disease hallmarks in an experimental mouse model of antigen-induced arthritis (AIA) (Nowell et al., 2003).

Fused soluble receptors

Another strategy to create an IL-6 inhibitor is based on the fusion of the extracellular parts of both gp130 and IL-6Rα with the constant part of a human IgG. Coexpression of both modified cDNAs in the expression host leads to Fc-mediated formation of disulfide-linked dimers (Economides et al., 2003). The limitation of this approach was the randomness of Fc-driven dimerization resulting in the expression of three distinct Fc-dimer populations, namely sgp130-Fc, sIL-6Rα:sgp130-Fc and sIL-6Rα-Fc.

In a parallel approach our lab developed a receptor fusion proteins targeting human IL-6 (hIL-6-RFP) based on the inline-fusion of the ligand binding domains of gp130 and IL-6Rα, inhibiting IL-6 classical and trans-signaling in a highly specific manner. hIL-6-RFP consists of domain D1-D3 of human gp130 fused to domains D2-D3 of human IL-6Rα and targets specifically human IL-6 (Ancey et al., 2003). Following the same design principle but based on the murine receptor subunits a murine IL-6 receptor fusion protein (mIL-6-RFP) was developed, including domains D1-D3 of murine IL-6Rα (instead of just D2-D3) and D1-D3 of murine gp130. mIL-6-RFP binds murine, rat as well as human IL-6 (Wiesinger et al., 2009, Metz et al., 2007). In contrast to neutralizing antibodies, RFPs are monogenic by design and therefore best suited for gene delivery approaches. They are useful tools to characterize cytokine contribution in murine models of human disease and could act as potential therapeutics in inflammatory diseases (Schwache and Müller-Newen, 2012).

1.6.2   Strategies targeting IL-31

As a potential therapeutic for pruritic skin diseases and to further clarify the contribution of IL-31 to pathogenesis, several biologicals targeting IL-31 have been developed.

Anti-IL-31 antibody

The first biological developed is a monoclonal antibody directly targeting IL-31, which is developed by ZymoGenetics (acquired by Brystol-Meyer-Squib) and currently goes through clinical phase I for the treatment of atopic dermatitis (ClinicalTrials.gov Identifier: NCT01614756).

Anti-IL-31R antibody

Another biological which targets IL-31 signal transduction is an anti-IL-31 receptor antibody, which has been shown to inhibit scratching behavior of IL-31 treated mice and to improve dermatitis scoring in a model of picryl-chloride induced contact hypersensitivity, which resembles AD (Kasutani et al., 2014).

OSMR-L-GPL

Following the design principle of hIL-6-RFP (Ancey et al., 2003), a receptor fusion protein for the inhibition of human IL-31 has been generated called OSMR-L-GPL consisting of D1–D4 of hOSMR connected with a flexible linker to D1–D2 of hIL-31R (Venereau et al., 2010). OSMR-L-GPL is a potent inhibitor of human IL-31 and does not inhibit human OSM signaling. In comparison to the previously described sOSMR and sIL-31R (sGPL) (Diveu et al., 2006), the inhibition of IL-31-dependent STAT3 phosphorylation by OSMR-L-GPL is more effective (Venereau et al., 2010).

2   Aim of the study

To further clarify the role and contribution of IL-31 to inflammatory and allergic diseases we wanted to develop a novel RFP based on the design of our previously described mOSM-RFP targeting murine interleukin-31. In addition an accompanying IL-31 responsive MEF cell system had to be developed for reliable analysis of IL-31 inhibitory studies.

As a proof-of-principle for other monogenic RFPs, we wanted to investigate the potential use of mIL-6-RFP in transgenic mouse models as an *in vivo* research tool. Therefore transgenic mice that express mIL-6-RFP in a doxycycline-inducible and tissue specific promoter driven manner were to be generated and characterized.

In a second approach we wanted to further optimize mIL-6-RFP to increase *in vitro* protein expression and facilitate protein purification. Additional improvements should lead to increased serum half-life *in vivo*. Therefore an engineered mIgG2a Fc-fragment followed by a transferable tag for detection and quantification should be added to the C-terminus to create mIL-6-RFP-Fc. To increase protein expression, mIL-6-RFP cDNA was optimized for mammalian codon usage. With the optimized mIL-6-RFP-Fc cDNA stably transfected producer cells were to be generated. The murine IgG2a Fc-fragment then should allow the purification of mIL-6-RFP-Fc through Protein A/G affinity chromatography for subsequent use of purified protein for *in vitro* and *in vivo* inhibition of IL-6.

As RFPs are encoded by a single gene, they are well suited for gene therapeutic approaches. As a proof-of-principle for the applicability of RFPs to gene therapy, the optimized mIL-6-RFP-Fc gene should delivered to mice by means of hydrodynamics-based transfection with subsequent analysis of pharmacodynamics of mIL-6-RFP-Fc and its therapeutic use in a model of ischemia/reperfusion in the kidney.

3 Materials and Methods

Materials and methods are described according to standard protocols used in the Institute of Biochemistry and Molecular Biology, RWTH Aachen University, and were modified regarding individual differences in experimental procedures.

3.1 Materials

3.1.1 Chemicals

All chemicals met at least the criteria for the purity standard *pro analysi* and were purchased from Merck, Sigma-Aldrich, Roth or Invivogen.

3.1.2 Buffers and Media

All buffers and media were prepared with double-distilled water (ddH$_2$O) unless stated otherwise.

PBS	137 mM	NaCl
	2.5 mM	KCl
	8 mM	Na$_2$HPO$_4$
	1.5 mM	KH$_2$PO$_4$
		adjusted to pH 7.4
RIPA lysis buffer	50 mM	Tris-HCl, pH 7.4
	150 mM	NaCl
	1 mM	EDTA
	0.5 %	Nonidet P-40
	1 mM	NaF
	15 %	glycerol
	1 mM	Na$_3$VO$_4$
	0.25 mM	phenylmethylsulfonylfluoride (PMSF)

	5 μg/ml	aprotinin
	2.5 μg/ml	leupeptin
TBS-N buffer	20 mM	Tris-HCl, pH 7.5
	135 mM	NaCl
	0.1 %	Nonidet P-40

3.1.3 Cytokines and soluble receptors

Recombinant murine IL-6 and murine IL-31 were purchased from ImmunoTools (Friesoythe, Germany). Recombinant murine OSM was purchased from PeproTech (Rocky Hill, NJ).

3.1.4 Oligonucleotides

All oligonucleotides were ordered from Eurofins Genomics (Cologne, Germany).

Table 1: List of sequencing primers

Name	Sequence 5' -> 3'
BGH_as (#1.15)	AACTAGAAGGCACAGTCG
AGS41_as (DS26)	CTTCCACCTCCACTACCAGC
MCS-Koz_s (DS34)	CGGTACTTAAGACAGGTACCGCCACC
PPT_s (DS35)	GATCCTAGCTCTTGTTGGAG
gp130-I_as (LB14)	TGAGGAGACCTTCCCAAGGG
gp130-I_s (LB16)	GAAGGTCTCCTCAGAGTCTATC
IL-6R_as (LB17)	GTTCTTCCGGAAGCAGGAGAGCTTG

Table 2: List of cloning primers

Name	Sequence 5'-3'
mIL-31R_as	GGCCAAGCTTTCAGGTACCTGGAACTTCCTCCATAGTCAC
mIL-31R_s	GTCCGCTAGCAGCCTGGCAGTCCTGCCGAC

3.1.5   Recombinant plasmids

Name	Description
pOG44	Expression vector (Invitrogen, Paisley, UK); CMV promoter; synthetic intron; FLP gene; ampicillin resistance (Amp^R); pUC origin (ori)
pUHrT 62-1	Expression vector (Urlinger et al., 2000); CMV promoter; Amp^R; ori; encodes for rtTA2^S-M2
pCMV-Sport6	Expression vector (Invitrogen, Paisley, UK); T7, SP6, and CMV promoters; lox P site; Amp^R; f1 ori
pcDNA3	Expression vector (Invitrogen, Paisley, UK); CMV promoter; T7 promoter; multiple cloning site (MCS); BGH polyadenylation signal (BGH-pA); f1 ori; SV40 promoter; neomycin resistance (Neo^R); Sv40-pA; β-Lactamase promoter (bla); Amp^R; pUC ori
pcDNA5/FRT/TO	Expression vector (Invitrogen, Paisley, UK); tetracycline controlled CMV promoter; T7 promoter; MCS; BGH-pA; Flp-In recombination target (FRT); Hygromycin resistance (Hygro^R) without ATG; Sv40-pA; pUC ori; bla; Amp^R; (After successful recombination into Flp-In sites hygromycin acquires the ATG required for expression.)
pcDNA5/FRT/TO-spezial	The vector pcDNA5/FRT/TO with a modified MCS
pMA	Transfer vector (Invitrogen, Paisley, UK)
pTZ-PEPCK	Expression vector

IL-31/mIL-31-RFP

Name	Insert
pCMV-Sport6	mIL-31R Isoform 4
pcDNA3	mIL-31-RFP-3V5-3HA
pcDNA5/FRT/TO	mIL-31-RFP-3V5-3HA-his
pcDNA5/FRT/TO	mIL-31R Isoform 1

IL-6/mIL-6-RFP

Name	Insert
pcDNA3	mIL-6-RFP-V5-his
pcDNA3	mIL-6-RFP-3V5-3HA
pMA	mIL-6-RFP-Fc-3V5-3HA (codon optimized cDNA)
pcDNA3	mIL-6-RFP-Fc-3V5-3HA (codon optimized cDNA)
pcDNA5/FRT/TO	mIL-6-RFP-Fc-3V5-3HA (codon optimized cDNA)
PTZ-PEPCK	mIL-6-RFP-Fc-3V5-3HA (codon optimized cDNA)

3.1.6 Antibodies

Anti-pY705-STAT3 (#9131), anti-STAT3 (#9139), anti-pERK1/2 (#4370), anti-ERK1/2 (#9102) from Cell Signaling (Danvers, MA), anti-V5 (#R960-25) from Invitrogen (Carlsbad, CA), anti-STAT3 C-20, anti-STAT3 K-15 (#sc-482, #sc-483), anti-ERK1 (#sc-093-G), anti-ERK2 (#sc-154-G), anti-GAPDH (#sc-32233) from Santa Cruz (Dallas, TX), anti-HSP70 (#ADI-SPA-820) from Enzo Life Sciences (Lörrach, Germany), and anti-HA (#H6908) from Sigma-Aldrich (St. Louis, MO) were used for immunoblotting. Anti-rabbit, anti-mouse and anti-goat antibodies conjugated to horseradish peroxidase were ordered from DAKO (Hamburg, Germany).

3.2 Prokaryotic cells

3.2.1 Bacterial strains

E.-coli-bacterial strains were used for transformation and amplification of plasmid DNA

DH5α	F- endA1 glnV44 thi-1 recA1 relA1 gyrA96 deoR nupG Φ80dlacZΔM15 Δ(lacZYA-argF)U169, hsdR17(rK- mK+), λ–
JM83	rpsL ara Δ(lac-proAB) Φ80dlacZΔM15
XL-1 blue	endA1 gyrA96(nal^R) thi-1 recA1 relA1 lac glnV44 F'[::Tn10 proAB$^+$ lacI^q Δ(lacZ)M15] hsdR17(r$_K^-$ m$_K^+$)
JM110	rpsL thr leu thi lacY galK galT ara tonA tsx dam dcm glnV44 Δ(lac-proAB) e14- [F' traD36 proAB$^+$ lacI^q lacZΔM15] hsdR17(r$_K^-$m$_K^+$)

3.2.2 Media and cultivation

Bacteria were either cultured in LB-medium, supplemented with a selection marker such as ampicillin or kanamycin (100 μg/ml) and incubated rocking with 250 rpm, or on LB-agar (1.5%) at 37°C. Storage of bacteria followed at -80°C in LB-Medium supplemented with 20% Glycerol (87%).

LB-Medium	10 g/l	Bacto-Tryptone (Difco, Detroit, MI)
	5 g/l	Yeast extract (Difco, Detroit, MI)
	5 g/l	NaCl
LB-Agar	15 g/l	Bacto-Agar (in LB-Medium) (MP Biomedicals, Eschwege)

3.2.3 Competent bacteria

50 ml LB-medium were inoculated with a trace of the corresponding *E. coli* cells (XL-1 blue, JM-83, JM-110, DH5α) from a glycerol stock vial and incubated at 37°C overnight to grow a preparatory culture, which is used the next day to inoculate 250 ml LB-medium to start the bacterial culture. Shake the culture at 37°C until an OD_{600} of 0.6-0.8 is reached (approximately 150 min). Cool the culture on ice for 5 min, and transfer the culture to a sterile, round-bottom centrifuge tube. Collect the cells by centrifugation (15 min, 6000 rpm, 4°C). Discard the supernatant carefully and resuspend the pellet gently in 25 ml cold LB/PEG.

LB-PEG	10 %	PEG (polyethylene glycol) 3350 or PEG 4000
	5 %	DMSO (dimethyl sulfoxide)
	100 mM	$MgCl_2$

Pass solution through a 0.2 μm sterile-filter and store at 4°C.

Prepare aliquots of 200 μl in sterile microcentrifuge tubes and freeze in liquid nitrogen. Store the competent cells at –80°C.

3.2.4 Transformation

A 10 μl aliquot of the DNA to be transformed was transferred into a 1.5 ml microcentrifuge tube, and kept on ice. An aliquot of frozen competent *E. coli* cells was thawed on ice. The bacteria were gently resuspended cells and 50 μl of the cell suspension was transferred into the microcentrifuge tube with the plasmid DNA, mixed carefully, and kept on ice for 30 min. The tube was then transferred to a 42°C heating block for 90 seconds and subsequently returned on ice for the next 2 min. The transformed bacteria

were then plated out on LB-agar plates containing the relevant antibiotic and incubated at 37°C overnight until colonies developed.

3.3 Molecular biological methods

3.3.1 Plasmid purification from bacterial cells

Plasmid DNA from prokaryotic cultures was extracted using the QIAprep Spin Miniprep Kit (Qiagen) for small-scale preparations (5-15 µg) and the HiSpeed Plasmid Maxi Kits (Qiagen) for large-scale preparations according to the manufacturer's recommendations. Plasmid DNA was eluted using Merck H_2O.

3.3.2 Quantification of DNA

Quantities of DNA were determined with NanoDrop 1000 spectrophotometer (Thermo Fisher Scientific, Waltham, MA) by photometric measurement of the absorption at 260 nm (A_{260}). An absorption-value of A_{260}=1.0 is equal to an amount of 50 µg double stranded DNA. Purity of prepared nucleic acids was analyzed by measuring absorption at 280 nm (A_{280}) additionally. For pure DNA the A_{260}/A_{280} ratio should correspond to 1.8 – 2.0.

3.3.3 Restriction endonuclease digestion of DNA

Enzymatic restriction of DNA was performed according to manufacturer's recommendations. Restriction enzymes were purchased from New England Biolabs (Ipswich, MA).

3.3.4 Agarose gel electrophoresis

DNA fragments from either digested plasmid DNA or PCR products were mixed with DNA loading buffer and loaded onto a 1-1.5% agarose gel (SeaKem-LE-Agarose, Biozym, USA). The gel was run at 5 V/cm^2 until the DNA fragments reached the required grade of separation. All agarose gels contained 0.5 µg/ml ethidium bromide for visualization of the DNA bands and were run in 1x TAE buffer. For size determination bands were compared with 1 Kb DNA ladder (Invitrogen, USA) marker.

10x DNA loading	0.25%	Xylencyanol
buffer	0.25%	Bromphenol blue
	30%	Ficoll 400
1x TAE buffer	40 mM	Tris-Base
	20 mM	Acetic acid
	1 mM	EDTA

3.3.5 Isolation of DNA fragments from agarose gels

The desired DNA fragments were cut out with a sterile scalpel and DNA was isolated using the QIAquick Gel Extraction Kit (Qiagen) following the manufacturer`s instructions. DNA was eluted in 30 µl chromatography grade water (Merck Millipore).

3.3.6 Ligation of DNA

The T4 DNA ligase (Roche, Mannheim, Germany) was used to ligate double stranded DNA fragments. 30 ng of linearized vector was incubated with a 3 fold molar excess of the insert for 60 min at room temperature. Then ligation preparations were transformed into competent bacteria.

3.3.7 DNA Sequencing

DNA was sequenced by Eurofins Genomics (Ebersberg, Germany). For sequencing 1 µg plasmid DNA was either premixed with 1.5 µl sequencing primer [10 pmol/µl] or standard primers supplied directly by Eurofins Genomics.

3.3.8 Polymerase chain reaction (PCR)

The PCR is used to selectively amplify a desired target DNA sequence. Standard PCR was performed according to the manufacturer's recommendations using Taq Polymerase. If the amplified DNA was to be used for further subcloning, the PCR was performded using Phusion High Fidelity (HF) Polymerase (Finnzymes), which exhibits an intrinisic proof reading activity.

Taq Polymerase	4 µl	Tail DNA
Master Mix	5 µl	5x Taq-Polymerase Buffer
for genotyping of	2 µl	DMSO
transgenic mice	2 µl	$MgCl_2$
	1.5 µl	dNTPs
	1.5 µl	Sense primer
	1.5 µl	Anti-sense primer
	0.3 µl	Taq Polymerase
	ad 25 µl	H_2O
Phusion HF	x µl	DNA (5-10 ng)
polymerase	10 µl	5x Phusion HF Buffer
	1 µl	dNTPs
	2.5 µl	Sense primer (10 pmol)
	2.5 µl	Anti-sense primer (10 pmol)
	0.5 µl	Phusion DNA Polymerase
	ad 50 µl	H_2O

3.3.9 RNA extraction

Total RNA from cells or tissues was extracted with the RNeasy Mini Kit (Qiagen) according to the manufacturer's recommendations. The cell lysates were homogenized using the QIAShredder (Qiagen) columns. Remaining genomic DNA was digested on column using the RNase free DNase Set (Qiagen) for 15 min at room temperature. RNA concentration was determined using the Nanodrop 100 UV/VIS Spectrophotometer (Thermo Scientific). RNA was stored at -80°C.

3.3.10 Reverse Transcription

Complementary DNA (cDNA) was synthesized from 1 µg RNA using the OmniScript RT Kit (Qiagen) according to the manufacturer's recommendations using either oligo-dT or random hexamer primers.

3.4   Eukaryotic cells

3.4.1   Cell lines

HEK293	Adherent human embryonic kidney cells
HepG2	Adherent human liver carcinoma cell line (ATCC HB-8065)
MEF	Adherent murine embryonic fibroblasts (Dr. B. Neel, Boston, USA)
muHepa	Murine hepatocarcinoma cells (kindly provided by Dr. Christian Liedtke, Department of Medicine III, RWTH Aachen University)
Primary murine keratinocytes	Kindly provided by Prof Dr. Jens Malte Baron, Department of Dermatology, RWTH Aachen University
PAM212	Mouse keratinocyte cell line (kindly provided by Prof Dr. Jens Malte Baron, Department of Dermatology, RWTH Aachen University)

3.4.2   Cultivation of eukaryotic cells

HEK293, MEF, PAM212 and muHepa cells were maintained in Dulbecco's modified Eagle's medium (DMEM, Lonza), supplemented with 10% fetal calf serum (FCS), 100 mg/l streptomycin, and 60 mg/l penicillin. HepG2 cells were maintained in DMEM-F12 medium (Lonza) supplemented with 10% FCS, 100 mg/l streptomycin, 60 mg/l penicillin and 2 mM l-glutamine. The cells were incubated at 37°C in a water-saturated atmosphere at 5% CO_2. All cells used were free of mycoplasma as determined by a PCR-based assay.

3.4.3   Cryoconservation of eukaryotic cells

Cells were grown to 80% confluency and either scraped or trypsinized. Cells were centrifuged, washed with PBS and resuspended in freezing medium. 1 ml aliquots were stored

3.4.4   Mammalian protein production and purification

Stable HEK293 Flp-In/T-Rex cells (Invitrogen) for the inducible production of mIL-6-RFP- Fc were generated with the Flp-In system using 250 µg/ml Hygromycin B (Invivogen) and 15 µg/ml Blasticidin (Invivogen). Protein expression was induced in serum-free medium with 400 ng/ml doxycycline (Sigma-Aldrich) for 72 hours. Harvested conditioned media were cleared through centrifugation, passed through a 0.20 µm sterile-filter and afterwards loaded onto an ÄKTA Purifier 10 system (GE Healthcare, Chalfont St. Giles, UK) for affinity purification on a 1 ml Protein A Sepharose Column (#89924, Thermo Fischer, Waltham, MA). The column was washed with 20 mM sodium phosphate buffer (pH 7). mIL-6-RFP-Fc was eluted in fractions of 1 ml using 12.5 mM citric acid (pH 2.7) and neutralized immediately by adding 50 µl of 2 M Tris/HCl (pH 8). Protein containing fractions were quantified using a BCA colorimetric assay (#500-0006, Bio-Rad, Munich, Germany) following manufacturer's instruction. Protein containing fractions were pooled and dialyzed against PBS.

3.4.5   Expression of mIL-6-RFP-Fc in vitro

Murine hepatocarcinoma cells (kindly provided by Dr. Christian Liedtke, Department of Medicine III, RWTH Aachen University) were cultivated in Dulbecco's Modified Eagle Medium (DMEM) with GlutaMax (Invitrogen) supplemented with 10% FCS (Lonza, Basel, Switzerland), 100 U/ml penicillin and 100 µg/ml streptomycin (Sigma-Aldrich). For the cultivation of HepG2 cells (ATCC HB-8065) DMEM/F12 (Invitrogen) was used. The cells were incubated at 37°C in a water saturated atmosphere at 5% CO_2 and grown on 6-well plates to 70% confluence. All cells used in this study were free of mycoplasma as determined by a PCR-based assay. Cells were transfected using TransIT-LT1 (Mirus Bio, Madison, WI) according to manufacturer's instructions. Medium was exchanged to DMEM with GlutaMax™ without FCS after 4 hours. For analysis of protein secretion conditioned media were harvested at the indicated time points and cleared by centrifugation.

3.5 Cell biological and immunological methods

3.5.1 Cell lysis

For the isolation of cellular proteins, cell cultures were lysed in RIPA-lysis buffer (50 mM Tris-HCl, pH 7.4, 150 mM NaCl, 0.5% NP-40, 15% glycerol, 1 mM NaF, and 1 mM Na_3VO_4) supplemented with 5 µg/ml of each aprotinin, leupeptin and 0.25 mM PMSF as well as 0.5 mM EDTA.

3.5.2 SDS-PAGE

Protein containing samples were separated on a 7.5% or 10% polyacrylamid separating gel at 35 mA by discontinuous sodium dodecyl sulfate polyacrylamide gel electrophoresis (SDS-PAGE).

3.5.3 Coomassie staining

Following SDS-PAGE, proteins could be visualized in the gel with Coomassie Brilliant-Blue G-250 (Diezel et al., 1972). The gels were first fixed in fixation solution (10% acetic acid, 25% isopropanol, H_2O). After fixation, the gels were stained in coomassie staining solution (10% acetic acid, 30% isopropanol, 0.006% Coomassie Brilliant-Blue G-250, H_2O) for 20 minutes at room temperature with constant agitation. The gels were then incubated in destaining solution (10% acetic acid, 40% methanol, H_2O) until the background of the gel disappeared.

3.5.4 Western blot and immuno-detection

Proteins were separated by SDS-PAGE and transferred to a polyvinylidene-difluoride (PVDF) membrane (GE Healthcare). Membranes were washed in TBS-N and then blocked with 10% bovine serum albumin in TBS-N for 30 min. Membranes were exposed to specific primary antibodies overnight at 4°C. Membranes were washed three times with TBS-N and subsequently incubated with horseradish-peroxidase (HRP)-conjugated secondary antibodies for 1h at room temperature. Primary and HRP-conjugated secondary antibodies were diluted in TBS-N buffer (20 mM Tris-HCl, pH

7.5, 135 mM NaCl, 0.1% Nonidet P-40). After washing the membrane three times sig-nals membrane-bound antibody complexes were detected by chemiluminescence (pCA-ECL solution (100 mM Tris-HCl pH 8.8, 2.5 mM luminol, 0.2 mM para coumaric acid, 2.6 mM hydrogenperoxide).

3.5.5   ELISA

anti-mIL-6-Rα

Concentrations of mIL-6-RFP were determined by a sandwich ELISA. A validated anti-body combination directed against domains D1–D3 of the murine IL-6Rα was used (R&D Systems). Soluble mIL-6Rα (R&D Systems) served as a standard.

anti-HA/anti-V5

Microtiter plates (Nunc Maxisorp, Sigma) were coated overnight with anti-HA antibody (#MMS-101R, BioLegend, Dedham, MA) in sterile filtered PBS at 4°C. After blocking the plate for 1 hour with 1% BSA/PBS diluted standard and samples were added and incubated for 2 hours at room temperature. mIL-6-RFP-Fc bound to the plate was de-tected by anti-V5-HRP (#R961-25, Invitrogen). The enzymatic reaction was performed with 3,3´,5,5´-tetramethylbenzidine (TMB) substrate, stopped in 2 M H_2SO_4 and the absorbance was measured at 450 nm on an EON Microplate Spectrophotometer (Bio-Tek, Winooski, VT) and analyzed with Gen5 Software (BioTek). mIL-6-RFP quantified with the mIL-6Rα ELISA served as a standard.

3.5.6   Inhibition of IL-6 in vitro

muHepa cells were grown on 6 cm dishes to 70% confluence. A mixture of IL-6 (20 ng/ml) and mIL-6-RFP-Fc (corresponding molar ratios) or PBS, respectively, was prein-cubated in 1 ml DMEM for 30 min and afterwards added to the cells for 20 min. For pretreatment the medium was supplemented with 1335 ng/ml mIL-6-RFP-Fc (10-fold molar excess) 90' prior stimulation with IL-6 (20 ng/ml). Subsequently, cells were washed with PBS once and lysed with RIPA lysis buffer. The proteins were separated by

SDS-PAGE and transferred to a PVDF membrane with subsequent immunodetection using specific antibodies. Primary and HRP-conjugated secondary antibodies were diluted in TBS-N buffer. The membrane was incubated with pCA-ECL solution (100 mM Tris-HCl pH 8.8, 2.5 mM luminol, 0.2 mM para coumaric acid, 2.6 mM hydrogenperoxide) and membrane-bound antibody complexes were detected by chemiluminescence using a digital imaging system (LAS 4000 mini, Fuji, Japan).

The murine pre-B cell line Ba/F3 was stably transfected through electroporation with an expression vector encoding murine gp130. Ba/F3-mgp130 cell pools expressing mgp130 in conjunction with the puromycin resistance gene were selected and maintained in the presence of 1.5 µg/ml puromycin (Invivogen) and IL-3. Ba/F3-mgp130 cells were retrovirally transduced with mIL-6Rα using the pMOWS system as described elsewhere 48, selected and maintained in the presence of 1.5 µg/ml puromycin and 10 ng/ml IL-6. Ba/F3 cell lines were cultured in DMEM containing 10% FCS, 100 U/ml penicillin and 100 U/ml streptomycin at 37°C with 5% CO_2 in a water-saturated atmosphere. For the proliferation assay Ba/F3-mgp130-mIL6Rα were seeded on 96-well plates (20,000 cells/well), and stimulated with IL-6 (37 pM) in the presence of either mIL-6-RFP-Fc- or mIL-6-RFP-conditioned media. After 60 h of incubation, metabolically active cells were quantified using a colorimetric assay based on the cell proliferation kit II XTT assay (Roche Diagnostics, Mannheim, Germany).

3.6   Animal experiments

All animal experiments have been approved by the local government authorities and were performed in accordance with relevant guidelines and regulations. Mice were held under a 12-hour light-dark cycle and had ad libitum access to drinking water and standard chow. Treatment groups were distributed equally among cages. For assessment of pharmacokinetics and for IL-6 injection experiments, matched male littermates aged 12-20 weeks were used. Volumes of 100 and 200 µl were administered for i.v. and i.p. injections, respectively. Blood draws and euthanasia for organ harvesting were performed at the time points indicated. For subsequent quantitative protein analysis samples for

comparison were assayed on a single membrane or ELISA plate with equal amounts loaded and the experimenter having animal numbers rather than specified treatment group information. qPCR, serum creatinine measurements and tissue analysis were conducted in a completely blinded fashion. Serum creatinine was analyzed as described (Nagayama et al., 2014).

3.6.1   Hydrodynamics-based in vivo gene delivery

To obtain maximal expression levels, younger, i.e., 7 week-old male littermates were transfected via tail vein injection of plasmid PTZ-PEPCK-b.glob.intron-mIL-6-RFP-Fc-3V5-3HA-b.glob.polyA prepared in delivery solution (TransIT-EE, Mirus Bio, Madison, WI).

3.6.2   Renal ischemia and reperfusion procedure

Seven-week-old male C57/Bl6J animals (purchased from Charles River, Sulzfeld, Germany; allowed 1 week of acclimatization) hydrodynamically pre-transfected and exhibiting mIL-6-RFP-Fc levels of 0.25-4.5 µg/ml (as assessed by serum ELISA at 20 h post transfection) or having received 100% of the control plasmid volume i.v. were subjected to I/R. Mice were anaesthetized using Ketamin/Xylazin, acclimatized on a warmed electrical plate for 15 min (constant plate temperature of 37°C), and subject to operation by midline laparotomy and subsequent clamping of both renal hila using mini clamps (#18055-04, Fine Science Tools, Heidelberg). Clamping was timed to be exactly 33 minutes per each kidney while animals were held at a constant plate temperature of 37°C. Completeness of ischemia of both kidney was assured by color changes of the entire organ to a dark and lighter color during and following ischemia, respectively. Mice were sutured using standard techniques. Surgeons were blinded to the animals' treatment groups. Upon euthanasia at sacrifice animals were perfused intraarterially with saline 0.9 % prior to organ harvest.

3.6.3   Immunofluorescence

Prior to liver harvesting by snap-freezing (TissueTek, Sakura, Japan) mice were perfused intra-arterially with saline 0.9 % upon euthanasia to minimize blood cell autofluorescence. Cryosections (5 μm) were fixed in 4 % paraformaldehyde for 15 min, blocked with 10 % donkey serum in PBS, and subsequently stained with rabbit anti-HA antibody (1:100), donkey anti-rabbit-cy3 (1:200, Dianova, Hamburg, Germany), and DAPI (4',6-diamidino-2-phenylindole, 1:10000, Roche, Mannheim, Germany). GFP fluorescence was preserved during this procedure. A BZ-9000 microscope (Keyence, Japan) was used for visualization.

3.6.4   Histology and renal tissue injury score

Following harvest, right kidney halves were fixed in methyl Carnoy's solution, embedded in paraffin, sectioned (2 μm), and stained by periodic acid-Schiff (PAS) as described (Nagayama et al., 2014). Left kidney tissue was not available for PAS stain due to processing for cryopreservation. Renal tissue injury was assessed in a blinded fashion by scoring the percentage of tubules in the outer medulla that exhibited tubular dilation / atrophy, cast formation, cellular necrosis and loss of brush border as follows: 0, none; 1, >0-25%; 2, 25 – 50%, 3, 50-75% and 4, > 75% as described (Howard et al., 2012). Six consecutive non-overlapping high-power fields (x 200) per section were examined.

3.6.5   Preparation of liver and kidney lysates

Tissue protein extracts were generated on ice using RIPA buffer and processed for Western blot analysis similar to cellular lysates (see above). Equal amounts of protein (30 μg) were loaded.

3.6.6   Quantitative mRNA analysis

Liver RNA isolation and cDNA synthesis were performed using standard columns (Qiagen, Hilden, Germany) and random primers (Roche), respectively. Real-time quantitative PCR was carried out using qPCR Core Kit for SYBR Green (Eurogentec, Liege, Bel-

gium) and an ABI Prism 7300 sequence detector (Life Technologies, Carlsbad, CA). Data were normalized using glyceraldehyde-3-phosphate dehydrogenase (Gapdh) as an internal control and calculated using the $\Delta\Delta$CT-method.

Table 3: List of qPCR primers

Name	Sequence 5'-3'
Gapdh_fwd	GGC AAA TTC AAC GGC ACA GT
Gapdh_rev	AGA TGG TGA TGG GCT TCC C
Saa1	QuantiTect Primer Assay, Mm_Saa1_1_SG, Catalog No. QT00196623, (Qiagen, Hilden, Germany)
A2m_fwd	TGC ATC CGG GTT GGT GTA C
A2m_rev	TTC ATA CAG ATG CAG TGA GAC TTT TG
IL-6_fwd	TGT TCA TAC AAT CAG AAT TGC CAT T
IL-6_rev	AGT CGG AGG CTT AAT TAC ACA TGT T
Ngal_fwd	GGC CTC AAG GAC GAC AAC A
Ngal_rev	TCA CCA CCC ATT CAG TTG TCA

Saa1, serum amyloid A1; A2M, a-2macro-globulin; Ngal, Neutrophil gelatinase-associated lipocalin (NGAL)/lipocalin-2 (Lcn2).

3.6.7 Statistical analysis

Unpaired one-sided student's t-test with Welch's correction when appropriate was performed at all instances when not otherwise specified to compare control- and RFP-treated groups as indicated using GraphPad Prism version 6.0b for Mac OS X, GraphPad Software (La Jolla, CA). The one-sided test approach was chosen since our hypothesis H1 was one-sided, i.e., mIL6-RFP-Fc inhibits IL-6 or is beneficial in the renal ischemia-reperfusion model compared to control.

4   Results

4.1   Development of mIL-31-RFP

The first part deals with the engineering and biochemical characterization of a receptor fusion protein targeting murine IL-31 (mIL-31-RFP). Through a combination of computational analysis and site-directed mutagenesis the critical amino acids of human IL-31 implicated in ligand receptor interaction with hOSM-R and hIL-31R were identified (Le Saux et al., 2010). As a site II/III cytokine IL-31 resembles OSM and LIF, which both signal through heterodimeric receptor complexes consisting of mgp130 (site II interaction) and a cytokine specific receptor subunit mOSM-R and mLIF-R (site III interaction), respectively.

4.1.1   Cloning and expression of mIL-31-RFP

The receptor signaling complex of IL-31 consists of OSMR and IL-31R. mIL-31-RFP is built up in analogy to the previously published receptor fusion protein for the inhibition of murine OSM (mOSM-RFP) (Brolund et al., 2011). mOSM-RFP consists of the four N-terminal domains of the murine OSM receptor (mOSMR) and domains D2 and D3 of murine gp130 (mgp130) connected by a flexible polypeptide linker. To create mIL-31-RFP the CBM of gp130 (D2 + D3) was replaced with the CBM of mIL-31R (Figure 6A). The CBM of mIL-31R is highly homologous to gp130, and is formed by its domain D1 and D2 (see Supplementary Figure 1). Furthermore, the flag-tag at the C-terminus of mOSM-RFP was replaced with a 3V5-3HA tag module consisting of three consecutive V5 and HA tags which improves protein detection and facilitates quantification through a α-HA/α-V5 based sandwich-ELISA. The cDNA of isoform 4 of murine IL-31R (Uniprot: Q8K5B1-4) was obtained from imaGenes. The nucleotide sequence encoding D1 and D2 of mIL-31R was amplified via PCR from pCMV-Sport6-mIL-31R and subsequently digested with NheI/HindIII. The digested PCR fragment was used to replace the

domains D2-D3 of mgp130 and the flag-tag in pcDNA3.1-mOSM-RFP-flag to create

pcDNA3.1-mIL-31-RFP. In a second construct we introduced the 3V5-3HA tag, ampli-

fied from pcDNA3-Albumin via PCR and digested with KpnI/HindIII, to create

pcDNA3.1-mIL-31-RFP-3V5-3HA. HEK293 cells were transfected with an expression

vector encoding for mIL-31-RFP-3V5-3HA. Conditioned media of the cells were con-

centrated 10-fold, quantified and analyzed under either reducing or non-reducing con-

ditions by Western blotting using an antibody directed against the HA-tag (Figure 6B).

The apparent molecular mass of reduced mIL-31-RFP is about 150 kDa, which is in

agreement with the expected molecular mass of the glycosylated mIL-31-RFP. Under

non-reducing conditions additional bands of higher molecular mass represent the for-

mation of mIL-31-RFP-3V5-3HA dimers and multimers.
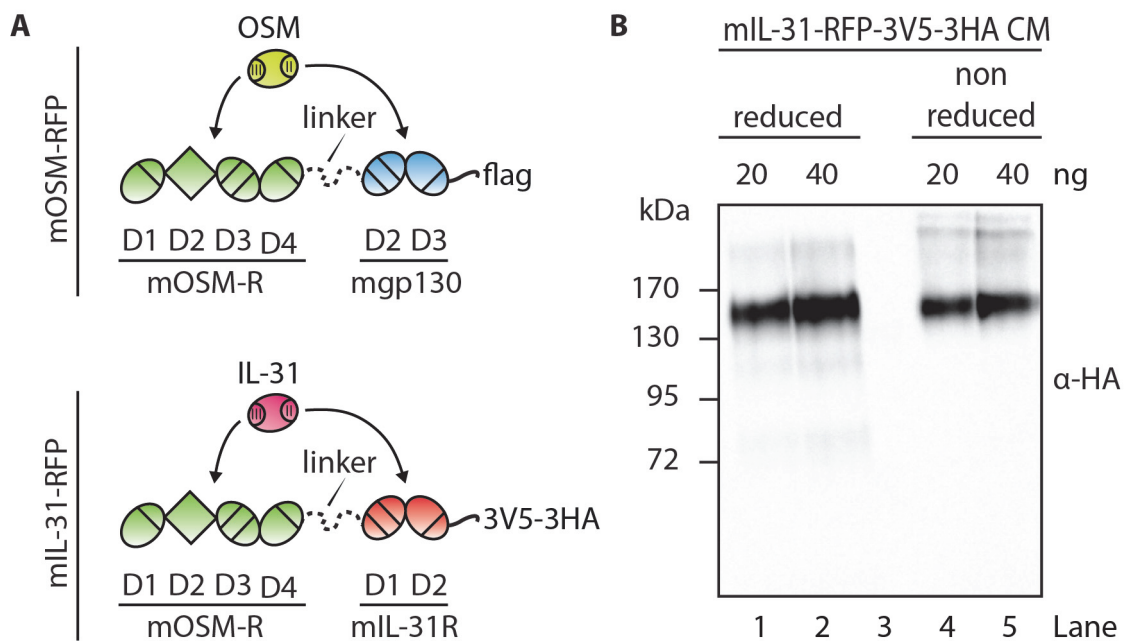
Figure 7: Design and expression of mIL-31-RFP (A) mIL-31-RFP was cloned on the basis of mOSM-RFP and consists of domain D1-D4 of murine OSMR connected through a flexible linker with D1-D2 of murine IL-31R followed by three V5 and three HA epitopes. Arrows indicate binding of IL-31 to mIL-31-RFP. (B) Western blot analysis of reduced and non-reduced 10-fold concentrated conditioned media from transiently transfected HEK293 cells, previously quantified with an α-V5/α-HA-based sandwich-ELISA for mIL-31-RFP-3V5-3HA.

4.1.2 Analysis of cell lines for IL-31 responsiveness

To analyze the inhibitory function of mIL-31-RFP a model system to validate its biological activity is needed. It is known, that undifferentiated normal human epidermal keratinocytes (NHEK) respond well to IFN-γ priming with increased IL-31R expression. Subsequent stimulation with IL-31 leads to phosphorylation of STAT3 (Heise et al., 2009). Therefore we first analyzed the IL-31 signaling capabilities of primary murine keratinocytes and PAM 212 cells, a murine keratinocyte cell line (Figure 8). To possibly enhance or induce IL-31R expression, both cell lines were additionally primed with 20 ng/ml IFN-γ for 24 hours prior to stimulation with IL-31. Stimulation with OSM served as a positive control for STAT3 phosphorylation.
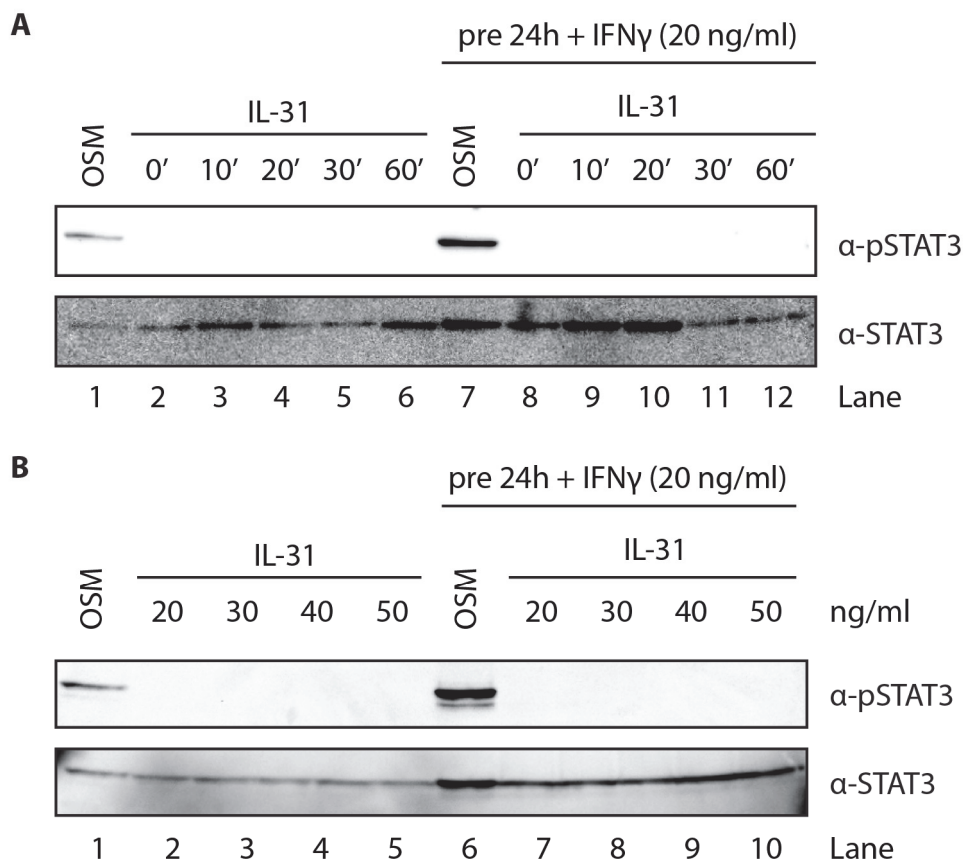
Figure 8: IL-31 responsiveness of primary murine keratinocytes and PAM212 cells
Western blot analysis of IL-31 induced STAT3 phosphorylation on whole cell lysates of (A) primary murine keratinocytes stimulated with 50 ng/ml IL-31 for 10 to 60 minutes or 5 ng/ml OSM for 20 minutes, or (B) PAM212 cells stimulated with different concentrations of IL-31 or 5 ng/ml OSM for 20 minutes.

Both, primary murine keratinocytes (Figure 8A) and PAM212 cells (Figure 8B), do not respond to IL-31 treatment with tyrosine phosphorylation of STAT3 (Figure 8A Lanes 2-6, Figure 8B Lanes 2-5). Even after priming with 20 ng/ml IFN-γ for 24h no STAT3 phosphorylation was detectable (Figure 8A Lanes 8-12, Figure 8B Lanes 7-10). In contrast, stimulation with OSM for 20 minutes resulted in STAT3 tyrosine phosphorylation (Figure 8A+B Lane 1), which was increased after IFN-γ priming (Figure 8A Lane 7, Figure 8B Lane 6).

4.1.3   Engineering of an IL-31 responsive cell system

To establish a reliable cellular system for subsequent analysis of IL-31 signaling and the inhibitory activity of mIL-31-RFP, mouse embryonic fibroblasts (MEF) cells, previously used to study the inhibitory function of mOSM-RFP and mLIF-RFP, were chosen. Wild-type (WT) MEF cells constitutively express the murine OSMR but lack mIL-31R and are therefore not capable of responding to IL-31 (Figure 9A). To obtain full-length mIL-31R the cDNA for isoform 4 of mIL-31R was amplified from pCMVSport6-mIL-31R via PCR and cloned into pcDNA3.1. In a second step exons 13-16 of the mIL-31R gene were amplified via PCR from genomic DNA, fused to isoform 4 (Figure 9B) and cloned into the pcDNA5FRT/TO vector to obtain pcDNA5FRT/TO-mIL-31-R encoding the full length receptor chain. This vector harbors a FLP recombination target (FRT) site which allows the Flp-recombinase-mediated integration of the vector into Flp-In host cell lines. Successful integration confers resistance to hygromycin B and allows selection of positive cells. To generate a stable mIL-31R cell line, MEF Flp-In cells were co-transfected through electroporation with pcDNA5FRT/TO-mIL-31R and pOG44, encoding Flp-In recombinase. Transfected cells were selected by addition of 200 μg/ml hygromycin B and seeded at low density to select single cell clones. Whole cell lysates of well-growing clones were analyzed for mIL-31R expression via Western blotting using an antibody targeting the N-terminal part of mIL-31R. All selected clones showed mIL31-R expression (Figure 9C).
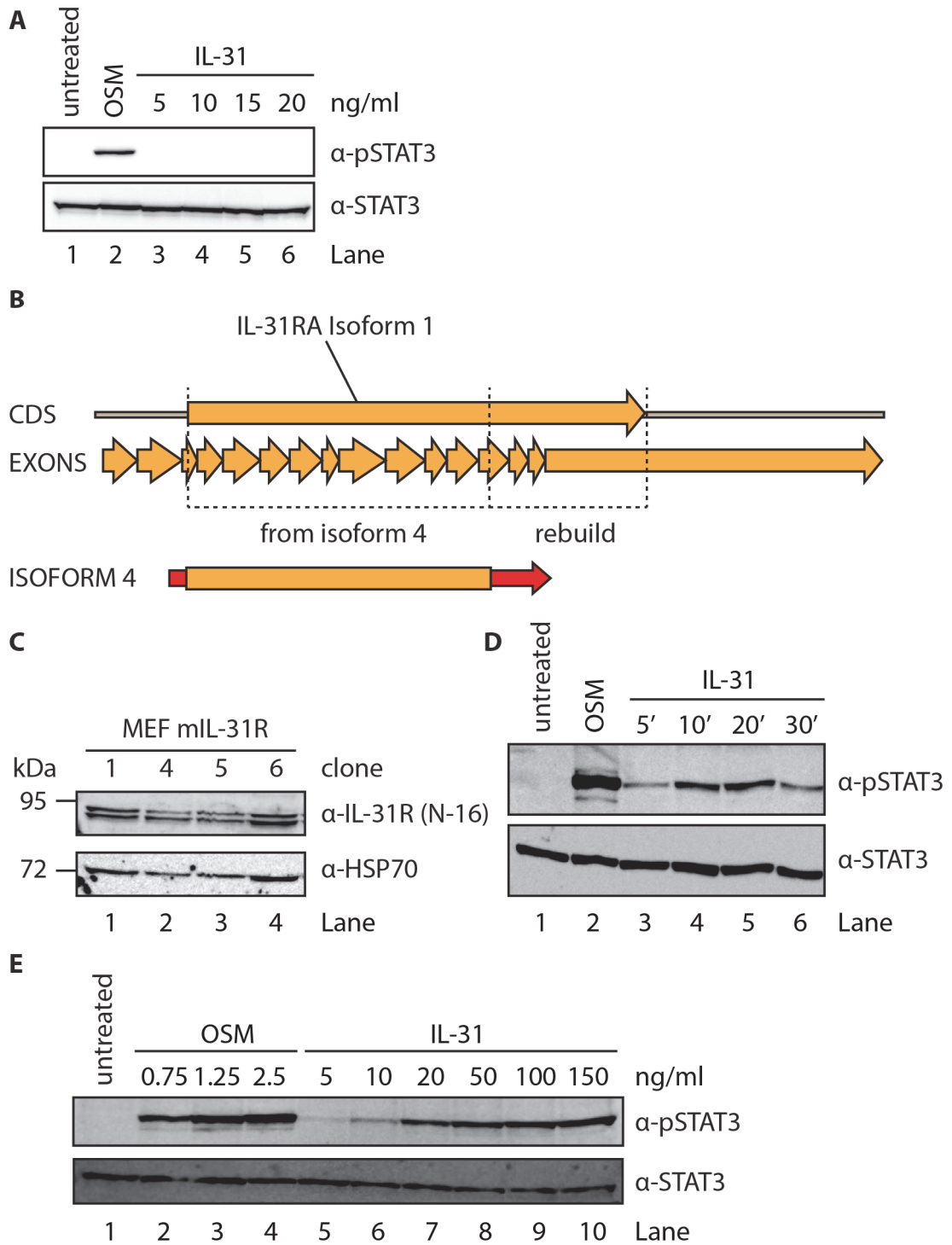
Figure 9: Rebuilding full-length mIL-31R cDNA from genomic DNA and generation of stably transfected MEF cells with IL-31 responsiveness (A) Western blot analysis of OSM- and IL-31 induced STAT3 phosphorylation on WT MEF cells. (B) Schematic view of the CDS of full-length mIL-31R and the corresponding exons needed to rebuild full-length mIL-31R. (C) Western blot analysis of whole cell lysates from stably transfected MEF mIL-31R clones. (D, E) Western blot analysis of (D) time- and (E) dose-dependent IL-31 induced STAT-3 phosphorylation on MEF mIL-31R clone 6.

For further experiments MEF mIL-31R clone 6 was selected. Time-dependent stimulation of MEF mIL-31R clone 6 with 20 ng/ml mIL-31 lead to tyrosine phosphorylated STAT3 with maximal phosphorylation at 20 minutes (Figure 9D Lanes 3-6). OSM stimulation served as a positive control (Figure 9D Lane 2). In comparison to OSM-induced STAT3 phosphorylation, where already low concentrations lead to strong STAT3 phosphorylation (Figure 9E Lanes 2-4), much higher concentrations of IL-31 are required to induce a similar degree of STAT3 phosphorylation (Figure 9E Lanes 5-10).

4.1.4   mIL-31-RFP inhibits IL-31 induced STAT3 phosphorylation

-	-	-	+	+	+	+	+	+	+	+	+	20' IL-31 | OSM
-	-	+	-	-	0.5	1	10	-	-	1	10	mIL-31-RFP (ratio)
-	+	-	-	+	-	-	-	-	+	-	-	control CM

												α-pSTAT3
												α-STAT3
1	2	3	4	5	6	7	8	9	10	11	12	Lane
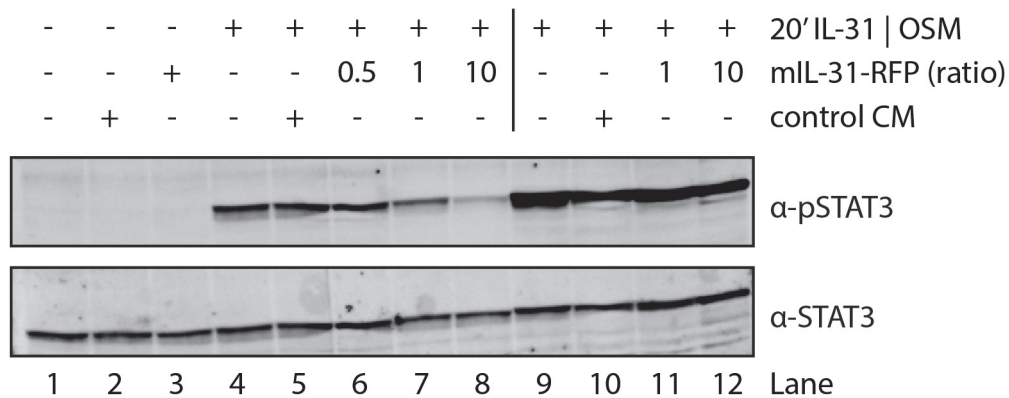
Figure 10: mIL-31-RFP inhibits IL-31 dependent STAT3 phosphorylation on MEF mIL-31R cells MEF mIL-31R cells were stimulated with 15 ng/ml of IL-31 or 2.5 ng/ml OSM for 20 min in the presence or absence of control or mIL-31-RFP conditioned media with corresponding molar ratios towards IL-31. Whole cell lysates were separated by SDS/PAGE and analyzed via Western blotting.

To test the IL-31 antagonizing activity of mIL-31-RFP, conditioned media of transiently transfected HEK293 cells were pre-incubated with IL-31 for 20 minutes to allow the cytokine to bind to the inhibitor. MEF mIL-31R cells were then stimulated for 20 minutes with either IL-31 alone or IL-31/mIL-31-RFP at different molar ratios. To assess the specificity of mIL-31-RFP cells were additionally stimulated with OSM and pre-incubated OSM/mIL-31RFP. After 20 minutes cells were lysed and STAT3 phosphorylation was analyzed. Stimulation with IL-31 alone or pre-incubated with control conditioned media from mock-transfected HEK293 cells lead to a prominent tyrosine phosphorylation of STAT3 (Figure 10 Lanes 4-5). Treatment of MEF cells with IL-31 pre-incubated with increased volumes of conditioned media containing mIL-31-RFP result-

ed in a reduction of tyrosine phosphorylation of STAT3 (Figure 10 Lanes 6-8). A 10-fold molar excess of mIL-31-RFP over IL-31 reduces STAT3 phosphorylation to nearly basal levels (Figure 10 Lane 8). mIL-31-RFP CM had no effect on OSM-induced STAT3-phosphorylation (Figure 10 Lanes 11-12). Thus mIL-31-RFP effectively and specifically inhibits IL-31 signaling.

4.1.5   Further modification of mIL-31-RFP

As conditioned media contain a plethora of different proteins, that possibly affect other signaling pathways, it was desired to clone a mIL-31-RFP variant that can be easily purified and therefore be used in a defined formulation. We chose to add six histidine residues to the C-terminus, which allow the purification of mIL-31-RFP through immobilized metal affinity chromatography (IMAC). Histidines bind to divalent metal ions like nickel around neutral pH, and can be eluted under specific buffer conditions. To clone this variant pcDNA5FRT/TO-mOSM-RFP-3V5-3HA-6his was digested with AgeI/KpnI to replace the gp130 CBM with the mIL-31R CBM from AgeI-/KpnI digested pcDNA3-mIL-31-RFP-3V5-3HA to obtain pcDNA5FRT/TO-mIL-31-RFP-3V5-3HA-6his.

4.1.6   Generation of mIL-31-RFP-3V5-3HA-his producing cell lines

The pcDNA5FRT/TO mIL-31-RFP-3V5-3HA-6his vector allows the Flp-In site-directed recombination of mIL-31-RFP-3V5-3HA-his into a Flp-In host cell line. Successful integration after stable transfection confers resistance to hygromycin B and allows selection of positive cells. To generate a stable mIL-31-RFP-3V5-3HA-his producer cell line HEK293 Flp-In/T-Rex cells were chosen. These cells contain a single stably integrated FRT site at a transcriptionally active genomic locus. In addition to the Flp-In site, these cells express the tet repressor (TR) protein, which binds a tetracycline responsive element (TRE) on the promoter under doxycycline (dox, a semisynthetic derivate of tetracycline) free conditions and thereby block transcription. Upon addition of doxycycline, the TR is released from the TRE, and the gene of interest will be expressed. Therefore, HEK293 Flp-In/T-Rex cells were co-transfected with pcDNA5FRT/TO-mIL-31-

RFP-3V5-3HA-his and pOG44, encoding Flp-In recombinase. After selection well-growing clones were then grown to 80% confluency, the medium exchanged to serum-free DMEM, and protein expression was induced with 200 ng/ml doxycycline. After 48h to 72h conditioned media were analyzed for mIL-31-RFP expression via Western blotting. All selected clones expressed mIL31-RFP (Figure 11). Clone 6 showed highest levels of mIL-31-RFP secretion. Already 48 hours following induction with doxycycline mIL-31-RFP secretion level of clone 6 (Figure 11 Lane 4) was higher than of clone 3 after 72h (Figure 11 Lane 2). For further protein production clone 6 was chosen.
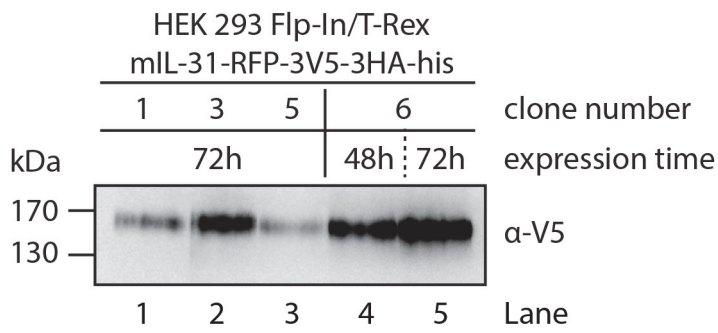
Figure 11: Analysis of conditioned media from HEK293 Flp-In/T-Rex mIL-31-RFP-3V5-3HA-his clones Western Blot analysis of conditioned media from stably transfected HEK293 mIL-31-RFP-3V5-3HA-6his clones under serum-free conditions. Protein expression was induced with 200 ng/ml doxycycline.

4.2 Modification of mIL-6-RFP for application *in vivo*

To transfer the previously described mIL-6-RFP (Wiesinger et al., 2009), consisting of the domains D1-D3 of murine gp130 and D1-D3 of murine soluble IL-6Rα, to an *in vivo* system, mIL-6-RFP was modified to facilitate serum detection, and sub-cloned into a tetracycline responsive vector system to regulate gene expression in specific tissues.

4.2.1 Modification for serum detection

For an increased sensitivity and the ability to specifically discriminate mIL-6-RFP from the soluble receptors sgp130 and sIL-6Rα present in the plasma of mice the V5/his tag was replaced with a 3V5-3HA tag module (Figure 12). This module is transferable to other proteins of interest and allows the use of α-HA/α-V5 based sandwich-ELISA to detect mIL-6-RFP in conditioned media or most importantly in plasma samples. The 3V5-3HA tag module was amplified from pcDNA3.1 AlbuminWT-3V5-3HA (Tenten et al., 2013) via PCR, subsequently digested with EcoRI/PmeI, and cloned into Eco-RI/PmeI digested pcDNA3 mIL-6-RFP-V5-his replacing V5-his with 3V5-3HA to create pcDNA3.1 mIL-6-RFP-3V5-3HA.
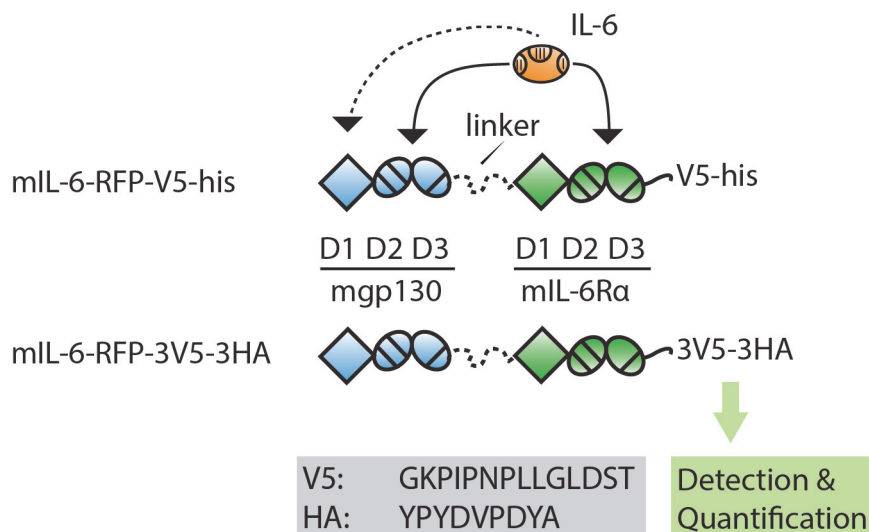
Figure 12: Schematic representation of mIL-6-RFP structure and exchange of tags Structural features of mIL-6-RFP. Arrows indicate binding of IL-6 to mIL-6-RFP with the dashed line indicating binding to a second mIL-6-RFP. Secretion of mIL-6-RFP-Fc is driven by the signal sequence of preprotrypsin (not shown).

A

-	+	-	-	+	-	-	-	-	-	-	-	control CM
-	-	-	-	-	1	5	7	-	-	-	-	mIL-6-RFP-V5-his
-	-	7	-	-	-	-	-	.2	1	5	7	mIL-6-RFP-3V5-3HA
-	-	-	+	+	+	+	+	+	+	+	+	IL-6 (10 ng/ml)

α-pSTAT3

α-STAT3

Lane 1 2 3 4 5 6 7 8 9 10 11 12

B

BSA Sepharose   IL-6 Sepharose

α-V5

Lane 1 2 3 4 5 6 7 8 9 10 11
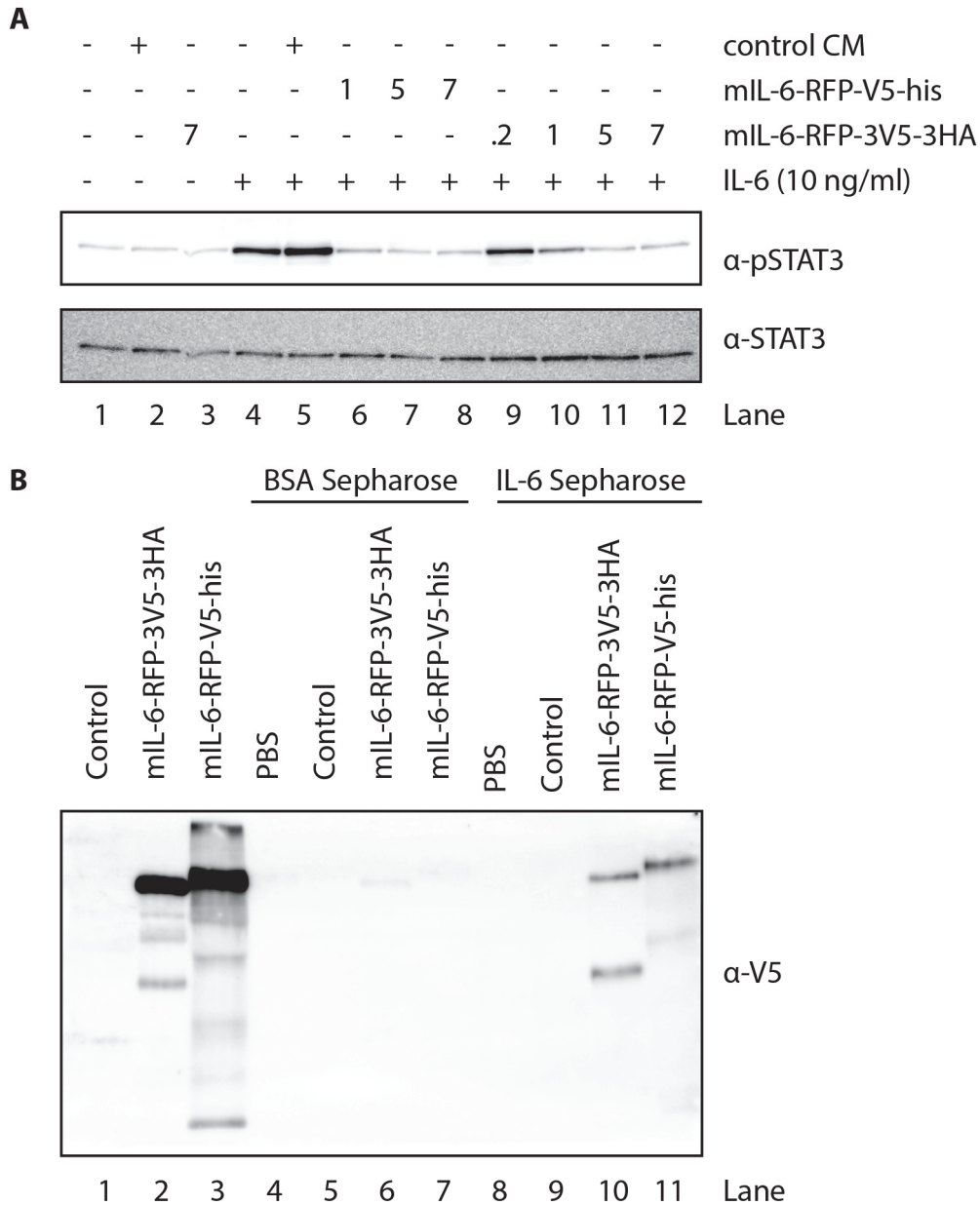
Figure 13: Biologic activity of mIL-6-RFP-3V5-3HA (A) Primary murine hepatocytes were stimulated for 20 min with IL-6 (20 ng/ml) preincubated with control conditioned media (CM), mIL-6-RFP-V5-his or mIL-6-RFP-3V5-3HA with molar ratios of mIL-6-RFP:IL-6 as indicated (x mol). Cellular lysates were analyzed by Western blotting for phosphorylation of STAT3 at Y705 (α-pSTAT3) and total STAT3 (α-STAT3) as a loading control. (B) Binding of either control, mIL-6-RFP-3V5-3HA or mIL-6-RFP-V5-his conditioned media to BSA-Sepharose or IL-6-Sepharose.

To address a possible influence of mIL-6-RFP tag exchange on biological activity, conditioned media of transiently transfected HEK293 cells were pre-incubated with IL-6 for 20 minutes to allow the fusion protein to bind to the cytokine. Primary murine hepatocytes were then stimulated for 20 minutes with either IL-6 alone or IL-6/mIL-6-RFP in different molar ratios. Conditioned media of mock-transfected HEK293 cells served as

control. Whole cell lysates were prepared, and STAT3 phosphorylation was analyzed.
The stimulation with IL-6 alone or pre-incubated with control conditioned media leads
to a prominent tyrosine phosphorylation of STAT3 (Figure 13A Lanes 4, 5). Treatment
with IL-6 pre-incubated with increased volumes of mIL-6-RFP conditioned media with
increasing molar ratios towards IL-6 resulted in a reduction of tyrosine phosphorylation
of STAT3 (Figure 13A Lanes 6-8, 9-12). Already at equal molar ratios both mIL-6-RFP-
V5-his and mIL-6-RFP-3V5-3HA reduce STAT3 phosphorylation to nearly basal levels
(Figure 13A Lanes 6, 10). To assess any influence on direct ligand binding, conditioned
media of both variants of mIL-6-RFP were precipitated with immobilized IL-6 (Figure
13B). The exchange of V5-his with 3V5-3HA did not alter binding of the fusion protein
to IL-6 covalently bound to Sepharose (Figure 13B Lanes 10, 11). Only weak unspecific
binding to BSA-Sepharose could be detected (Figure 13B Lanes 6, 7). PBS and condi-
tioned media from mock-transfected cells served as additional controls. Thus the ex-
change of the tag did not affect direct binding to IL-6 and IL-6 antagonizing activity of
mIL-6-RFP.

4.2.2 Cloning of the transgene expression vector
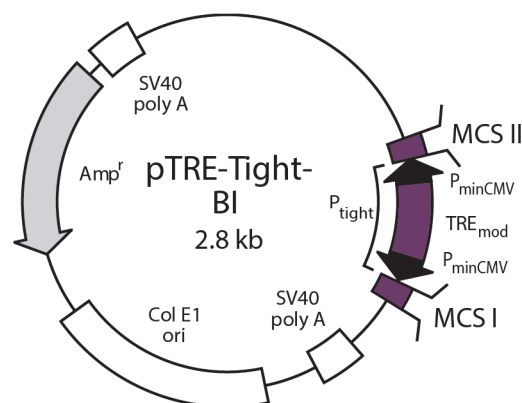
Figure 14: Transgene expression vector pTRE-Tight-BI TRE_{mod}: modified tet responsive
element; MCS: multiple cloning site; P_{minCMV}: two mini CMV promoters, which lack the en-
hancer that is part of the complete CMV promoter. Both genes inserted into MCS I and MCS II
will be responsive to the tTA and rtTA regulatory proteins in the Tet-Off and Tet-On systems,
respectively (Clontech, 2010).

The pTRE-Tight-BI vector system is a well-suited system to generate transgenic mice which express a gene of interest in a tissue-specific and inducible manner (Figure 14). It contains a modified Tet response element (TRE$_{mod}$) flanked by two minimal CMV promoters. This bidirectional Tet responsive promoter can be used to express either a reporter gene and one gene of interest, or two genes of interest. In both scenarios the Tet-responsive promoter element needs to be induced by a doxycycline-activated reverse tetracycline Trans-Activator (rtTA) to initiate gene expression. To sub-clone the fusion protein into this system, two fragments of mIL-6-RFP-3V5-3HA were amplified via PCR from pcDNA3.1 mIL-6-RFP-3V5-3HA – a gp130 portion and an IL-6R-3V5-3HA portion, which were subsequently digested with KpnI/AgeI and AgeI/NotI, respectively. The digested fragments were subjected to three-fragment-ligation into a KpnI/NotI digested pTRE-Tight-BI VEGF loxp/nlacZ vector replacing the VEGF loxp with mIL-6-RFP-3V5-3HA, and thereby creating pTRE-Tight-BI mIL-6-RFP-3V5-3HA/nlacZ. This vector contains the nlacZ reporter gene encoding for β-Galactosidase with a nuclear localization signal.

4.2.3 *In vitro* characterization of pTRE-Tight-BI mIL-6-RFP-3V5-3HA

HepG2 cells were transiently transfected with combinations of pUHRT 62-1, encoding rtTA-M2 (Urlinger et al., 2000), and pTRE-Tight-BI mIL-6-RFP-3V5-3HA plasmids. Cells were grown to 80% confluency, the medium was exchanged to serum-free medium, and cultured in the presence or absence of doxycycline for 48 h. Conditioned media were collected, whole cell lysates were prepared, separated by SDS-Page and analyzed for mIL-6-RFP-3V5-3HA expression and secretion via Western Blotting (Figure 15). mIL-6-RFP-3V5-3HA expression strictly depends on the presence of the rtTA, as transfection of mIL-6-RFP-3V5-3HA encoding plasmids alone (Figure 15 Lanes 4, 8) or in combination with doxycycline (Figure 15 Lanes 5, 9) did not lead to any detectable fusion protein. Co-transfection with the rtTA encoding plasmid already lead to low mIL-6-RFP expression even without addition of doxycycline albeit with low secretion levels (Figure 15 Lanes 6, 10). Addition of doxycycline to co-transfected cells strongly induces

mIL-6-RFP expression and secretion (Figure 15 Lane 7, 11) demonstrating functionality of the expression system.
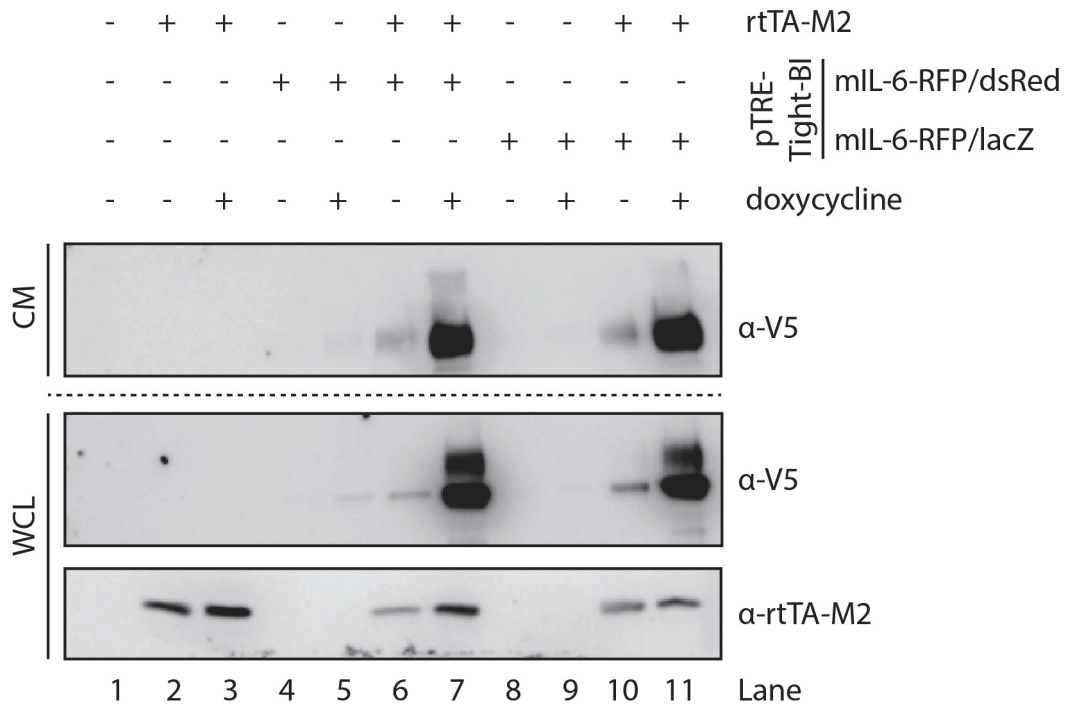
Figure 15: In vitro characterization of pTRE-Tight-BI mIL-6-RFP-3V5-3HA Western Blot analysis of mIL-6-RFP-3V5-3HA and rtTA-M2 expression from transiently transfected HepG2 cells in conditioned media (CM) and whole cell lysates (WCL).

4.2.4 Generation of mIL-6-RFP transgenic mice

For the generation of Tg(TRE:mIL-6-RFP) mice, pTRE-Tight-BI-lacZ-mIL-6-RFP-3V5-3HA vector DNA was linearized with PacI and injected into the pronucleus of fertilized eggs. The eggs were transferred into pseudo-pregnant recipient mice. To discriminate gp130 and IL-6Rα genes are located on chromosome 13 and chromosome 3 in the mouse genome, primer combinations that amplify either fused gp130/IL-6Rα fragments or vector elements like the bovine growth hormone poly adenylation signal (BGH pA) that are normally not encoded in the mouse genome, are ideally suited for genetic screening by PCR as they show no background signal (Figure 16A-C).
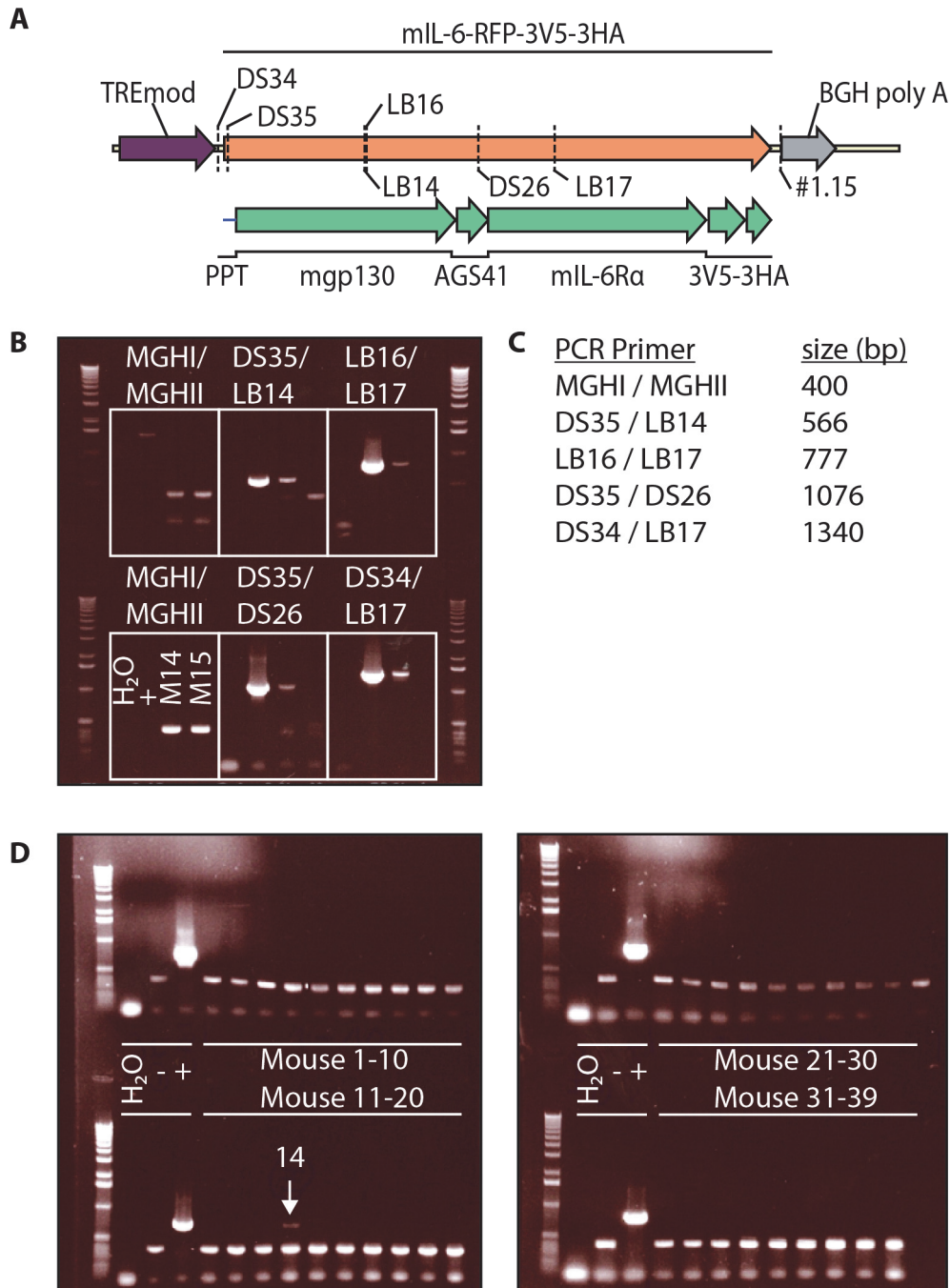
Figure 16: Genetic screening of mice following pronucleus injection (A) Schematic representation of TREmod promoter (purple) mIL-6-RFP gene (orange) including substructure (green) and bovine growth hormone polyadenylation signal (BGH poly A) (grey) and localization of sense (labels above mIL-6-RFP gene) and anti-sense (label below) primer binding sites (B) mIL-6-RFP transgene detection by PCR with genomic tail DNA as template with primer combinations depicted. (C) Expected PCR product size with the various primer combinations. (D) mIL-6-RFP transgene detection by PCR with genomic tail DNA as template with primer combination LB16/LB17. H_2O and random mice tail DNA (-) served as negative control, pTRE-Tight-BI-mIL-6-RFP plasmid (+) as positive control.

Genetic screening by PCR from tail biopsies of 39 newborn mice revealed 1 mice (Figure 16D) where the DNA has integrated into the host genome (2.6% transgene submission). This founder mouse was used for subsequent transgenic breeding to establish a homozygous mouse line Tg(TRE:mIL-6-RFP)1. A second pronucleus injection provided another transgene positive mouse that was used for the generation of a second transgenic mouse line Tg(TRE:mIL-6-RFP)2, where genetic screening by PCR from 7 newborn mice revealed 1 mice (data not shown) where the DNA has integrated into the host genome (14.3% transgene submission). As the expression of mIL-6-RFP strictly depends on the presence of rtTA, both founder lines need to be crossed with mice that express rtTA in desired tissues.

4.2.5   Double transgenic mice

In this study, we sought to develop a system to temporally control the onset of transgene expression in a systemic or localized manner with mice as a model system. For systemic expression of the fusion protein Tg(TRE:mIL-6-RFP-3V5-3HA) mice were crossed with Tg(LAP:rtTA) mice. The latter express rtTA under control of the liver activator protein (LAP) promoter, which is mainly active in the liver and to a lesser extent in the kidney (Hasan et al., 2001, Schonig et al., 2002, Gallagher et al., 2003). The double transgenic animals are expected to produce mIL-6-RFP in hepatocytes of the liver followed by secretion of the protein into the bloodstream for systemic availability. For a more localized expression and specific use in renal disease models Tg(TRE:mIL-6-RFP-3V5-3HA) mice were crossed with Tg(Pod:rtTA) mice, where rtTA expression is under the control of a promoter, consisting of a 2.5-kb fragment of the human podocin gene *NPHS2*, which is mainly active in podocytes of the kidney (Shigehara et al., 2003). Each founder animal was crossed with rtTA mouse strains to establish different transgenic lines. For all litters PCR was used for identification of transgenic mice.
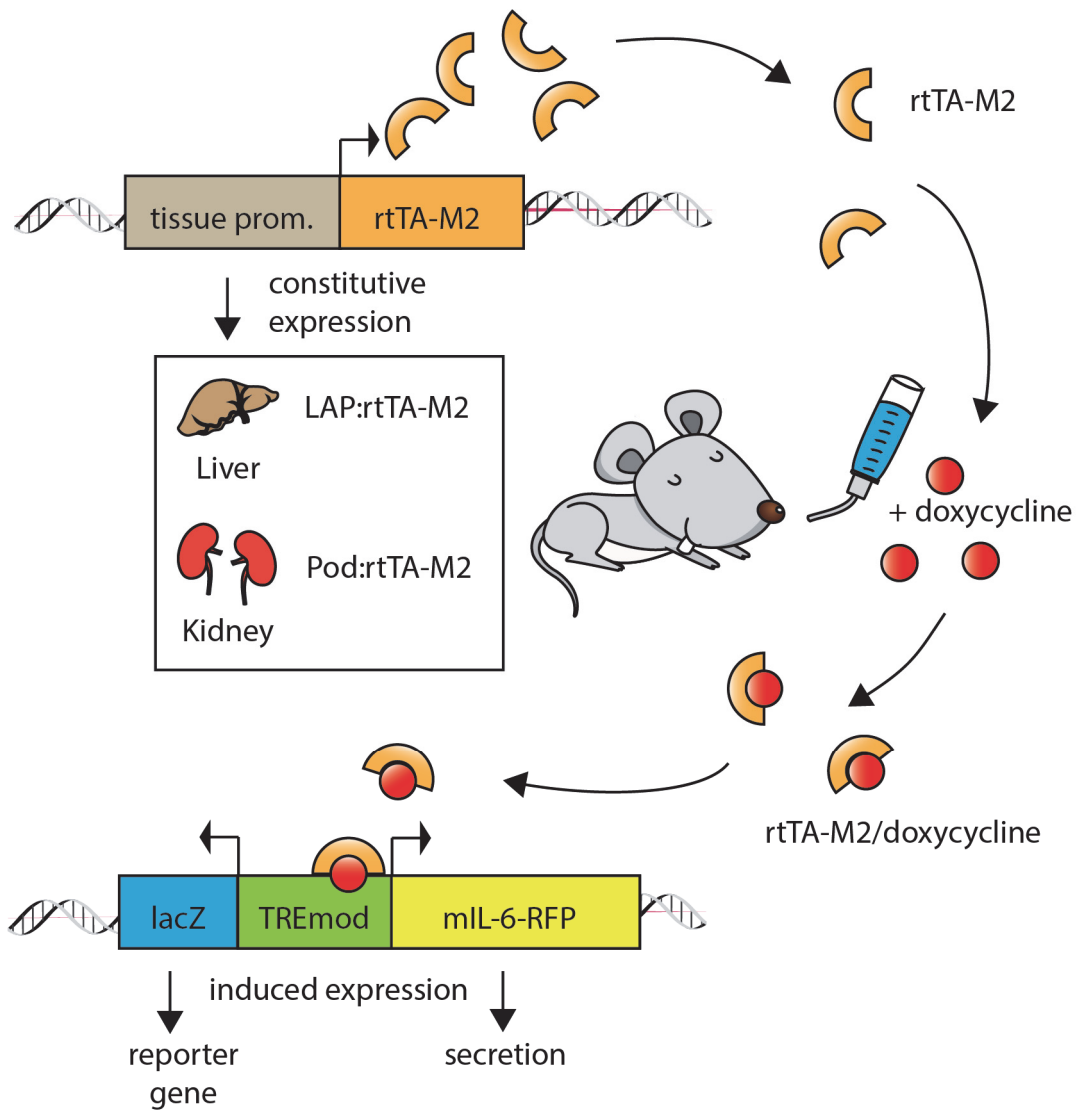
Figure 17: Tetracycline responsive system for mIL-6-RFP expression in vivo A schematic diagram showing the principle of induction of mIL-6-RFP and lacZ expression from genomically integrated pTRE-Tight-BI expression cassette in double transgenic mice. rtTA-M2, constitutively expressed in corresponding tissues governed by the activity of either LAP- or Podocin-promoter, binds after complexing with doxycycline administered by drinking water to TREmod element, and induces the expression of both lacZ and mIL-6-RFP.

4.2.6 Analysis of Tg(LAP:rtTA/TRE:mIL-6-RFP) mice
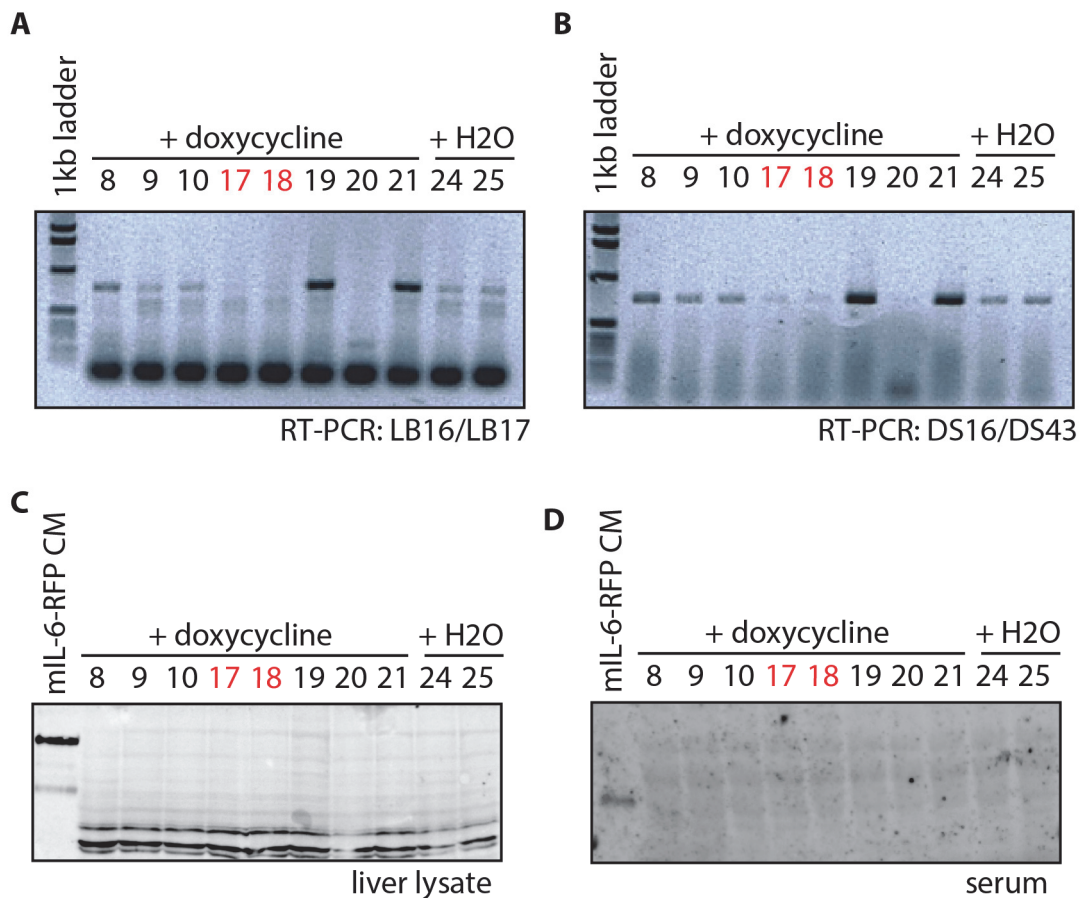
Figure 18: Analysis of Tg(TRE:mIL-6-RFP, LAP:rtTA)1F1 mice Transgene negative mice are marked in red (A) RT-PCR analysis for mIL-6-RFP mRNA from liver RNA from mice treated for 14 days either with doxycycline or H_2O. (B) RT-PCR analysis for β-Galactosidase mRNA from liver RNA samples from mice treated for 14 days either with doxycycline or H_2O. (C) Western Blot analysis of liver lysates separated by SDS-Page and stained with α-V5 antibody. (D) Western Blot analysis of mouse serum separated by SDS-Page and stained with α-V5 antibody.

In double transgenic mice Tg(TRE:mIL-6-RFP-3V5-3HA, LAP:rtTA) both the fusion protein and β-Galactosidase are expressed under the transcriptional control of the rtTA controlled promoter. rtTA expression is driven through LAP promoter, which is mostly hepatocyte-specific, but also drives expression in proximal tubular cells of the kidney to a lesser extent. Since hepatocytes exhibit a high synthetic capacity, mIL-6-RFP should be secreted into the serum in high amounts. Therefore RNA, liver lysates and serum of doxycycline treated mice were examined for mIL-6-RFP and rtTA expression. Although there was mRNA of mIL-6-RFP-3V5-3HA (Figure 18A) and β-Galactosidase (Figure

18B) detectable, mIL-6-RFP protein could be detected neither in liver lysates (Figure 18C) nor in serum (Figure 18D) of any Tg(TRE:mIL-6-RFP-3V5-3HA, LAP:rtTA) mice tested.

X-Gal   IF: GFP
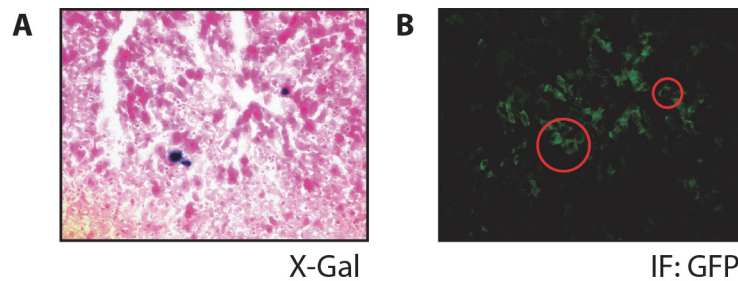
Figure 19: Hydrodynamic co-transfection of pTRE-Tight-BI mIL-6-RFP + nlacZ & pEGFP into doxycycline treated Tg(LAP:rtTA) mice (A) X-Gal staining and (B) Immunofluorescence from serial sections of liver tissue

As it was shown in the *in vitro* characterization of the vector system (Chapter 4.2.3) the expression strictly depends on rtTA expression. Therefore we hydrodynamically co-transfected Tg(LAP:rtTA) mice with pTRE-Tight-BI-mIL-6-RFP-3V5-3HA/nlacZ and pEGFP-N1. In serial sections of the liver only low and mosaicism-like expression of β-Galactosidase is detectable (Figure 19A), whereas GFP is strongly expressed throughout the liver (Figure 19B).

4.2.7   Analysis of Tg(Pod:rtTA/TRE:mIL-6-RFP) mice

A

X-Gal Line 998 male (2390/12)

B
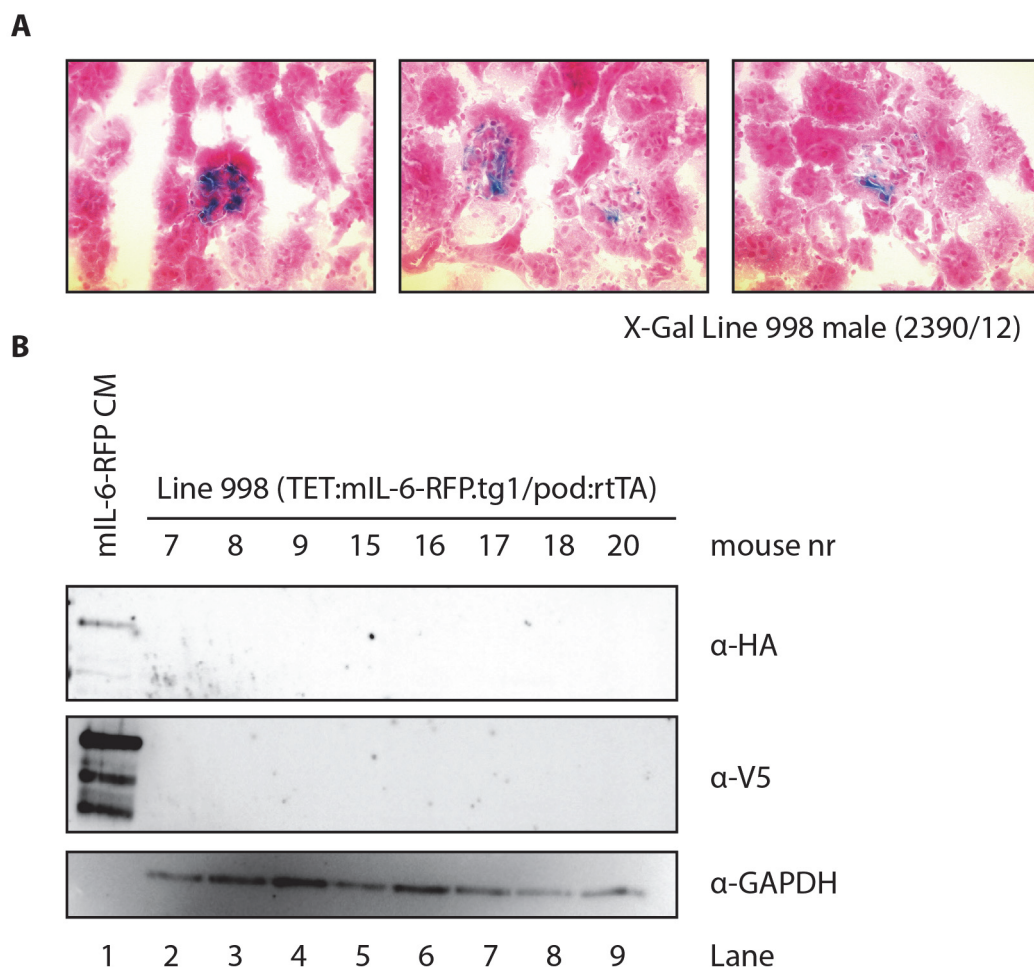
Figure 20: Analysis of Tg(TET:mIL-6-RFP.tg1/pod:rtTA)2F1 mice (A) β-Galactosidase expression in the kidney sections of Tg(TET:mIL-6-RFP.tg1/pod:rtTA) mice. Doxycycline (2 mg/ml) was administered in drinking water for 14 days. (B) Western Blot analysis of whole kidney lysates from doxycycline treated mice.

In Tg(TRE:mIL-6-RFP-3V5-3HA, Pod:rtTA) mice transgene expression is controlled by podocyte specific rtTA expression. Therefore tissue sections and kidney lysates of doxycycline-treated mice were examined for β-Galactosidase or mIL-6-RFP expression, respectively. X-Gal staining showed an expression pattern of β-Galactosidase, that was localized predominantly to the periphery of glomeruli (Figure 20A). There was no mIL-6-RFP detectable in whole kidney lysates (Figure 20B) of any Tg(TRE:mIL-6-RFP-3V5-3HA, Pod:rtTA) mice tested.

4.3 Re-Engineering of mIL-6-RFP-3V5-3HA

As the initial approach to establish mIL-6-RFP as an *in vivo* research tool in a transgenic mouse model was not successful due to the lack of any detectable mIL-6-RFP protein in either serum or tissues, another approach was considered. Therefore we thought to further modify mIL-6-RFP by the addition of the constant fragment of an antibody to allow protein purification through affinity chromatography and to improve its pharmacokinetics. To enhance mammalian expression the cDNA was codon optimized and introduced into expression vectors suitable for transient or stable expression and finally, as receptor fusion proteins are encoded by a single gene, into vectors suitable for gene transfer approaches.

4.3.1 Generation of mIL-6-RFP-Fc

mIL-6-RFP-Fc-3V5-3HA (Figure 21A) was generated by adding an engineered mIgG2a Fc-fragment (hinge-CH2-CH3) followed by a transferable 3V5-3HA tag for detection and quantification to the C-terminus of our previously reported receptor fusion protein mIL-6-RFP for the inhibition of human, rat and murine IL-6. The Fc region of mouse IgG2a normally mediates high antibody-dependent cellular cytotoxicity (ADCC) and complement-dependent cytotoxicity (CDC). To reduce its cytotoxicity, mIgG2a-Fc was engineered by mutating the amino acids that are critical for Fcγ receptor (FcγR) and C1Q complex binding of the complement system (Steurer et al., 1995). The Fc fragment facilitates purification through protein A/G affinity chromatography and is expected to increase serum half-life of the recombinant protein through interaction with the neonatal Fc receptor (FcRn) (Kuo and Aveson, 2011). Moreover, the Fc-fragment enforces dimerization of the fusion protein through disulfide bond formation increasing its avidity towards IL-6. The dimer is perfectly tailored for adapting the conformation of the hexameric IL-6 receptor complex required for high-affinity IL-6-binding (Figure 21B).
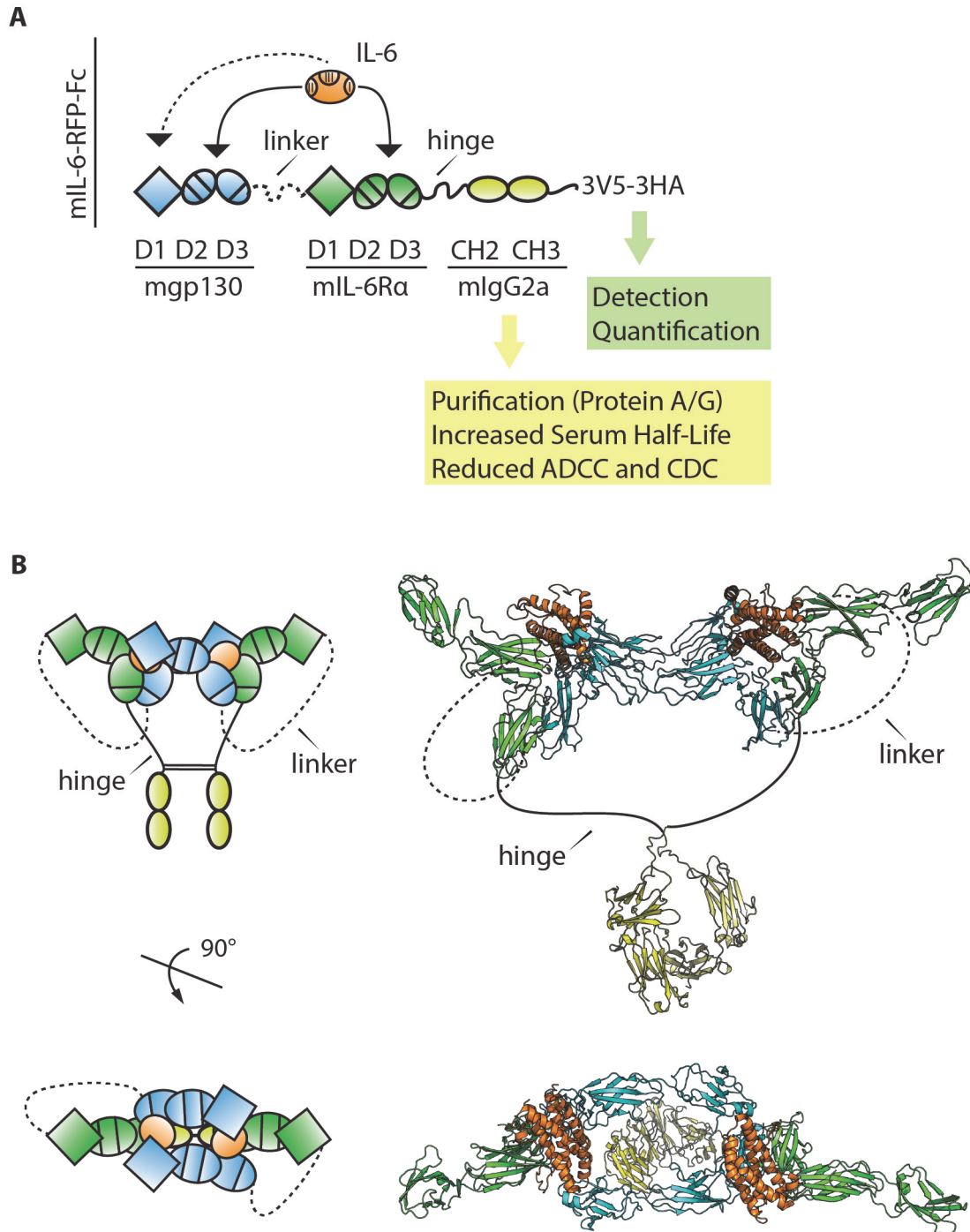
Figure 21: Design, characterization and structural model of mIL-6-RFP-Fc (A) Schematic representation of the structural features of mIL-6-RFP-Fc. Arrows indicate binding of IL-6 to mIL-6-RFP-Fc with the dashed line indicating binding to a second mIL-6-RFP-Fc resulting in the formation of a complex in analogy to the hexameric IL-6 receptor complex (shown in B). Secretion of mIL-6-RFP-Fc is driven by the signal sequence of preprotrypsin (not shown) (B) Schematic representation (left panel) and structural model (right panel) of the $(IL-6)_2(mIL-6-RFP-Fc)_2$ inhibitory complex. The structural model is based on the crystal structures of the human hexameric IL-6 signaling complex (PDB: 1P9M), human IL-6Rα (PDB: 1N26), and the hinge region, CH2 domain and CH3 domain of murine IgG2A (PDB: 1IGT).

4.3.2   Codon Optimization of mIL-6-RFP-Fc

The cDNA encoding mIL-6-RFP-Fc was optimized for gene delivery in mice by replac-
ing 32% of the codons for those being preferred in mice (Figure 22). In addition, poten-
tial internal inhibitory motifs, AT-rich instability motifs, repeat sequences, internal pol-
yadenylation sites, as well as splice donor and acceptor sites were eliminated. The fully
synthesized cDNA coding for mIL-6-RFP-Fc was flanked with restriction sites to facili-
tate sub-cloning into the pcDNA3, pcDNA5 and pTZ18R-PEPCK vector systems for
transient, stable expression and gene transfer approaches, respectively. The transfer vec-
tor pMA-mIL-6-RFP-Fc-3V5-3HA containing the optimized mIL-6-RFP-Fc was syn-
thesized by GeneArt (Regensburg).
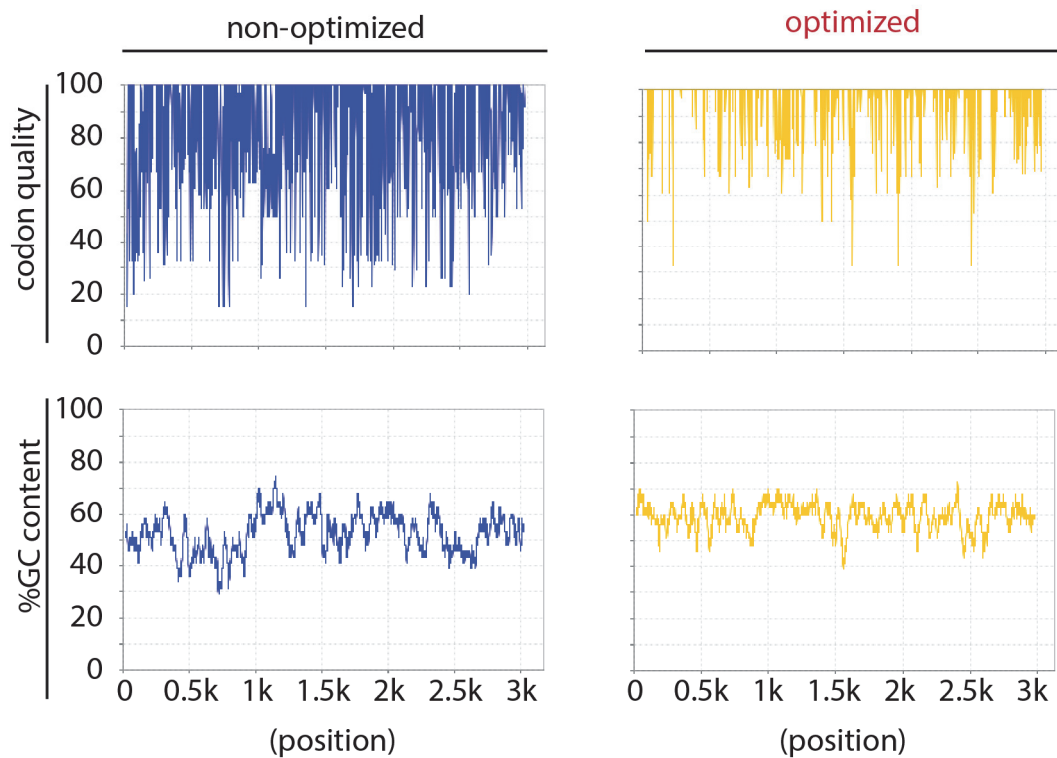
Figure 22: Codon quality and %GC content plot Comparison of codon quality and %GC
content of the non-optimized vs. optimized mIL-6-RFP-Fc cDNA sequence.

4.3.3   Cloning of expression vectors

The optimized cDNA for mIL-6-RFP-Fc was excised from the transfer vector pMA-
mIL-6-RFP-Fc-3V5-3HA with HindIII/NotI and transferred through direct restriction

cloning into HindIII/NotI digested pcDNA3 and pcDNA5/FRT/TO vectors to generate the expression vectors pcDNA3-mIL-6-RFP-Fc-3V5-3HA, pcDNA5/FRT/TO-mIL-6-RFP-Fc-3V5-3HA, respectively. For gene delivery approaches we chose to adapt a vector system that was previously described to successfully overexpress sgp130-Fc, a fusion protein specifically targeting IL-6 trans-signaling, in transgenic mouse models (Rabe et al., 2008). The optimized mIL-6-RFP-Fc cDNA was excised from pMA-mIL-6-RFP-Fc-3V5-3HA by XhoI digestion and cloned into XhoI digested pTZ-PEPCK-bglob.intron-sgp130-Fc-b.glob.polyA vector thereby creating PTZ-PEPCK-b.glob.intron-mIL-6-RFP-Fc-3V5-3HA-b.glob.polyA.

4.3.4 Comparative expression of optimized mIL-6-RFP-Fc *in vitro*
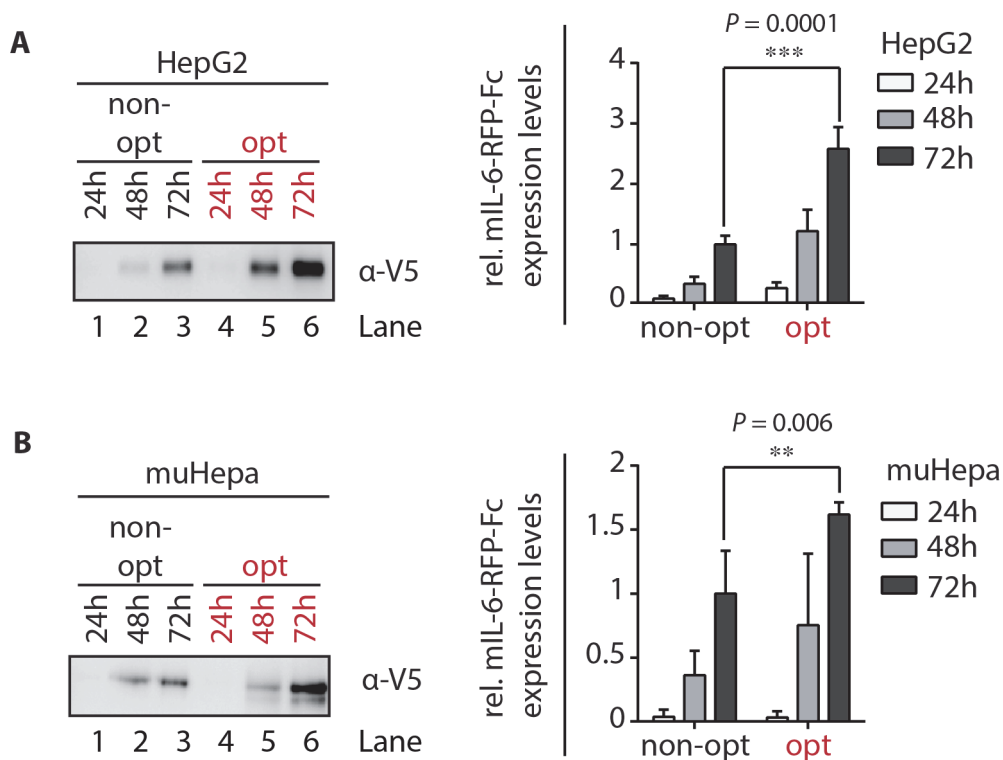
Figure 23: Comparative transient expression of mIL-6-RFP-Fc Western blot analysis (left panel) of equal volumes of conditioned media harvested from (A) HepG2 and (B) muHepa cells transiently transfected with optimized (opt) or non-optimized (non-opt) mIL-6-RFP-Fc expression plasmids after the indicated time points using an antibody directed against the V5-epitope (α-V5). Bar charts show relative expression of mIL-6-RFP-Fc from densitometric analyses of Western blots. For comparison, densitometric levels from the secretion of non-opt mIL-6-RFP-Fc at 72 hours were set to 1. Results of five independent experiments are presented (means ± SD).

To evaluate the effects of codon optimization on protein expression levels of mIL-6-RFP-Fc, murine hepatocarcinoma cells (muHepa) and HepG2 cells were transiently transfected with expression vectors encoding for either the non-optimized or optimized cDNA for mIL-6-RFP-Fc. Over time increasing amounts of the recombinant protein were detected in conditioned media (Figure 23 A + B). Compared to the original cDNA the optimized cDNA yielded an about 2.5-fold increase in protein secretion in HepG2 over 72 hours (Figure 23A Lane 3 vs. 6) and a 1.6-fold increase in muHepa cells over 72 hours (Figure 23B Lane 3 vs. 6).

4.3.5   Generation of single clone stable producer cell lines
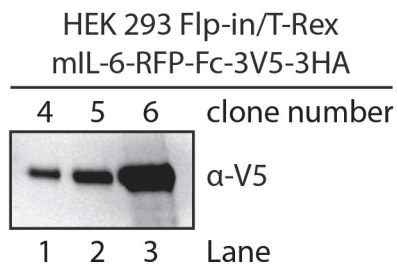
Figure 24: mIL-6-RFP-Fc expression in stably transfected HEK 293 Flp-In/T-Rex single cell clones Western Blot analysis of conditioned media from stably transfected HEK 293 Flp-In/T-Rex clones. Equal volumes of conditioned media harvested from different clones were loaded and separated by SDS-Page.

For continuous protein production a stable producer cell line was to be generated. We chose again the HEK293 Flp-In/T-Rex cell system for targeted integration of the gene of interest together with the ability to induce protein expression. HEK293 Flp-In/T-Rex cells were co-transfected with pcDNA5/FRT/TO-mIL-6-RFP-Fc-3V5-3HA and pOG44. Transfected cells were selected by addition of 200 µg/ml hygromycin B and seeded at low density to select single cell clones. Well-growing clones were then grown to 80% confluency, the medium exchanged to serum-free DMEM, and protein expression was induced with 200 ng/ml doxycycline. After 72h conditioned media were analyzed for mIL-6-RFP-Fc expression via Western Blotting. All selected clones showed expression of the receptor fusion protein (Figure 24). Clone 6 showed the highest secretion levels

for mIL-6-RFP-Fc (Figure 24 Lane 3) and was therefore chosen for continuous protein production.

4.3.6 mIL-6-RFP-Fc purification and characterization
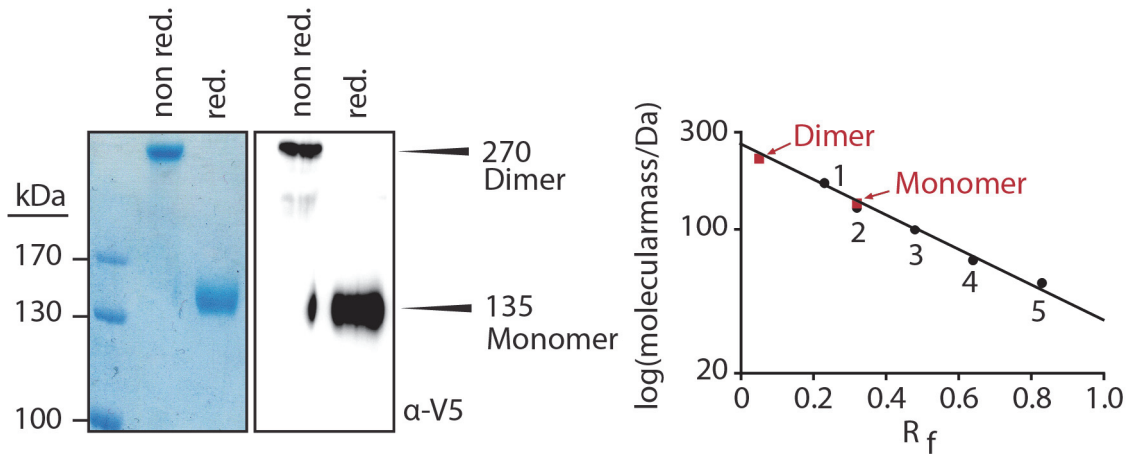
Figure 25: Purified mIL-6-RFP-Fc and Rf-value based calculation of molecular mass
Purified mIL-6-RFP-Fc was analyzed by 7.5% SDS/PAGE. Purity and identity was determined by staining with Coomassie brilliant blue and Western blotting, respectively, under non-reducing and reducing conditions. The molecular mass of mIL-6-RFP-Fc was determined by calculating the R_f of five marker proteins and inserting the R_f of mIL-6-RFP-Fc monomer and dimer into the equation for the linear regression.

To calculate the molar mass of mIL-6-RFP-Fc in its monomeric and dimeric form purified mIL-6-RFP-Fc was analyzed by SDS-PAGE under non-reducing and reducing conditions, then stained with Coomassie and destained to visualize the protein bands of the marker and purified mIL-6-RFP-Fc proteins (Figure 25 left panel). The gel was analyzed to obtain the R_f values for each band. A plot of log MW versus R_f was generated (Figure 25 right panel). Apparent molecular masses of 270 kDa for the dimer and 135 kDa for the monomer have been calculated.

4.3.7 Inhibitory activity *in vitro*
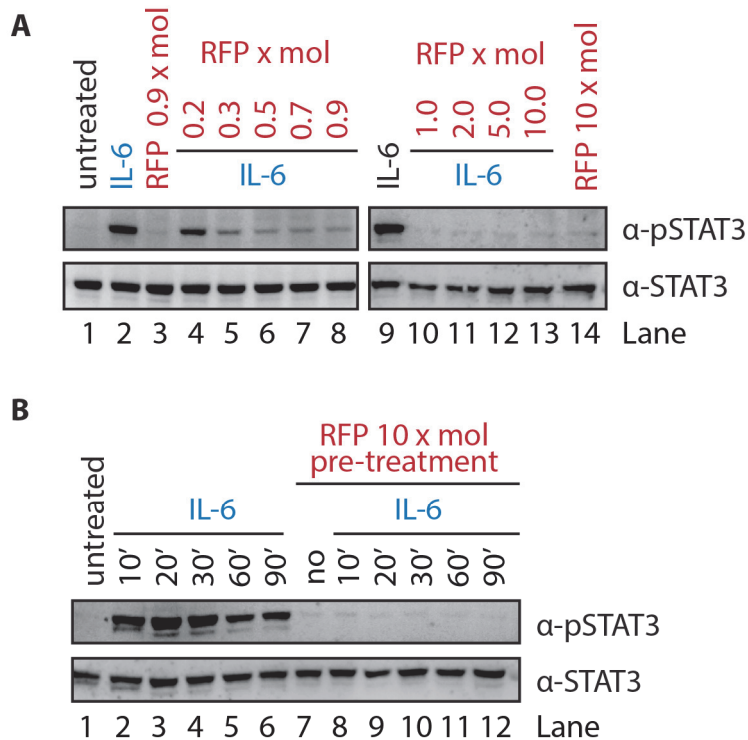
Figure 26: mIL-6-RFP-Fc mediated inhibition of IL-6 induced STAT3 phosphorylation
(A) muHepa cells were stimulated for 20 min with IL-6 (20 ng/ml), mIL-6-RFP-Fc (RFP) or IL-6 (20 ng/ml) preincubated with mIL-6-RFP-Fc (RFP) at concentrations ranging from 22.25 to 1335 ng/ml for 15 min corresponding to molar ratios of mIL-6-RFP-Fc:IL-6 as indicated (x mol). Cellular lysates were analyzed by Western blotting for phosphorylation of STAT3 at Y705 (α-pSTAT3) and total STAT3 (α-STAT3) as a loading control. (B) muHepa cells were pretreated for 120 min with a 10-fold molar excess of mIL-6-RFP-Fc (1335 ng/ml) and subsequently stimulated with IL-6 (20 ng/ml) for 20 min. Phosphorylation of STAT3 was analyzed as described in A.

To characterize the bioactivity of mIL-6-RFP-Fc, muHepa cells were stimulated with mIL-6 that had been pre-incubated with purified mIL-6-RFP-Fc in molar ratios ranging from 0.2 to 10 (Figure 26A). As a read-out of IL-6 activity tyrosine phosphorylation of STAT3 was analyzed. Complete inhibition of IL-6 was already achieved at about equimolar concentrations of mIL-6-RFP-Fc and IL-6 (Figure 26A Lane 10). In the next experiment, mIL-6-RFP-Fc and IL-6 were not pre-incubated, but cells were pretreated with mIL-6-RFP-Fc (Figure 26B). Subsequent addition of IL-6 did not elicit phosphorylation of STAT3 over a prolonged period of time indicating that even in direct competi-

tion with the cell surface receptors mIL-6-RFP-Fc neutralizes IL-6 immediately and completely.
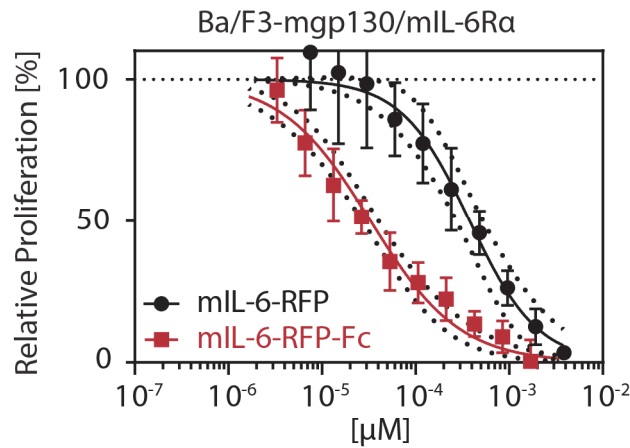
Figure 27: mIL-6-RFP-Fc inhibits IL-6 dependent cell proliferation Equal numbers of Ba/F3-mgp130/mIL-6Rα cells were incubated with a constant amount of IL-6 (37 pM) and serial 2-fold dilutions of either mIL-6-RFP-Fc (starting concentration 3.9 nM) or mIL-6-RFP (starting concentration 3.4 nM). After 60 h of incubation, viable cells were quantified using a colorimetric XTT assay. Data shown are means ± SD (n=6).

After showing that mIL-6-RFP-Fc inhibits IL-6 dependent STAT3 phosphorylation in muHepa cells, we wanted to compare the inhibitory activity of mIL-6-RFP-Fc to the previously described mIL-6-RFP. We chose the murine pre-B-cell line Ba/F3, which does not express murine gp130 and murine IL-6Rα, and only proliferates in the presence of IL-3. By stable transfection with cDNA encoding mgp130 and mIL-6Rα we generated a Ba/F3-mgp130/mIL-6Rα cell line that proliferates IL-6 dependently, and is therefore well suited to compare the inhibitory activities of mIL-6-RFP and mIL-6-RFP-Fc. IL-6-dependent proliferation of Ba/F3-mgp130/mIL-6Rα cells was inhibited in a concentration-dependent manner by both inhibitors. However, mIL-6-RFP- Fc's inhibitory activity was one order of magnitude higher compared to the non-optimized version mIL-6-RFP (Figure 27; IC50 mIL-6-RFP-Fc: 3.3×10^{-5} µM, IC50 mIL-6-RFP: 3.8×10^{-4} µM) which is in agreement with the higher avidity of mIL-6-RFP-Fc as proposed in our model (Figure 21B) and with the increase of the activity of the IL-6 trans-signaling inhibitor sgp130 upon Fc fusion (Jostock et al., 2001).

4.4   *In vivo* application of mIL-6-RFP-Fc

The continuous mIL-6-RFP-Fc production with subsequent purification through affinity chromatography allows the use of recombinant protein for determination of its pharmacokinetics in animals and additionally the evaluation of its therapeutic potential *in vivo*.

4.4.1   Pharmacokinetics of recombinant mIL-6-RFP-Fc
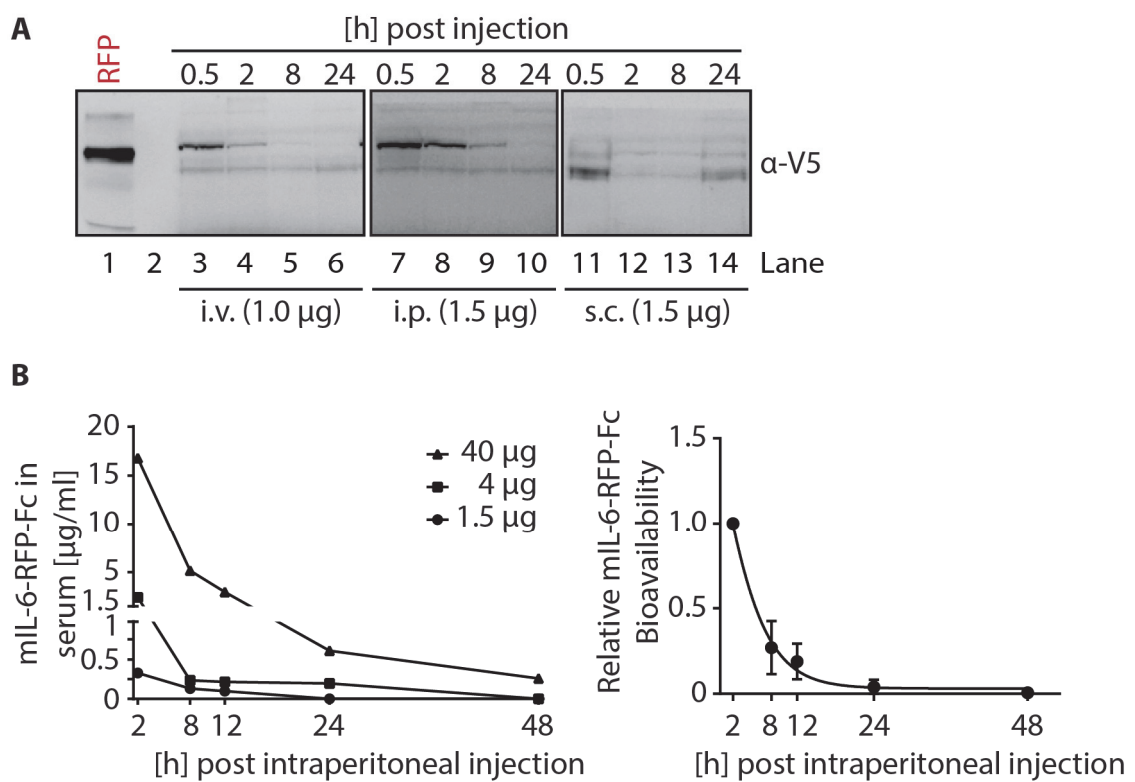
Figure 28: Pharmacokinetics of recombinant mIL-6-RFP-Fc (A) Western blot analysis of mIL-6-RFP-Fc in mouse serum samples (2 µl serum/lane) obtained at the indicated time points following administration of indicated amounts of mIL-6-RFP-Fc either intravenously (i.v.), intraperitoneally (i.p.) or subcutaneously (s.c.) using an antibody directed against the V5-epitope (α-V5). (B) Left: mIL-6-RFP-Fc serum concentrations over time following intraperitoneal administration of the indicated amounts of recombinant protein as determined by an ELISA based on capture and detection of the HA- and V5-epitopes, respectively. Depicted are individual animals. Right: Statistical evaluation by normalization of each animals' values on its 2 h serum level (n=3). Calculated time constant: $t_{1/2}$ = 3.5 h.

To establish its bioavailability in a mammalian system, mIL-6-RFP-Fc was administered to mice 1 µg intravenously (i.v.), 1.5 µg intraperitoneally (i.p.) and 1.5 µg subcutaneous-

ly (s.c.) and recovered via blood sampling. For i.v. injection a lower amount was chosen because a higher recovery was expected upon direct administration to the blood stream.. As determined by Western blot analysis of serum samples (Figure 28A), the i.v. and i.p. routes gave rise to the highest systemic levels with the latter resulting in prolonged serum detectability with no signs of major degradation of the fusion protein (Figure 28A Lane 3-4; Lane 7-9). Subcutaneous application did not result in significant plasma levels (Figure 28A Lane 11-14), which might be explained by the known slow-onset and prolonged pharmacokinetics of this route. It should be noted that a non-optimized, non-Fc-containing variant of mIL-6-RFP (Wiesinger et al., 2009) was successfully applied s.c. for local IL-6 antagonism in a cutaneous tumor model (Schroeder et al., 2014). To further characterize the pharmacokinetics of mIL-6-RFP-Fc, different amounts were injected i.p. followed by quantitative serum ELISA directed against the epitope tags. At the highest amount (40 μg) applied in one single administration, mIL-6-RFP-Fc could be detected in serum for up to 48 h (Figure 28B left diagram). Normalization of the different animals' serum mIL-6-RFP-Fc levels on their respective 2 h value, allowed for statistical analysis and determination of a time constant ($t_{1/2}$ = 3.5 h) across the amounts of protein spiked (Figure 28B, right diagram). The observed half-life is identical with the initial clearing determined for an IL-2-Fc fusion protein harbouring the same Fc-fragment (mIgG2a) (Zheng et al., 1999).

4.4.2   mIL-6-RFP-Fc inhibits IL-6-induced STAT3 and ERK phosphorylation *in vivo*
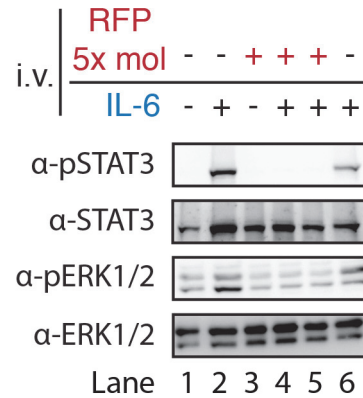
Figure 29: Coincubation of IL-6 with mIL-6-RFP-Fc inhibits IL-6-dependent STAT3 and ERK phosphorylation in vivo Western blot analysis of mouse liver lysates prepared 15 min following intravenous administration of either PBS, IL-6 (100 ng) or preincubated IL-6/mIL-6-RFP-Fc-complexes (100 ng/3.5 µg, corresponding to a molar ratio 1:5, incubation for 30 min).

To determine the efficacy of mIL-6-RFP-Fc in mice we established a model of IL-6-stimulated STAT3 and ERK1/2 phosphorylation in liver and kidney tissues. In analogy to the *in vitro* experiments, mIL-6-RFP-Fc was either pre-incubated with IL-6 (Figure 29) or the proteins were administered sequentially (Figure 30). In both scenarios mIL-6-RFP-Fc significantly reduced IL-6 downstream signaling. Pretreatment with 40 µg (70x molar excess) of mIL-6-RFP-Fc i.p. for 45 min attenuated STAT3 and ERK1/2 phosphorylation by 12 and 63 % in the liver and by 80 and 50 % in the kidney, respectively (Figure 30). Collectively, these data established mIL-6-RFP-Fc as a potent therapeutic agent for the inhibition of IL-6 *in vitro* and *in vivo*. Phosphorylation was assessed by the ratio of phosphorylated versus total STAT3 or ERK1/2 (Figure 30). Variations of total STAT3 levels might be due to the fact that activated STAT3 induces its own gene expression (Hutchins et al., 2013, Nagayama et al., 2014).
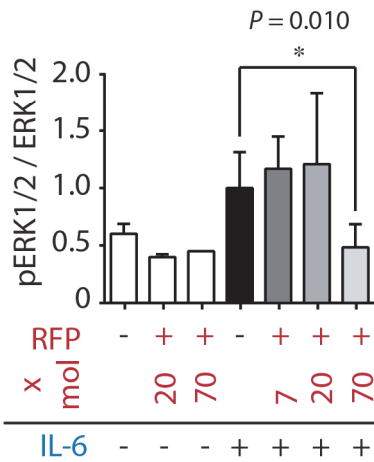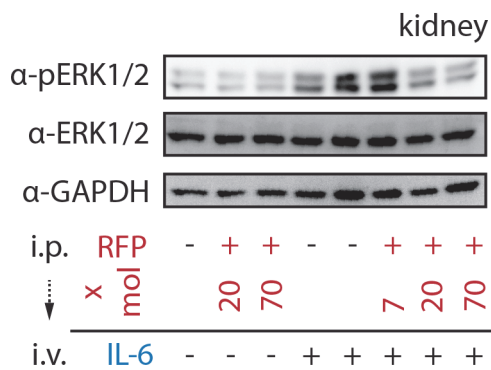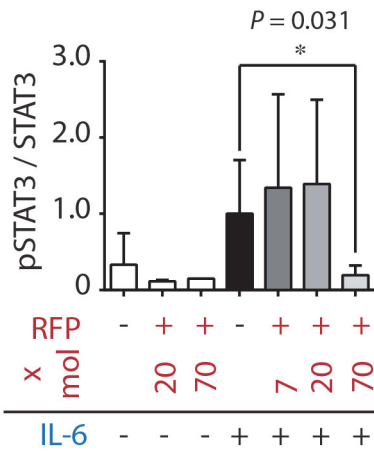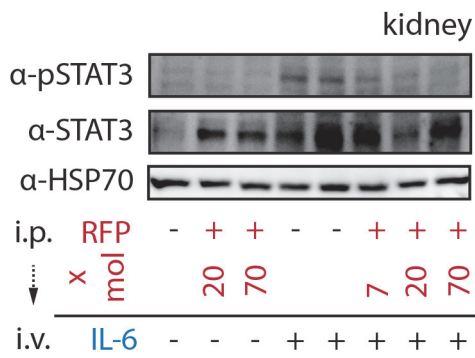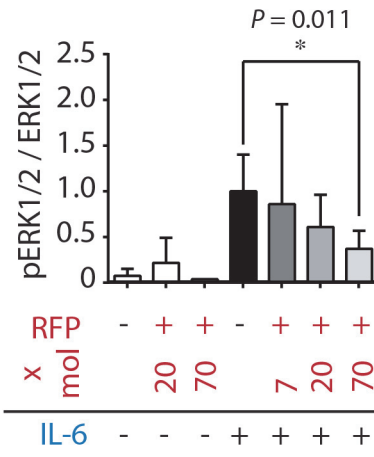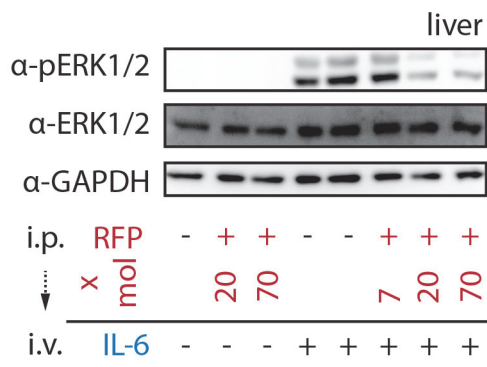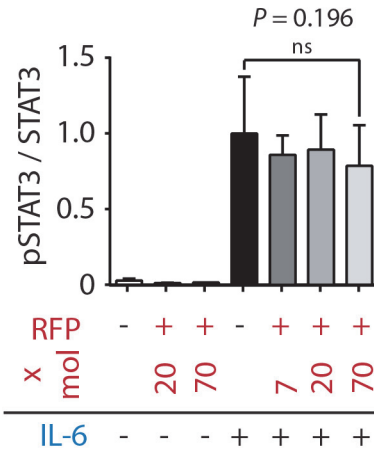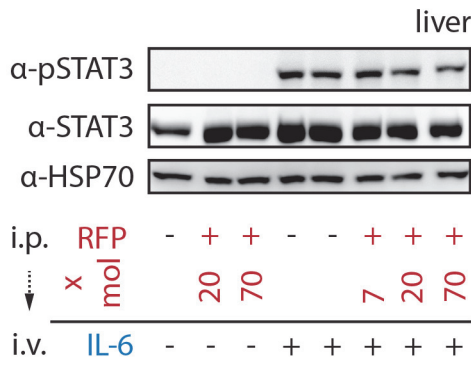
Figure 30: mIL-6-RFP-Fc pretreated mice exhibit reduced IL-6 dependent STAT3 activation (Left) Representative Western blots of mouse liver and kidney lysates prepared 15 min following intravenous administration of either PBS or IL-6 (100 ng). Mice were pretreated for 45 min with PBS or mIL-6-RFP-Fc i.p. at dosages of 4, 12 or 40 µg, corresponding to molar IL-6/mIL-6-RFP-Fc (RFP) ratios as indicated. Phosphorylated STAT3 (α-pSTAT3), phosphory-lated ERK1/2 (α-pERK1/2), total STAT3 (α-STAT3) and total ERK1/2 (α-ERK1/2) were detected. GAPDH and HSP70 served as loading controls. (Right) Statistical evaluation of experiments depicted in D. Data shown are means ± SD. *$p \leq 0.05$, one-sided t-test (n=2 for PBS i.v. stimu-lated groups; n=5 for PBS i.p. / IL-6 i.v.; n=3 for RFP 7x i.p. / IL-6 i.v.; n=3 for RFP 20x i.p. / IL-6 i.v.; n=4 for RFP 70x i.p. / IL-6 i.v.). Because of variations in STAT3 expression levels, pSTAT3 was normalized relative to total STAT3. Similarly, pERK1/2 was normalized relative to total ERK1/2.

4.4.3   mIL-6-RFP-Fc gene delivery by hydrodynamic transfection

Although anti-cytokine therapy through application of recombinant protein has been shown to be effective, protein production is expensive and tedious. We argued that a gene therapeutic approach, where small amounts of a delivered plasmid generates sub-stantial protein levels by the recipient himself, might be much more efficient. mIL-6-RFP-Fc is encoded by a single gene and therefore ideally suited for gene delivery. In or-der to achieve high systemic levels of circulating mIL-6-RFP-Fc we used the method of hydrodynamic plasmid delivery via the tail vein, which mainly results in transfection of the liver and to a much lower extent of the kidney and other organs (Liu et al., 1999). The phosphoenolpyruvate carboxykinase (PEPCK) promoter was chosen because it is active in the liver and generates high systemic levels of soluble proteins (Beale et al., 1992, Rabe et al., 2008). Following gene delivery, mIL-6-RFP-Fc was detected in liver tissue (Figure 31A) and serum (Figure 31B). The concentration of expressed protein in the liver correlated well with the amount of plasmid used for transfection (i.e. 10 and 37 µg/animal, respectively). Using the latter amount, a mIL-6-RFP-Fc serum level at 24 h of 1.3 ± 1.5 µg/ml (mean ± SD; n=4) was achieved, thus corresponding to the 2 h and 12-24 h levels upon singular i.p. spiking of 4 and 40 µg of mIL-6-RFP-Fc, respectively (Figure 28B). Subsequently, 37 µg of plasmid per animal were used for hydrodynamic transfection throughout all experiments. Analysis of liver sections of mice that were simultaneously transfected with plasmid encoding mIL-6-RFP-Fc and eGFP revealed that a single cell either expresses the fusion protein or eGFP but rarely both (Figure 31C). This finding emphasizes the advantage of a single gene construct such as receptor

fusion proteins over proteins encoded by multiple genes such as antibodies for gene transfer approaches.
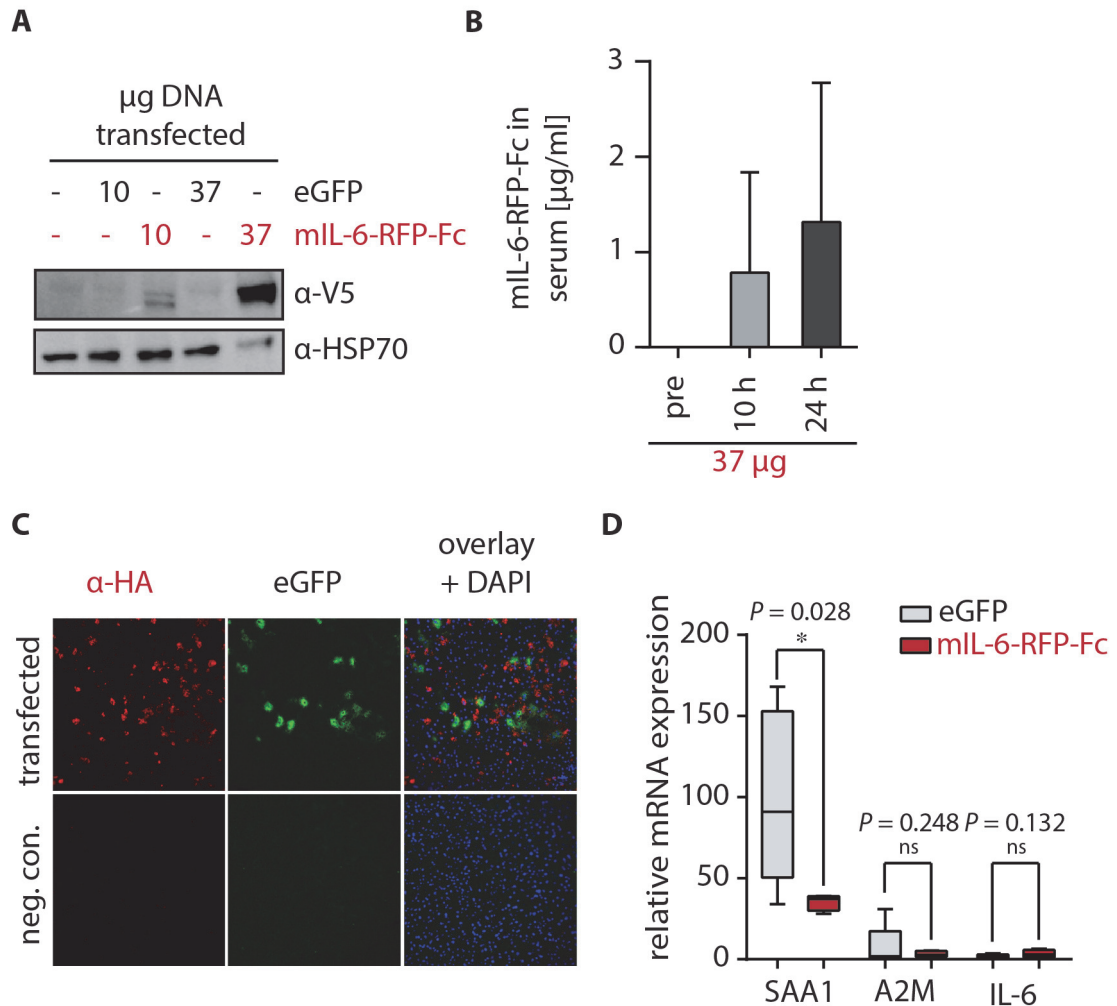
Figure 31: Hydrodynamics-based transfection of PEPCK-mIL-6-RFP-Fc (A) Western blot analysis of liver lysates from mice hydrodynamically transfected with control vector (eGFP) lacking the epitopes or mIL-6-RFP-Fc using an antibody directed against the V5-epitope of mIL-6-RFP-Fc (α-V5). Amounts of plasmid transfected were as indicated. Mice were sacrificed 24 hours post transfection. As a negative control, a mouse treated with transfection agent without plasmid is shown. Detection of HSP70 served as a loading control (α-HSP70). (B) mIL-6-RFP-Fc serum concentrations as determined by ELISA at time points indicated. n=4 animals; subsequently analyzed in (D). (C) Immunofluorescence of liver cryosections 24 hours post hydrodynamic gene delivery. Cotransfection with expression vectors encoding mIL-6-RFP-Fc (as detected by α-HA, red) and eGFP (green) was performed. As a negative control, a mouse treated with transfection agent without plasmid is shown. (D) qRT-PCR of liver acute phase mRNAs 24 hours after hydrodynamic delivery of 37 µg of either control plasmid or mIL-6-RFP-Fc-endocing plasmid. SAA1, serum amyloid A; A2M, α2-macroglobulin. Data were normalized and calculated using the housekeeper GAPDH and the ΔΔCT method (Livak and Schmittgen, 2001). X-fold expression relative to mean of healthy normal mice. n=4 (mIL-6-RFP-Fc) and n=5 (eGFP) animals/group. Box plots, whiskers indicating minimal to maximal values, *p≤0.05, one-sided t-test.

The bioactivity of mIL-6-RFP-Fc administered through gene transfer could be directly confirmed by the suppression of hepatic acute phase protein production which had been induced by the invasive transfection procedure. Expression of mRNA for serum amyloid A1 (SAA1) was significantly reduced and expression of mRNA for α2-macroglobulin (A2M) showed a trend of a reduction (Figure 31D). Both molecules are known to be governed by IL-6 (Sander et al., 2010). A trend for slightly increased IL-6 mRNA levels in the mIL-6-RFP-Fc treated group might reflect compensatory IL-6 production (Figure 31D). The fact that SAA1 is not completely suppressed in this model might be potentially explained by other SAA1-governing cytokines such as IL-1 and TNF being released following hydrodynamic transfection.

4.4.4 mIL-6-RFP-Fc pharmacokinetics after gene delivery
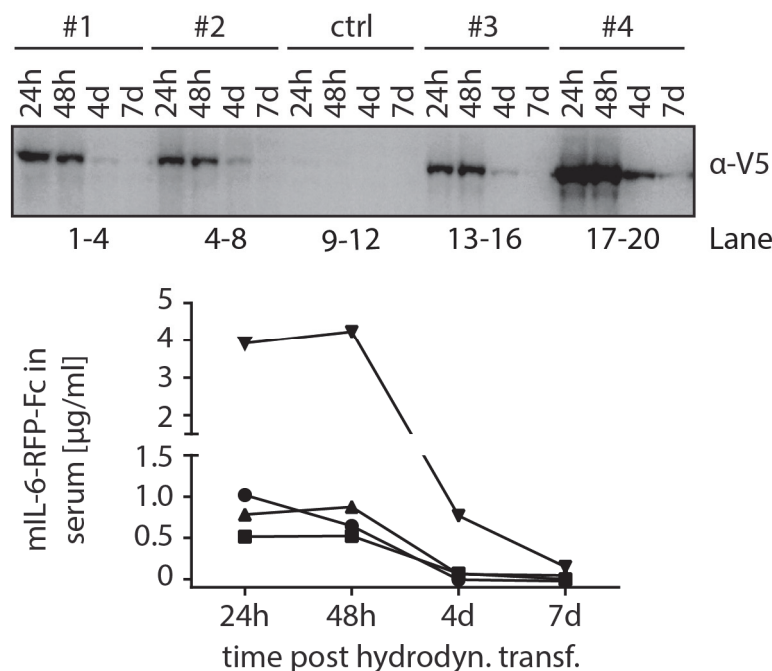
Figure 32: mIL-6-RFP-Fc pharmacokinetics following mIL-6-RFP-Fc gene delivery Serum levels of mIL-6-RFP-Fc from 4 mice (#1-#4) over time following hydrodynamic transfection with 37 µg plasmid. Western blot using an antibody directed against the V5-epitope (α-V5, upper panel) and corresponding quantification by ELISA (lower panel). ctrl, mouse transfected with empty vector.

To assess the usefulness of the hydrodynamic transfection approach for disease models, the pharmacokinetics of mIL-6-RFP-Fc were evaluated in more detail. mIL-6-RFP-Fc was detected in serum for up to one week after gene transfer, again with no signs of degradation. Average serum levels of 1.6 µg/ml (±1.6 SD; n=4) mIL-6-RFP-Fc were achieved for at least 48 h (Figure 32), indicating continuous synthesis as opposed to singular spike and turnover (Figure 28).

4.4.5 Model of ischemia and reperfusion injury in the kidney
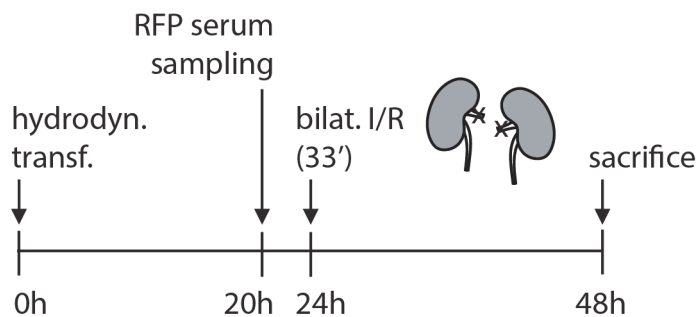
Figure 33: Experimental outline of the used acute kidney injury model by ischemia/reperfusion Bilateral (bilat.) renal ischemia-reperfusion (I/R, 33 min of ischemia) performed 24 hours following hydrodynamic transfection (hydrodyn. transf.) of 37 µg mIL-6-RFP-Fc or 37 µg empty vector. Serum levels of mIL-6-RFP-Fc was measured at 20 h post hydrodynamic transfection. Serum creatinine was assessed 5 days prior to gene delivery and at sacrifice.

To assess the therapeutic potential of mIL-6-RFP-Fc produced via gene delivery in a relevant disease model we applied a model of acute kidney injury (AKI) by transient bilateral renal ischemia for 33 minutes followed by reperfusion for 24 hours (I/R). This well-established model of tubular cell necrosis (Wei and Dong, 2012) has been previously demonstrated to depend critically on IL-6 (Jones et al., 2015). Injury is significantly reduced in IL-6^{-/-} mice and can also be alleviated by the adoptive transfer of IL-6^{-/-} bone marrow or by treatment with IL-6 neutralizing antibodies, resulting in improved renal serum and histological parameters (Patel et al., 2005, Kielar et al., 2005). The current experimental design is outlined in Figure 33. Mice with detectable mIL-6-RFP-Fc serum levels (0.25 - 4.5 µg/ml; mean 1.5 µg/ml ± SD 1.5) at 20 h post hydrodynamic transfec-

tion or equally treated mice having received control vector were subjected to bilateral

I/R of 33 minutes duration at 24 h and sacrificed at 48 h for further organ analysis.
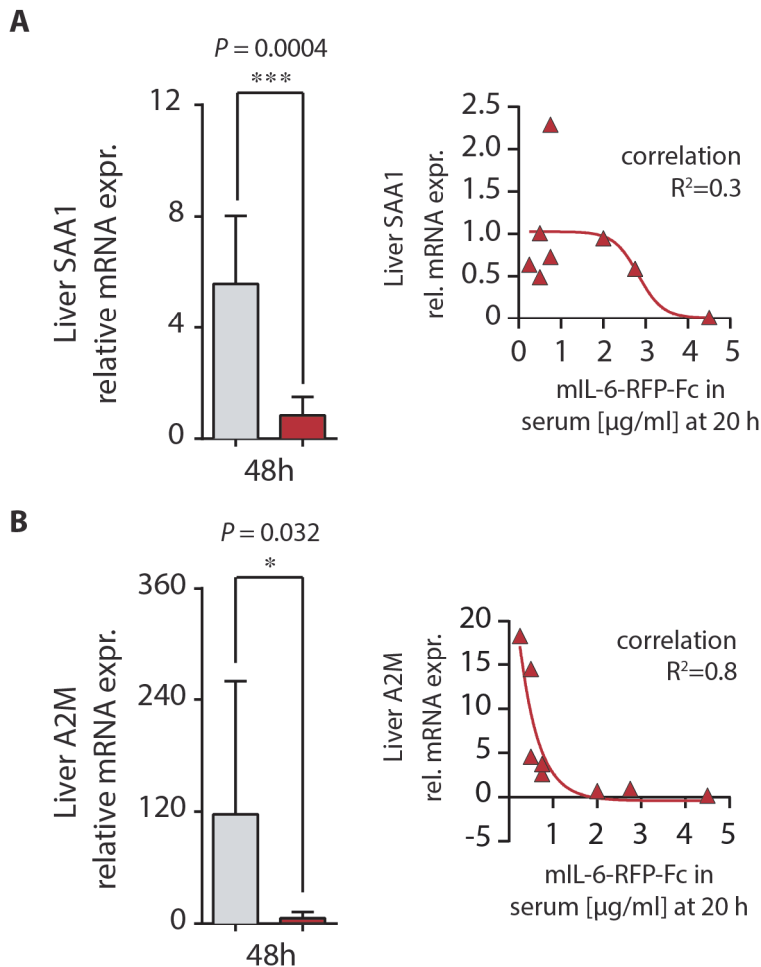
Figure 34: mIL-6-RFP-Fc blocks acute phase protein synthesis in the I/R injury model
qRT-PCR of acute phase mRNAs from liver of sacrificed mice as calculated relative (x-fold) to mean of healthy control mice using housekeeper GAPDH and the ΔΔCT method. Expression of both acute phase proteins by mIL-6-RFP-Fc transfection is significantly reduced (red bars) in comparison to control vector (grey bars). Nonlinear regression analysis revealed that suppression of SAA1 and A2M correlates with serum mIL-6-RFP-Fc levels. Red bar, mIL-6-RFP-Fc; grey bar, empty vector. All data are from n=8 animals/group, shown as means ± SD and/or single values, *p≤0.05, **p≤0.01, ***p≤0.001 one-sided t-test.

Successful transfection and biological activity of mIL-6-RFP-Fc was confirmed by suppressed hepatic (Figure 34A) SAA1 and (Figure 34B) A2M mRNAs, which also correlated with the 20 h serum level of mIL-6-RFP-Fc (Figure 34A+B, right panels).

A

B

C

healthy   I/R - control   I/R - mIL-6-RFP-Fc
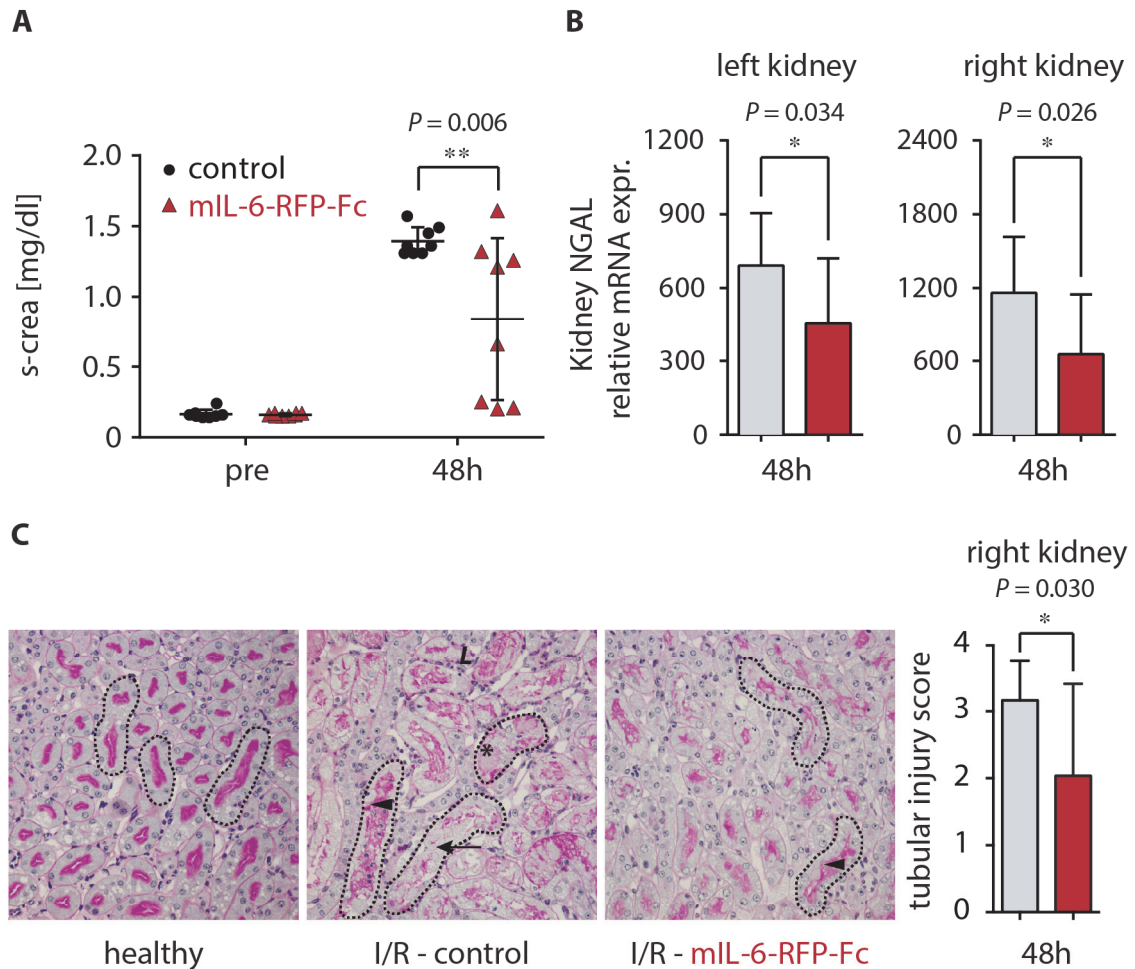
Figure 35: mIL-6-RFP-Fc ameliorates kidney damage (A) Increased serum creatinine following I/R is significantly reduced by prior transfection with mIL-6-RFP-Fc. Verification of t-test results by ANOVA with Tuckey multiple group analysis revealed an overall p≤0.0001 and an identical significance level of ≤0.01 for I/R control versus mIL-6-RFP-Fc. (B) Transcription of the tubular injury marker NGAL in both kidneys as assessed using housekeeper GAPDH and the ΔΔCT method (Livak and Schmittgen, 2001), indicating the significant mitigation of renal injury upon hydrodynamic transfection of mIL-6-RFP-Fc (red bars) compared to empty vector (grey bars). (C) Representative renal tissue sections, original magnifications, x200. Dotted lines, representative renal tubules. Normal healthy kidney showing homogeneous basophilic and eosinophilic staining of the cytoplasm and of the apical brush border membrane, respectively. Following I/R, tubular dilatation/atrophy (arrowheads), loss of the brush border (arrow), tubular necrosis (asterisk) and leukocyte infiltration (L) ensue, the degree of which is mitigated following transfection with mIL-6-RFP-Fc. Far right: statistical analysis of tissue injury score for the right kidney (left kidney not assessed). Red bar, mIL-6-RFP-Fc; grey bar, empty vector. All data are from n=8 animals/group, shown as means ± SD and/or single values, *p≤0.05, **p≤0.01, ***p≤0.001 one-sided t-test.

In line with the previous studies (Patel et al., 2005, Kielar et al., 2005), we observed similar beneficial effects on renal endpoints. Serum creatinine (Figure 35A), intrarenal mRNA synthesis of the acute kidney injury marker neutrophil gelatinase-associated lipocalin (NGAL)/lipocalin-2 (Lcn2) (Ko et al., 2010, Nickolas et al., 2008) (Figure 35B)

and histologic tubular injury scoring (Figure 35C) were significantly reduced following transfection with mIL-6-RFP-Fc. These data are also in line with another report in which IL-6$^{-/-}$ mice were protected in the initial phase of a mercury-induced proximal tubular injury model (Nechemia-Arbely et al., 2008). It must be noted that the renal functional and renal histologic endpoints of the mIL-6-RFP-Fc group exhibited a comparatively wide variance (Figure 35A, C). This is in agreement with published data on this complex acute kidney injury model (Kielar et al., 2005). By combining the data from the hydrodynamic transfections of 16 individual animal described herein (Figure 31B n=4, Figure 32 n=4, Figure 34 n=8), a very consistent mean serum expression level of mIL-6-RFP-Fc within the first 20-48 h of 1.5 µg/ml; ± SD 1.4 can be inferred.

Collectively, the consistent reduction of the hepatic acute phase response in both the hepatic transfection and the I/R model (Figure 31D and Figure 34, respectively) and the significant – though variant – benefit of renal endpoints in I/R (Figure 35) establish endogenous expression of mIL-6-RFP-Fc via gene transfer as an effective treatment in murine disease models.

5   Discussion

5.1   Biochemical characterization of mIL-31-RFP

In the first part of this study we developed a novel receptor fusion protein for the inhibition of murine IL-31. The receptor fusion protein mIL-31-RFP consists of domains D1-D4 of murine OSMR connected with a flexible polypeptide linker to domains D1-D2 of mIL-31R. Starting with our previously cloned mOSM-RFP (Brolund et al., 2011), we exchanged the domains D2+D3 of murine gp130 with the CBM of murine IL-31R, transforming the fusion protein from an OSM-specific to an IL-31-specific cytokine inhibitor (Figure 7). An additional tag exchange from flag to a 3V5-3HA module allowed reliable quantification with an ELISA directed against the two triple tags. As primary murine keratinocytes as well as PAM212 cells did not respond to IL-31 stimulation before and after IFN-γ priming, which is known to upregulate IL-31R expression (Figure 8), we established a reliable cell system for the analysis of IL-31-dependent signal transduction by stably transfecting MEF cells with murine full-length IL-31R cDNA, rebuilt by PCR-based fusion of exon fragments (Figure 9). MEF mIL-31R cells allowed us to analyze IL-31 signaling, and assay the inhibitory activity of mIL-31-RFP. As expected mIL-31-RFP is a potent inhibitor of IL-31 induced STAT3 phosphorylation (Figure 10).

5.1.1   Specificity of mIL-31-RFP

OSMR acts as the common receptor subunit involved in the formation of the heterotrimeric signaling complex for both IL-31 and OSM, with either IL-31R or gp130 as the second receptor subunit, respectively. In regards to cytokine specificity, the question arises whether mIL-31-RFP is able to at least partially inhibit OSM signaling due to the N-terminal domains D1-D4 of murine OSMR. Even a 10-fold molar excess of mIL-31-RFP did not inhibit OSM bioactivity on MEF cells (Figure 10). This suggests that the

affinity between the OSMR component of the mIL-31-RFP and murine OSM is very low and is not sufficient for high-affinity binding over the membrane bound full-length receptors OSMR and gp130, which are both present on MEF cells.

5.1.2 Potential use of mIL-31-RFP

The contribution of IL-31 to atopic dermatitis was first discovered in a mouse model with transgenic IL-31 overexpression. Thus IL-31 has been implicated as a key factor in pruritic skin and other allergic diseases like asthma (Dillon et al., 2004, Neis et al., 2006, Sonkoly et al., 2006). Recent evidence shows its direct involvement with neurons in dorsal root ganglia (Bando et al., 2006).

For the inhibition of human IL-31 the fusion protein OSMR-L-GPL (Venereau et al., 2010) was constructed following the design principles of hIL-6-RFP (Ancey et al., 2003). As there exists a strict species specifity regarding receptor interaction of human and murine IL-31 (Broxmeyer et al., 2007) OSMR-L-GPL cannot be used in murine models of atopic dermatitis. Therefore mIL-31-RFP will be a useful tool to decipher the role of murine IL-31 in mouse models of pruritic skin diseases and the further dissection of cytokine signaling networks. Although there already exists an antibody targeting murine IL-31 (Grimstad et al., 2009), mIL-31-RFP allows refined targeting of cytokines in murine disease models. Because of its monogenic nature, mIL-31-RFP is well suited for transgenic or gene delivery approaches. Transfer vectors can be designed for temporal and spatial expression of mIL-31-RFP through organ- or tissue-specific promoters so that the consequences of local IL-31 inhibition can be studied.

Besides its contribution to skin diseases recent evidence suggests a role of IL-31 and OSM in itch and neuroimmune communication (Cevikbas et al., 2014). By using gene delivery by adeno-associated virus-derived (AAV) vectors it is possible to target specific tissues. The AAV serotype 5 has been reported to mediate effective gene delivery to dorsal root ganglia (DRG) (Mason et al., 2010), and further improvements to vectors have been made for simultaneous expression of two genes of interests (Fagoe et al., 2014). Combined or single gene delivery to DRG of i.e. mOSM-RFP and mIL-31-RFP could

further clarify the distinct contribution and role of both cytokines to itch and neuroimmune communication mediated by DRG signaling in pruritic skin tissues.

Another role has been proposed for IL-31 in the regulation of intestinal barrier function contributing to the pathogenesis of IBD. Both IL-31R and OSMR are expressed on intestinal epithelial cells (IEC). Additionally colonic lesions of IBD patients show increased IL-31 mRNA expression (Dambacher et al., 2007). Interestingly recent evidence hints at a similar role for OSM in IBD. OSM signaling through type II OSM receptor complex (OSMR/gp130) leads to increased IEC proliferation and wound healing. Further colonic biopsies of patients with active IBD (Beigel et al., 2014) show upregulated OSM protein expression. Again concurrent use of both mOSM-RFP and mIL-31-RFP could help to further dissect cytokine networks in IBD.

5.2   Transgenic mice with inducible expression of mIL-6-RFP

In this project, the previously described mIL-6-RFP-V5-his (Wiesinger et al., 2009) was optimized for the transfer to a tetracycline inducible system that is well suited for the generation of transgenic mice and allows controlled expression of the fusion protein in space and time. First the V5-his tag was replaced with a 3V5-3HA tag module (Figure 12), allowing reliable ELISA based quantification from conditioned media and serum samples. The tag exchange did not influence biological activity in terms of IL-6 binding and inhibition of IL-6 induced STAT3 phosphorylation (Figure 13). The vector system of choice was the tetracycline controlled pTRE-Tight-BI vector system (Figure 14). Transient expression analysis in HEK293 cells revealed a strong dependence on the presence of the rtTA-M2. Basal expression, but low secretion levels, of mIL-6-RFP-3V5-3HA could be observed even without the addition of doxycycline in cells co-transfected with the corresponding vectors encoding for rtTA-M2 and mIL-6-RFP-3V5-3HA. But treatment with doxycycline led to a strong induction of mIL-6-RFP expression and secretion. Without the presence of the rtTA-M2 no mIL-6-RFP expression was detectable (Figure 15). The latter is an important aspect in the generation of mice with rtTA-M2-/doxycycline-controlled mIL-6-RFP expression. Tissues and cells that don't carry the

rtTA-M2 transgene will not express any mIL-6-RFP. Therefore localized expression is governed by the activity of the promoter controlling rtTA-M2 expression.

In the next step we were able to create two independent transgenic founder mice identified through PCR based genotyping from tail DNA (Figure 16), that were subsequently crossed with LAP:rtTA and Pod:rtTA mouse lines to target the liver and podocytes of the kidney for localized mIL-6-RFP expression (Figure 17). Additional pronuclear injections failed to generate transgene positive mice. As we are dealing with transgenic mice, each Tg(TET:mIL-6-RFP) founder mice has a random insertion site for the transgene accompanied with different transcriptional activity. In the analysis of Tg(TRE:mIL-6-RFP, LAP:rtTA)1F1 mice we were able to detect some mIL-6-RFP and lacZ mRNA expression in mice (Figure 18 A+B), but we failed to detect any mIL-6-RFP protein by means of Western Blot of liver lysates and serum (Figure 18 C+D), or ELISA from serum samples directed against the V5-HA tag module. We then co-transfected Tg(LAP:rtTA) mice with vectors encoding doxycycline-inducible and rtTA-dependent mIL-6-RFP/lacZ expression and constitutive expression of eGFP. X-Gal staining from liver sections revealed low and mosaicism-like lacZ expression (Figure 19 A), whereas immunofluorescence analysis showed eGFP expression in more than 50% of the liver tissue (Figure 19 B). In this scenario lacZ expression depends on rtTA-M2 expression and doxycycyline activation, whereas eGFP is expressed constitutively. This either speaks for either low to none rtTA-M2 levels in liver of Tg(LAP:rtTA).

In Tg(TET:mIL-6-RFP.tg1/pod:rtTA)2F1 mice we could detect lacZ gene expression through X-Gal staining from kidney sections (Figure 20 A). This staining is in line with a report originally describing the podocyte specific expression of the lacZ gene (Shigehara et al., 2003). Unfortunately we also failed to detect any mIL-6-RFP protein by means of Western blot analysis from kidney lysates (Figure 20 B), or ELISA from serum samples directed against the V5-HA tag module (data not shown).

For missing protein expression in transgenic mice various factors have to be considered: Effective transgene expression depends on the place of integration, and as mentioned before pronucleus injection of linearized DNA leads to random integration into the host

genome. Heterochromatin regions of the mouse genome are often affected by gene silencing effects. Therefore the histone and DNA methylation status of the inserted transgene in different tissues would be worth to investigate. Also tissue-specific silencing of the CMV promoter has been reported. In the liver silencing of the CMV promoter might not be due to DNA methylation but instead through transcriptional repressors binding to elements on the promoter (Loser et al., 1998). A specific repressive factor may act upon the minimal CMV promoter. It may therefore be necessary to screen cell types with poor CMV activity with different minimal promoters to find their most active enhancer elements. In our system another important factor that controls transgene expression is the tissue penetration of the administered doxycycline. Protein expression could further be negatively influenced by transcript regulation through cell-type specific microRNA expression patterns that target in the case of mIL-6-RFP either the gp130 or IL-6Rα portion. Taken together expression of mIL-6-RFP transgene could be silenced or negatively regulated due to yet unknown reasons or mechanisms on either genetic or transcriptional levels. Further clarification would be necessary.

5.3   Optimization of mIL-6-RFP

5.3.1   Design of mIL-6-RFP-Fc

Although the first transgenic approach described previously did not result in any measurable and detectable protein, we thought about further modifications to the design, expression system and type of transgene delivery of mIL-6-RFP-3V5-3HA. As a first measure we added the hinge region and crystallizable fragment (Fc) domain of an engineered mIgG2a to mIL-6-RFP-3V5-3HA. The resulting fusion protein mIL-6-RFP-Fc-3V5-3HA (mIL-6-RFP-Fc) is homodimeric, containing two entities mIL-6-RFP-3V5-3HA (Figure 21). Responsible are cysteine residues within the Fc-fragment that enforce dimerization through disulfide bond formation thereby favoring the formation of an inhibitory complex consisting of a mIL-6-RFP-Fc dimer that binds two IL-6 molecules. This stoichiometry is analogous to the high-affinity hexameric receptor complex con-

sisting of two molecules of each IL-6, sIL-6Rα and gp130 that has been verified by X-ray crystallography (Boulanger et al., 2003). Earlier work demonstrated that IL-6-RFP indeed forms complexes similar to the native IL-6 receptor complex (Metz et al., 2007). The homodimeric character of mIL-6-RFP-Fc increases its avidity towards IL-6, which is reflected in the tenfold increase of its inhibitory activity on IL-6-dependent cell proliferation compared to the original mIL-6-RFP (Figure 27). Furthermore, the Fc-fragment of IgG interacts with the neonatal Fc receptor (FcRn) that mediates recycling of pinocytosed protein, thus increasing the plasma half-life of the fusion protein (Rath et al., 2013). This feature can be further modulated through mutations that affect the Fc-FcRn interaction (Vaccaro et al., 2005). Finally, when mIL-6-RFP-Fc is produced as a recombinant protein the Fc fragment allows convenient purification through affinity chromatography with immobilized Protein A or G. As its predecessor, mIL-6-RFP-Fc can be reliably quantified with an ELISA directed against the two triple tags (3V5-3HA) that follow the Fc-fragment. By simple cloning procedures, the Fc-3V5-3HA module can be easily transferred to other receptor fusion proteins so that different proteins can be quantified by the same assay and acquire additionally the Fc mediated properties.

5.3.2 Codon Optimization

In a second step we optimized the cDNA of mIL-6-RFP-Fc based on mammalian codon usage (Figure 22). Further sequences that could interfere with stability and translation of the transcribed mRNA were removed. Recently it was reported that optimization of codons modulate the translational elongation rates. Significant alterations in tRNA concentrations between cells and tissues can alter the mRNA expression profile and dynamically change mRNA stability (Presnyak et al., 2015). Also negative regulatory effects on mIL-6-RFP-Fc expression at the translational level mediated by cell-type specific miRNAs would be avoided by codon optimization.

The optimized cDNA was subcloned into various vector systems suited for either *in vitro* protein expression, in a transient or stable manner, and finally a vector system well suited for the generation of either transgenic mice or gene delivery approaches to ana-

lyze the efficacy of mIL-6-RFP-Fc *in vivo*. Comparative analysis following transient transfection of the optimized mIL-6-RFP-Fc cDNA vs. non-optimized cDNA revealed a 2.5-fold or 1.6-fold increase in protein secretion from either human or murine liver de-rived cells, respectively (Figure 23). HEK293 Flp-In/T-Rex were stably transfected with the optimized mIL-6-RFP-Fc cDNA and subjected to clonal selection (Figure 24). Con-tinuous protein production yielded about 4 mg mIL-6-RFP-Fc per liter of conditioned medium (data not shown). The purity of recombinant mIL-6-RFP-Fc was high as there were no impurities and signs of degradations in the Coomassie stained gel (Figure 25).

5.3.3 Biochemical characterization of mIL-6-RFP-Fc

mIL-6-RFP-Fc inhibited IL-6-dependent STAT3-phosphorylation already at equimolar concentration in muHepa cells, whereas pretreatment with a 10-fold molar excess of mIL-6-RFP-Fc completely inhibited signal transduction by IL-6 (Figure 26). Further mIL-6-RFP-Fc inhibits IL-6-induced proliferation of Ba/F3-mgp130/mIL-6Rα cells. The forced dimerization through Fc-fusion leads to an improved inhibitory profile as evi-dent by the 10-fold lower IC50 in comparison to the monomeric mIL-6-RFP (Figure 27). This is in agreement with the higher avidity of mIL-6-RFP-Fc as proposed in our model and with the increase of the activity of the IL-6 trans-signaling inhibitor sgp130 upon Fc fusion (Jostock et al., 2001).

Complete blockade of all receptor binding sites of IL-6 by mIL-6-RFP-Fc could have a direct impact on its activity in a clinical setting. A direct comparison of two TNF-α in-hibitors, namely Etanercept, a TNFR-Fc fusion protein, and infliximab, an anti-TNF-α antibody, has shown that differences in binding stoichiometry and affinity might lead to different clinical outcomes (Scallon et al., 2002). Etanercept can interact by design just with two binding sites within the TNF-α trimer in a 1:1 stoichiometry even in molar excess, leaving one available binding site, whereas infliximab binds the TNF-α trimer in a 3:1 stoichiometry, fully blocking all binding sites. Both biologics ameliorate disease characteristics in RA patients, whereas only infliximab seems to be effective in the treatment of Crohn's disease patients.

5.3.4 Pharmacological properties of recombinant mIL-6-RFP-Fc

To assess the usefulness as a potential therapeutic the pharmacokinetics of mIL-6-RFP-Fc were analyzed. Intraperitoneally injected mIL-6-RFP-Fc showed the highest serum-bioavailability compared to intravenous or subcutaneous administration (Figure 28 A). Two hours following intraperitoneal delivery mIL-6-RFP-Fc serum bioavailability was about 40%. At the highest amount (40 μg) applied in one single administration, mIL-6-RFP-Fc could be detected in serum for up to 48 h (Figure 28 B). The dominant half-life of mIL-6-RFP-Fc was about 3.5 h and is identical with the initial clearing determined for an IL-2-Fc fusion protein harboring the same Fc-fragment of mIgG2a (Zheng et al., 1999).

5.3.5 mIL-6-RFP-Fc inhibits IL-6 signaling *in vivo*

The pretreatment of mice through systemic administration of recombinant mIL-6-RFP-Fc by intraperitoneal injection decreased IL-6-induced STAT3 and ERK phosphorylation in the liver and the kidney of IL-6 treated mice (Figure 30). Thus circulating mIL-6-RFP-Fc penetrates into the liver and kidney, is biologically active and inhibits IL-6 dependent signal transduction *in vivo*.

5.3.6 Gene delivery of monogenic RFPs

As production and purification of recombinant protein is time-consuming, tedious and costly, we explored the potential use of monogenic RFPs for gene therapy. Targeted gene transfer allows cytokine inhibition at sites of inflammation by enabling local, sustained and potentially regulated expression of receptor fusion proteins. Endogenously produced proteins as a result of gene transfer are nascent molecules that have undergone post-translational modification with glycosylation patterns that are entirely host-like. This feature is expected to dramatically reduce immunogenicity which often is a result of aberrant non-host-like glycosylation by i.e. recombinant protein production in different expression systems (Baker et al., 2010).

In our study, we used the experimental method of hydrodynamic transfection for gene delivery of mIL-6-RFP-Fc (Liu et al., 1999). For gene delivery we chose a vector system under the transcriptional control of the PEPCK promoter, previously described for the generation of transgenic mice expressing either sIL-6Rα (Peters et al., 1996) or sgp130-Fc (Rabe et al., 2008). The PEPCK promoter is mainly active in the liver and kidney (Beale et al., 1992). A β-globin intron, located between promoter and open-reading-frame (ORF) should lead to more efficient translation of the intron-containing transcript or spliced mRNA (Lee et al., 2009). Previous experiments of *Wiesinger et al.* initially tested intramuscular electrotransfer of the previously reported mIL-6-RFP-V5-his to rats. 72 hours after electroporation of rat serum levels were in the range of 0.4 to 0.7 ng/ml (Wiesinger, 2008). Following hydrodynamics-based transfection of mIL-6-RFP-Fc into mice, obtained serum levels of the fusion protein were stable for at least 48 hours in the range of 0.5 to 4 μg/ml (Figure 32), which marks a 1.000 to 10.000 fold increase when compared to mIL-6-RFP-V5-his serum levels after electrotransfer into rats. Host-expressed mIL-6-RFP-Fc was detectable for up to 7 days (Figure 32).

Resolution of the Acute Phase Response

The acute phase response (APR) is part of the innate immune response and is triggered by pro-inflammatory cytokines as a result of local or systemic disturbances (Ruminy et al., 2001). Acute phase proteins (APP) are produced predominantly by hepatocytes and are induced by the pro-inflammatory cytokines IL-1, TNF-α and IL-6 under acute inflammatory conditions. In mice, the predominant APP belong to the SAA family. IL-6 is regarded as the major inducer of acute phase protein synthesis in the liver (Ritchie and Fuller, 1983, Gabay and Kushner, 1999).

The experimental procedure of hydrodynamics-based transfection leads to liver stress as evident by the transient increase of alanine aminotransferase (ALT) levels, a marker for hepatocyte damage, post injection independent of the presence of plasmid DNA (Liu et al., 1999). Following hydrodynamic delivery we could observe upregulated mRNA expression of the two acute phase proteins SAA1 and A2M 24 hours post transfection

(Figure 31D) and also in the I/R model 48 hours after transfection (Figure 34). Expression for both SAA1 and A2M mRNAs was markedly reduced in mIL-6-RFP-Fc transfected mice compared to control animals (Figure 31D and Figure 34). This result demonstrates that host-produced mIL-6-RFP-Fc is biologically active and mIL-6-RFP-Fc serum levels are sufficient to resolve IL-6-dependent acute phase response as a consequence of local disturbances caused by the hydrodynamic events in the liver. Resolution of the acute phase protein synthesis correlated with increased mIL-6-RFP-Fc levels (Figure 34, right panels).

5.3.7   IL-6 in ischemia reperfusion injury of the kidney

Finally we used the host-expressed inhibitor to assess its bioactivity and therapeutic potential in an experimental model of acute kidney injury (AKI). We employed the model of bilateral ischemia/reperfusion injury of the kidney (Figure 33). Ischemia/reperfusion shows a complex pathophysiology. It affects many regulatory systems at the cellular level, i.e. on energy metabolism, loss of tubular cell polarity and development of acute tubular necrosis (ATN) (Devarajan, 2005). Release of chemokines and cytokines in renal tissues leads to the activation of distinct inflammatory events (Salvadori et al., 2015).

Although the role of IL-6 in renal ischemic injury is controversial, studies in mice highlight a contribution of IL-6 to the development of AKI, and that inhibition of IL-6 ameliorates kidney damage (Kielar et al., 2005, Patel et al., 2005). Renal injury by ischemia/reperfusion has been mainly attributed to increased IL-6 production of macrophages in the context of injured proximal tubular cells (Kielar et al., 2005). IL-6^{-/-} mice or mice that were treated with a neutralizing anti-IL-6 antibody show a reduction of the increased plasma urea and serum creatinine levels caused by I/R (Patel et al., 2005).

We investigated the potential of mIL-6-RFP-Fc to ameliorate acute kidney injury caused by I/R. Indeed mice that underwent hydrodynamic transfection of mIL-6-RFP-Fc prior to induction of ischemic renal injury showed a significant reduction of serum creatinine levels compared to control mice (Figure 35A), reduced tubular damage as assessed by reduced NGAL mRNA expression (Figure 35B) and tubular injury scoring (Figure 35C).

A large variance within the IL-6$^{-/-}$ groups in the I/R model was also observed in another study (at least twofold of the wildtype control groups) (Kielar et al., 2005). To better understand this phenomenon a careful correlation analysis of the 20 h serum mIL-6-RFP-Fc levels and the associated renal outcomes was undertaken. While the animal with the highest serum level of 4.5 μg/ml exhibited the lowest serum creatinine level (0.21 mg/dl) and the lowest average NGAL expression level (right kidney: 40-fold, left kidney 156-fold of normal) no clear correlation between these outcome markers and the mIL-6-RFP-Fc level was found in the other animals (data not shown). On the other hand, a clear dose-response effect was observed in the inhibition of the hepatic acute phase response (Figure 34, right panels).

Intriguingly, in the hepatic stress response at 24 h following hydrodynamics based transfection (Figure 31D) acute phase transcriptional suppression by mIL-6-RFP-Fc is significant but incomplete while in the I/R model it is total with some animals ranging below the level of healthy controls (Figure 34, right panels). Indeed, as discussed above, 24 h post hydrodynamics stress non-IL-6 driven SAA1 transcription by IL-1 or TNF might be the case, while for the I/R model it has been elegantly established that IL-6 is mainly derived from the kidney contributing to high systemic levels (Kielar et al., 2005). Renal IL-1 and TNF release is a feature of I/R but not in the setting of IL-6$^{-/-}$ or antagonism (Patel et al., 2005). Collectively, this could explain the discrepancy between acute phase transcriptional suppression in hepatic stress and I/R.

5.4 Outlook

5.4.1 Design of hIL-6-RFP-Fc

In this study we found a rather short circulating $t_{1/2}$ for mIL-6-RFP fused to Fc from mIgG2A. An analogous hIL-6-RFP should be fused to Fc of human IgG1 that harbors the M252Y/S254T/T256E (YTE) mutations to improve serum half-life. The YTE triple mutation has been shown to increase affinity of IgG1-Fc to human FcRn tenfold, resulting in a 4-fold increase in serum-half-life in cynomolgus monkeys (Dall'Acqua et al.,

2006). Other hIgG1-Fc-fusion proteins exert variable half-life's, ranging from 4 to 23 d (Suzuki et al., 2010). Additionally species identity of the human Fc part should reduce immunogenicity.

For other analogous hIgG1-Fc-fusion proteins that are to be used in a murine model of human disease, there is also to keep in mind that human IgG1 has a stronger affinity to murine FcRn than to human FcRn (Neuber et al., 2014). Therefore for pharmacological studies, mouse strains that express human rather than murine FcRn should be used (Roopenian et al., 2010, Tam et al., 2013).

5.4.2   Design of an RFP targeting IL-11

The approach of gene delivery of monogenic cytokine inhibitors is not confined to IL-6 and can be exploited to target other cytokines that signal through heteromeric cytokine receptors. For instance, through replacement of the IL-6Rα moiety by the IL-11Rα, a mIL-11-RFP-Fc can be generated that is expected to potently block IL-11, another cytokine of the IL-6 family (Schwache and Müller-Newen, 2012). IL-11 has been recently identified as a dominant cytokine during gastrointestinal tumorigenesis (Putoczki et al., 2013).

5.4.3   Gene therapy

The main advantages of gene therapy over the use of recombinant proteins are maintenance of sustained and therapeutically relevant concentration of the protein eliminating the limitations of recombinant protein production and delivery. Additionally gene therapy allows for targeted and local gene expression rather than systemic availability of the therapeutic protein.

Methods for non-viral gene delivery of monogenic RFPs

Hydrodynamic Gene Delivery The experimental method of hydrodynamic transfection allowed us to effectively characterize the biological action of mIL-6-RFP-Fc *in vivo* but obviously this mode of gene delivery will not be suited for the treatment of humans

but is an option to consider in preclinical animal models (Katsimpoulas et al., 2012). Hydrodynamics-based transfection of naked plasmid DNA is of transient nature. A recent study reported the use of a cationic polymer carrier solution, which improved transfection efficiency of murine liver hepatocytes 2.5-fold in the liver of transfected animals compared to the conventional use of naked plasmid DNA (Nakamura et al., 2013).

Minicircular DNA (Minicircle) Another possibility to non-virally transfer monogenic RFPs *in vivo* uses minicircular DNA. Minicircular DNA (Minicircle) lacks bacterial sequences and has been shown to express superior amounts of serum human factor IX and α1-antitrypsin compared to standard plasmid DNAs transfected into mouse liver (Chen et al., 2003). Meanwhile bacterial systems have been developed that facilitate the production of purified minicircles in a time frame and quantity similar to those of routine plasmid DNA preparation (Kay et al., 2010). Recently, the well-established anti-IL-6-Rα antibody tocilizumab has been demonstrated to be effectively deliverable through hydrodynamic gene delivery by minicircular DNA (Yi et al., 2014). However this antibody required two separate minicircles, given the nature of antibody assembly from two chains. This is simplified by the approach presented herein.

DNA-functionalized gold-nanoparticles (GNP) For the therapy of inflammatory bowel diseases, a proof-of-concept study described the encapsulation of DNA-functionalized GNPs into primary isolated intestinal stem cells that could act as a Trojan horse for gene regulation therapies in inflammatory bowel disease (IBD). (Peng et al., 2015).

Methods for safe viral gene delivery of monogenic RFPs

For future therapeutic applications in patients, an analogous hIL-6-RFP-Fc designed for delivery through safe virus-based transfection methods such as integrating lentiviral vectors or non-integrating adeno-associated virus-derived vectors will be required.

Adeno-associated Virus (AAV) Adeno-associated viruses (AAV) are non-pathogenic in humans, and most importantly replication-defective in the absence of a helper virus (Mingozzi and High, 2011). Therefore AAVs are considered safe and have been successfully used in gene therapeutic studies. Wildtype (wt) AAV contains a single-stranded DNA genome within an icosahedric capsid of 25 nm diameter. The different AAV serotypes have tropism for a number of post-mitotic, long-lived cell types. AAV2, the best characterized of 12 different AAV serotypes, has a genome size of 4680 nucleotides with two open reading frames (ORFs) encoding for the capsid proteins (cap) and replication proteins (rep). The ORFs are further flanked by the inverted terminal repeats (ITR). In recombinant AAV (rAAV) the cap and rep ORFs are replaced with a transgene of interest. The transgene, composed of the therapeutic gene of interest, introns, polyadenylation signals and controlling promoter, should not exceed 5 kb and is integrated between both ITRs. For rAAV production rep/cap are delivered in *trans* with helper plasmids in HEK293 cells (Grimm et al., 2003) or in the insect cell line Sf9 (Mietzsch et al., 2014).

After transduction and transformation of the recombinant genome into stable episomal forms within the cell, long-term expression can be achieved even though integration into the genome has not occurred. The fusion protein p75-TNFR:Fc has been successfully delivered by AAV in animal models of rheumatoid arthritis as an alternative approach to TNF-α blockade with recombinant protein and showed long-term disease suppression (Sandalon et al., 2007). Similarly, rAAVs can be designed for targeted gene delivery and controlled expression of murine or human IL-6-RFP-Fc by different choices of organ- or tissue-specific promoters so that the consequences of local IL-6 inhibition can be studied.

5.4.4   Decyphering cytokine networks of IL-6 type cytokines

The IL-6 family of cytokines shares gp130 as a common β-chain receptor, which already hints at a system with great plasticity (Garbers et al., 2012). RFP are great tools to clarify the individual contributions of IL-6-type cytokines. Both for rheumatoid arthritis

(Wong et al., 2003) and inflammatory bowel disease (Neurath, 2014) the complex networks of cytokines including the IL-6 family of cytokines have been recognized.

Cytokine networks in IBD

OSM signal transduction in humans and rats can occur through two different types of receptors. OSM either signals through type I receptor complex consisting of LIFR/gp130, or the type II receptor complex consisting of OSMR/gp130, whereas in mice OSM signaling only occurs through the type II receptor complex (Drechsler et al., 2012). An important structural aspect in OSM that governs receptor affinity in humans is the presence of a BC-loop. Besides OSM the novel cytokine IL-31 has been shown to signal through OSMR. It has been described that IL-31R$^{-/-}$ mice show increased responsiveness to OSM (Bilsborough et al., 2010). So far it has not been shown, if either IL-31 dampens OSM-dependent signaling through OSMR by competition for receptor binding, or the other way around. In MEF mIL-31R cells OSM leads to more potent STAT3 activation than IL-31. It would be interesting to further dissect if shifts of target gene expression profiles can occur *in vivo* by interference through receptor fusion proteins targeting either IL-31 or OSM. A similar type of regulation has already been described for the LIF/OSM system. Cytokine signaling at the receptor level is governed by the individual affinity of cytokine-receptor interactions, soluble and membrane-bound receptor expression levels, and finally local cytokine levels.

5.4.5   Potential therapeutic applications for IL-6-RFPs in anti-IL-6 therapy

Lipid apheresis

Similar to the observed reduction of lipoprotein(a) serum levels in RA patients by anti-IL-6R treatment (Schultz et al., 2010), a recent study highlights the ability of anti-IL-6 treatment to lower elevated serum lipoprotein(a) concentrations leading to a reduced risk in developing cardiovascular diseases which presents a convenient alternative to costly and invasive lipid apheresis (Mueller et al., 2015).

Rheumatoid arthritis

Preclinical studies should explore modes of local inhibition of IL-6 by gene therapy as an alternative to systemic administration of antibodies targeting IL-6 in models of rheumatoid arthritis. Hybrid promoter systems consisting of the human IL-1 enhancer sequence in front of the human IL- 6 promoter allows autoregulation of transgene expression during arthritis (van de Loo et al., 2004) and could be used to express IL-6-RFPs in synovial joints.

6   Summary

Cytokines are small soluble proteins with regulatory functions in many biological processes including immune responses. Dysregulated cytokine signaling is often responsible for the development and maintenance of acute and chronic inflammation. Current anti-cytokine therapies have substantially improved the treatment of inflammatory diseases. Cytokine-targeting drugs are usually biologics such as neutralizing antibodies or soluble receptors. To target cytokines that signal through heteromeric receptor complexes we developed a strategy that involves the inline fusion of the ligand binding domains of the corresponding receptor subunits. These receptor fusion proteins (RFPs) are highly potent and specific, monogenic by design, and therefore well suited for gene transfer approaches.

The first part of this project deals with the development of a novel RFP targeting murine interleukin-31 (IL-31). IL-31, mostly involved in skin diseases, signals through heterodimeric receptor complexes comprised of the interleukin-31 receptor (IL-31R) and the oncostatin M receptor (OSMR) subunits.

- mIL-31-RFP was created by inline fusion of domains D1-D4 of murine OSMR and domains D1-D2 of murine IL-31R connected by a flexible linker and equipped with a 3V5-3HA-tag module to facilitate protein quantification and detection.

- Full-length mIL-31R cDNA was rebuilt by PCR fusion of missing exons from genomic DNA to Isoform 4. Subsequently MEF cells were stably transfected with mIL-31R to establish a cell-based system for the analysis of murine IL-31 and OSM signaling.

- mIL-31-RFP effectively and specifically inhibited IL-31-dependent signal-transduction and did not interfere with the activity of mOSM.

- HEK293 Flp-In/T-Rex cells were stably transfected with mIL-31-RFP cDNA, subjected to clonal selection for the production of recombinant mIL-31-RFP.

In the second part of this project, we investigated, as a proof-of-principle for other monogenic RFPs, the potential of the previously described mIL-6-RFP to inhibit interleukin-6 (IL-6) *in vivo*. Dysregulated persistent IL-6 production plays a pathological role in various autoimmune and chronic inflammatory diseases. Therefore, transgenic mice, that express mIL-6-RFP in an inducible and tissue-specific manner, were generated and characterized.

- First the V5-his-tag of the previously described mIL-6-RFP was exchanged with a 3V5-3HA-tag module to facilitate protein detection and quantification from serum of mice. The tag exchange did not influence its biological activity of mIL-6-RFP.

- mIL-6-RFP-3V5-3HA was efficiently expressed and secreted from HepG2 cells transiently transfected with the individual components of the expression system to be used in transgenic mice.

- Two independent Tg(TRE:mIL-6-RFP-3V5-3HA) mouse lines could be generated following pronucleus injection, and were subjected to further breeding. Generated mouse lines were crossed with Tg(LAP:rtTA) and Tg(Pod:rtTA) to generate double transgenic mice.

- Unfortunately, double transgenic mice did not express any measurable protein levels of mIL-6-RFP-3V5-3HA in either serum or in corresponding tissues.

In a parallel approach, we re-engineered mIL-6-RFP by fusion to the Fc of mIgG2a (mIL-6-RFP-Fc) for enhanced inhibitory activity and improved protein expression by codon optimization.

- Codon optimization led to increased mIL-6-RFP-Fc protein expression in HepG2 (2.5 fold) and muHepa cells (1.6 fold) compared to non-optimized cDNA following transient transfection of vectors encoding for mIL-6-RFP-Fc.

- HEK293 Flp-In/T-Rex cells were stably transfected with optimized mIL-6-RFP-Fc cDNA, and subjected to clonal selection for the production of recombinant mIL-6-RFP-Fc.

- mIL-6-RFP-Fc inhibited IL-6-dependent STAT3 phosphorylation in muHepa cells *in vitro* already at equimolar concentrations.

- mIL-6-RFP-Fc inhibited IL-6-dependent Ba/F3-mgp130/mIL-6Rα cell proliferation with a tenfold increased inhibitory activity when compared to mIL-6-RFP-V5-his.

- Upon application in mice, recombinant mIL-6-RFP-Fc inhibited IL-6-induced activation of the transcription factor STAT3 and ERK1/2 kinases in liver and kidney.

- Gene transfer through hydrodynamic plasmid delivery in mice resulted in hepatic production and secretion of mIL-6-RFP-Fc into the blood in considerable amounts, blocked hepatic acute-phase protein synthesis and improved kidney function in an ischemia and reperfusion injury model.

Our study establishes receptor fusion proteins as promising agents in anti-cytokine therapies through gene therapeutic approaches for future targeted and cost-effective treatments. The strategy described here is applicable for many cytokines involved in inflammatory and other diseases.

7   References

ANCEY, C., KUSTER, A., HAAN, S., HERRMANN, A., HEINRICH, P. C. & MÜLLER-NEWEN, G. 2003. A fusion protein of the gp130 and interleukin-6Ralpha ligand-binding domains acts as a potent interleukin-6 inhibitor. *J Biol Chem,* 278**,** 16968-72.

ANDUS, T., GEIGER, T., HIRANO, T., NORTHOFF, H., GANTER, U., BAUER, J., KISHIMOTO, T. & HEINRICH, P. C. 1987. Recombinant human B cell stimulatory factor 2 (BSF-2/IFN-beta 2) regulates beta-fibrinogen and albumin mRNA levels in Fao-9 cells. *FEBS Lett,* 221**,** 18-22.

ARAI, I., TSUJI, M., MIYAGAWA, K., TAKEDA, H., AKIYAMA, N. & SAITO, S. 2015. Repeated administration of IL-31 upregulates IL-31 receptor A (IL-31RA) in dorsal root ganglia and causes severe itch-associated scratching behaviour in mice. *Exp Dermatol,* 24**,** 75-8.

ATREYA, R., MUDTER, J., FINOTTO, S., MULLBERG, J., JOSTOCK, T., WIRTZ, S., SCHUTZ, M., BARTSCH, B., HOLTMANN, M., BECKER, C., STRAND, D., CZAJA, J., SCHLAAK, J. F., LEHR, H. A., AUTSCHBACH, F., SCHURMANN, G., NISHIMOTO, N., YOSHIZAKI, K., ITO, H., KISHIMOTO, T., GALLE, P. R., ROSE-JOHN, S. & NEURATH, M. F. 2000. Blockade of interleukin 6 trans signaling suppresses T-cell resistance against apoptosis in chronic intestinal inflammation: evidence in crohn disease and experimental colitis in vivo. *Nat Med,* 6**,** 583-8.

BAKER, M. P., REYNOLDS, H. M., LUMICISI, B. & BRYSON, C. J. 2010. Immunogenicity of protein therapeutics: The key causes, consequences and challenges. *Self Nonself,* 1**,** 314-322.

BANDO, T., MORIKAWA, Y., KOMORI, T. & SENBA, E. 2006. Complete overlap of interleukin-31 receptor A and oncostatin M receptor beta in the adult dorsal root ganglia with distinct developmental expression patterns. *Neuroscience,* 142**,** 1263-71.

BAZAN, J. F. 1990. Haemopoietic receptors and helical cytokines. *Immunol Today,* 11**,** 350-4.

BEALE, E. G., CLOUTHIER, D. E. & HAMMER, R. E. 1992. Cell-specific expression of cytosolic phosphoenolpyruvate carboxykinase in transgenic mice. *FASEB J,* 6**,** 3330-7.

BEIGEL, F., FRIEDRICH, M., PROBST, C., SOTLAR, K., GOKE, B., DIEGELMANN, J. & BRAND, S. 2014. Oncostatin M mediates STAT3-dependent intestinal epithelial restitution via increased cell proliferation, decreased apoptosis and upregulation of SERPIN family members. *PLoS One,* 9**,** e93498.

BETTELLI, E., CARRIER, Y., GAO, W., KORN, T., STROM, T. B., OUKKA, M., WEINER, H. L. & KUCHROO, V. K. 2006. Reciprocal developmental pathways for the generation of pathogenic effector TH17 and regulatory T cells. *Nature,* 441**,** 235-8.

BILSBOROUGH, J., LEUNG, D. Y., MAURER, M., HOWELL, M., BOGUNIEWICZ, M., YAO, L., STOREY, H., LECIEL, C., HARDER, B. & GROSS, J. A. 2006. IL-31 is associated with cutaneous lymphocyte antigen-positive skin homing T cells in patients with atopic dermatitis. *J Allergy Clin Immunol,* 117**,** 418-25.

BILSBOROUGH, J., MUDRI, S., CHADWICK, E., HARDER, B. & DILLON, S. R. 2010. IL-31 receptor (IL-31RA) knockout mice exhibit elevated responsiveness to oncostatin M. *J Immunol,* 185**,** 6023-30.

BOULANGER, M. J., CHOW, D. C., BREVNOVA, E. E. & GARCIA, K. C. 2003. Hexameric structure and assembly of the interleukin-6/IL-6 alpha-receptor/gp130 complex. *Science,* 300**,** 2101-4.

BROLUND, L., KUSTER, A., KORR, S., VOGT, M. & MÜLLER-NEWEN, G. 2011. A receptor fusion protein for the inhibition of murine oncostatin M. *BMC Biotechnol,* 11**,** 3.

BROXMEYER, H. E., LI, J., HANGOC, G., COOPER, S., TAO, W., MANTEL, C., GRAHAM-EVANS, B., GHILARDI, N. & DE SAUVAGE, F. J. 2007. Regulation of myeloid progenitor cell proliferation/survival by IL-31 receptor and IL-31. *Exp Hematol,* 35**,** 78-86.

CEVIKBAS, F., KEMPKES, C., BUHL, T., MESS, C., BUDDENKOTTE, J. & STEINHOFF, M. 2014. Role of Interleukin-31 and Oncostatin M in Itch and Neuroimmune Communication. *In:* CARSTENS, E. & AKIYAMA, T. (eds.) *Itch: Mechanisms and Treatment.* Boca Raton (FL).

CHEN, Z. Y., HE, C. Y., EHRHARDT, A. & KAY, M. A. 2003. Minicircle DNA vectors devoid of bacterial DNA result in persistent and high-level transgene expression in vivo. *Mol Ther,* 8**,** 495-500.

CLONTECH 2010. pTRE-Tight-BI Vector Information (PT3893-5). Clontech Laboratories.

COLLISON, L. W., DELGOFFE, G. M., GUY, C. S., VIGNALI, K. M., CHATURVEDI, V., FAIRWEATHER, D., SATOSKAR, A. R., GARCIA, K. C., HUNTER, C. A., DRAKE, C. G., MURRAY, P. J. & VIGNALI, D. A. 2012. The composition and signaling of the IL-35 receptor are unconventional. *Nat Immunol,* 13**,** 290-9.

CONTENT, J., DE WIT, L., POUPART, P., OPDENAKKER, G., VAN DAMME, J. & BILLIAU, A. 1985. Induction of a 26-kDa-protein mRNA in human cells treated with an interleukin-1-related, leukocyte-derived factor. *Eur J Biochem,* 152**,** 253-7.

CORNELISSEN, C., BRANS, R., CZAJA, K., SKAZIK, C., MARQUARDT, Y., ZWADLO-KLARWASSER, G., KIM, A., BICKERS, D. R., LUSCHER-FIRZLAFF, J., LUSCHER, B. & BARON, J. M. 2011. Ultraviolet B radiation and reactive oxygen species modulate interleukin-31 expression in T lymphocytes, monocytes and dendritic cells. *Br J Dermatol,* 165**,** 966-75.

COULIE, P. G., CAYPHAS, S., VINK, A., UYTTENHOVE, C. & VAN SNICK, J. 1987a. Interleukin-HP1-related hybridoma and plasmacytoma growth factors induced by lipopolysaccharide in vivo. *Eur J Immunol,* 17**,** 1217-20.

COULIE, P. G., VANHECKE, A., VAN DAMME, J., CAYPHAS, S., POUPART, P., DE WIT, L. & CONTENT, J. 1987b. High-affinity binding sites for human 26-kDa protein (interleukin 6, B cell stimulatory factor-2, human hybridoma plasmacytoma growth factor, interferon-beta 2), different from those of type I interferon (alpha, beta), on lymphoblastoid cells. *Eur J Immunol,* 17**,** 1435-40.

DALL'ACQUA, W. F., KIENER, P. A. & WU, H. 2006. Properties of human IgG1s engineered for enhanced binding to the neonatal Fc receptor (FcRn). *J Biol Chem,* 281**,** 23514-24.

DAMBACHER, J., BEIGEL, F., SEIDERER, J., HALLER, D., GOKE, B., AUERNHAMMER, C. J. & BRAND, S. 2007. Interleukin 31 mediates MAP kinase and STAT1/3 activation in intestinal epithelial cells and its expression is upregulated in inflammatory bowel disease. *Gut,* 56**,** 1257-65.

DEVARAJAN, P. 2005. Cellular and molecular derangements in acute tubular necrosis. *Curr Opin Pediatr,* 17**,** 193-9.

DIEZEL, W., KOPPERSCHLAGER, G. & HOFMANN, E. 1972. An improved procedure for protein staining in polyacrylamide gels with a new type of Coomassie Brilliant Blue. *Anal Biochem,* 48**,** 617-20.

DILLON, S. R., SPRECHER, C., HAMMOND, A., BILSBOROUGH, J., ROSENFELD-FRANKLIN, M., PRESNELL, S. R., HAUGEN, H. S., MAURER, M., HARDER, B., JOHNSTON, J., BORT, S., MUDRI, S., KUIJPER, J. L., BUKOWSKI, T., SHEA, P., DONG, D. L., DASOVICH, M., GRANT, F. J., LOCKWOOD, L., LEVIN, S. D., LECIEL, C., WAGGIE, K., DAY, H., TOPOUZIS, S., KRAMER, J., KUESTNER, R., CHEN, Z., FOSTER, D., PARRISH-NOVAK, J. & GROSS, J. A. 2004. Interleukin 31, a cytokine produced by activated T cells, induces dermatitis in mice. *Nat Immunol,* 5**,** 752-60.

DIVEU, C., LELIEVRE, E., PERRET, D., LAK-HAL, A. H., FROGER, J., GUILLET, C., CHEVALIER, S., ROUSSEAU, F., WESA, A., PREISSER, L., CHABBERT, M., GAUCHAT, J. F., GALY, A., GASCAN, H. & MOREL, A. 2003. GPL, a novel cytokine receptor related to GP130 and leukemia inhibitory factor receptor. *J Biol Chem,* 278**,** 49850-9.

DIVEU, C., VENEREAU, E., FROGER, J., RAVON, E., GRIMAUD, L., ROUSSEAU, F., CHEVALIER, S. & GASCAN, H. 2006. Molecular and functional

characterization of a soluble form of oncostatin M/interleukin-31 shared receptor. *J Biol Chem,* 281**,** 36673-82.

DRECHSLER, J., GROTZINGER, J. & HERMANNS, H. M. 2012. Characterization of the rat oncostatin M receptor complex which resembles the human, but differs from the murine cytokine receptor. *PLoS One,* 7**,** e43155.

DREUW, A., RADTKE, S., PFLANZ, S., LIPPOK, B. E., HEINRICH, P. C. & HERMANNS, H. M. 2004. Characterization of the signaling capacities of the novel gp130-like cytokine receptor. *J Biol Chem,* 279**,** 36112-20.

ECONOMIDES, A. N., CARPENTER, L. R., RUDGE, J. S., WONG, V., KOEHLER-STEC, E. M., HARTNETT, C., PYLES, E. A., XU, X., DALY, T. J., YOUNG, M. R., FANDL, J. P., LEE, F., CARVER, S., MCNAY, J., BAILEY, K., RAMAKANTH, S., HUTABARAT, R., HUANG, T. T., RADZIEJEWSKI, C., YANCOPOULOS, G. D. & STAHL, N. 2003. Cytokine traps: multi-component, high-affinity blockers of cytokine action. *Nat Med,* 9**,** 47-52.

EDUKULLA, R., SINGH, B., JEGGA, A. G., SONTAKE, V., DILLON, S. R. & MADALA, S. K. 2015. Th2 cytokines augment IL-31/IL-31RA interactions via STAT6-dependent IL-31RA expression. *J Biol Chem.*

EULENFELD, R., DITTRICH, A., KHOURI, C., MULLER, P. J., MUTZE, B., WOLF, A. & SCHAPER, F. 2012. Interleukin-6 signalling: more than Jaks and STATs. *Eur J Cell Biol,* 91**,** 486-95.

FAGOE, N. D., EGGERS, R., VERHAAGEN, J. & MASON, M. R. 2014. A compact dual promoter adeno-associated viral vector for efficient delivery of two genes to dorsal root ganglion neurons. *Gene Ther,* 21**,** 242-52.

GABAY, C. & KUSHNER, I. 1999. Acute-phase proteins and other systemic responses to inflammation. *N Engl J Med,* 340**,** 448-54.

GALLAGHER, A. R., SCHONIG, K., BROWN, N., BUJARD, H. & WITZGALL, R. 2003. Use of the tetracycline system for inducible protein synthesis in the kidney. *J Am Soc Nephrol,* 14**,** 2042-51.

GARBERS, C., HERMANNS, H. M., SCHAPER, F., MÜLLER-NEWEN, G., GROTZINGER, J., ROSE-JOHN, S. & SCHELLER, J. 2012. Plasticity and cross-talk of interleukin 6-type cytokines. *Cytokine Growth Factor Rev,* 23**,** 85-97.

GARBERS, C., THAISS, W., JONES, G. W., WAETZIG, G. H., LORENZEN, I., GUILHOT, F., LISSILAA, R., FERLIN, W. G., GROTZINGER, J., JONES, S. A., ROSE-JOHN, S. & SCHELLER, J. 2011. Inhibition of classic signaling is a novel function of soluble glycoprotein 130 (sgp130), which is controlled by the ratio of interleukin 6 and soluble interleukin 6 receptor. *J Biol Chem,* 286**,** 42959-70.

GARMAN, R. D., JACOBS, K. A., CLARK, S. C. & RAULET, D. H. 1987. B-cell-stimulatory factor 2 (beta 2 interferon) functions as a second signal for

interleukin 2 production by mature murine T cells. *Proc Natl Acad Sci U S A,* 84**,** 7629-33.

GAULDIE, J., RICHARDS, C., HARNISH, D., LANSDORP, P. & BAUMANN, H. 1987. Interferon beta 2/B-cell stimulatory factor type 2 shares identity with monocyte-derived hepatocyte-stimulating factor and regulates the major acute phase protein response in liver cells. *Proc Natl Acad Sci U S A,* 84**,** 7251-5.

GHILARDI, N., LI, J., HONGO, J. A., YI, S., GURNEY, A. & DE SAUVAGE, F. J. 2002. A novel type I cytokine receptor is expressed on monocytes, signals proliferation, and activates STAT-3 and STAT-5. *J Biol Chem,* 277**,** 16831-6.

GRIMM, D., KAY, M. A. & KLEINSCHMIDT, J. A. 2003. Helper virus-free, optically controllable, and two-plasmid-based production of adeno-associated virus vectors of serotypes 1 to 6. *Mol Ther,* 7**,** 839-50.

GRIMSTAD, O., SAWANOBORI, Y., VESTERGAARD, C., BILSBOROUGH, J., OLSEN, U. B., GRONHOJ-LARSEN, C. & MATSUSHIMA, K. 2009. Anti-interleukin-31-antibodies ameliorate scratching behaviour in NC/Nga mice: a model of atopic dermatitis. *Exp Dermatol,* 18**,** 35-43.

GRIVENNIKOV, S., KARIN, E., TERZIC, J., MUCIDA, D., YU, G. Y., VALLABHAPURAPU, S., SCHELLER, J., ROSE-JOHN, S., CHEROUTRE, H., ECKMANN, L. & KARIN, M. 2009. IL-6 and Stat3 are required for survival of intestinal epithelial cells and development of colitis-associated cancer. *Cancer Cell,* 15**,** 103-13.

GUSCHIN, D., ROGERS, N., BRISCOE, J., WITTHUHN, B., WATLING, D., HORN, F., PELLEGRINI, S., YASUKAWA, K., HEINRICH, P., STARK, G. R. & ET AL. 1995. A major role for the protein tyrosine kinase JAK1 in the JAK/STAT signal transduction pathway in response to interleukin-6. *EMBO J,* 14**,** 1421-9.

HASAN, M. T., SCHONIG, K., BERGER, S., GRAEWE, W. & BUJARD, H. 2001. Long-term, noninvasive imaging of regulated gene expression in living mice. *Genesis,* 29**,** 116-22.

HEINRICH, P. C., BEHRMANN, I., HAAN, S., HERMANNS, H. M., MÜLLER-NEWEN, G. & SCHAPER, F. 2003. Principles of interleukin (IL)-6-type cytokine signalling and its regulation. *Biochem J,* 374**,** 1-20.

HEISE, R., NEIS, M. M., MARQUARDT, Y., JOUSSEN, S., HEINRICH, P. C., MERK, H. F., HERMANNS, H. M. & BARON, J. M. 2009. IL-31 receptor alpha expression in epidermal keratinocytes is modulated by cell differentiation and interferon gamma. *J Invest Dermatol,* 129**,** 240-3.

HERMANNS, H. M., RADTKE, S., SCHAPER, F., HEINRICH, P. C. & BEHRMANN, I. 2000. Non-redundant signal transduction of interleukin-6-type cytokines. The adapter protein Shc is specifically recruited to rhe oncostatin M receptor. *J Biol Chem,* 275**,** 40742-8.

HIBI, M., MURAKAMI, M., SAITO, M., HIRANO, T., TAGA, T. & KISHIMOTO, T. 1990. Molecular cloning and expression of an IL-6 signal transducer, gp130. *Cell,* 63**,** 1149-57.

HIRANO, T., MATSUDA, T., TURNER, M., MIYASAKA, N., BUCHAN, G., TANG, B., SATO, K., SHIMIZU, M., MAINI, R., FELDMANN, M. & ET AL. 1988. Excessive production of interleukin 6/B cell stimulatory factor-2 in rheumatoid arthritis. *Eur J Immunol,* 18**,** 1797-801.

HIRANO, T., TAGA, T., YASUKAWA, K., NAKAJIMA, K., NAKANO, N., TAKATSUKI, F., SHIMIZU, M., MURASHIMA, A., TSUNASAWA, S., SAKIYAMA, F. & ET AL. 1987. Human B-cell differentiation factor defined by an anti-peptide antibody and its possible role in autoantibody production. *Proc Natl Acad Sci U S A,* 84**,** 228-31.

HIRANO, T., YASUKAWA, K., HARADA, H., TAGA, T., WATANABE, Y., MATSUDA, T., KASHIWAMURA, S., NAKAJIMA, K., KOYAMA, K., IWAMATSU, A. & ET AL. 1986. Complementary DNA for a novel human interleukin (BSF-2) that induces B lymphocytes to produce immunoglobulin. *Nature,* 324**,** 73-6.

HOREJS-HOECK, J., SCHWARZ, H., LAMPRECHT, S., MAIER, E., HAINZL, S., SCHMITTNER, M., POSSELT, G., STOECKLINGER, A., HAWRANEK, T. & DUSCHL, A. 2012. Dendritic cells activated by IFN-gamma/STAT1 express IL-31 receptor and release proinflammatory mediators upon IL-31 treatment. *J Immunol,* 188**,** 5319-26.

HOWARD, C., TAO, S., YANG, H. C., FOGO, A. B., WOODGETT, J. R., HARRIS, R. C. & RAO, R. 2012. Specific deletion of glycogen synthase kinase-3beta in the renal proximal tubule protects against acute nephrotoxic injury in mice. *Kidney Int,* 82**,** 1000-9.

HUTCHINS, A. P., DIEZ, D., TAKAHASHI, Y., AHMAD, S., JAUCH, R., TREMBLAY, M. L. & MIRANDA-SAAVEDRA, D. 2013. Distinct transcriptional regulatory modules underlie STAT3's cell type-independent and cell type-specific functions. *Nucleic Acids Res,* 41**,** 2155-70.

IVANOV, II, MCKENZIE, B. S., ZHOU, L., TADOKORO, C. E., LEPELLEY, A., LAFAILLE, J. J., CUA, D. J. & LITTMAN, D. R. 2006. The orphan nuclear receptor RORgammat directs the differentiation program of proinflammatory IL-17+ T helper cells. *Cell,* 126**,** 1121-33.

JONES, S. A., FRASER, D. J., FIELDING, C. A. & JONES, G. W. 2015. Interleukin-6 in renal disease and therapy. *Nephrol Dial Transplant,* 30**,** 564-74.

JOSTOCK, T., MULLBERG, J., OZBEK, S., ATREYA, R., BLINN, G., VOLTZ, N., FISCHER, M., NEURATH, M. F. & ROSE-JOHN, S. 2001. Soluble gp130 is the natural inhibitor of soluble interleukin-6 receptor transsignaling responses. *Eur J Biochem,* 268**,** 160-7.

KANG, S., TANAKA, T. & KISHIMOTO, T. 2015. Therapeutic uses of anti-interleukin-6 receptor antibody. *Int Immunol,* 27**,** 21-9.

KASUTANI, K., FUJII, E., OHYAMA, S., ADACHI, H., HASEGAWA, M., KITAMURA, H. & YAMASHITA, N. 2014. Anti-IL-31 receptor antibody is shown to be a potential therapeutic option for treating itch and dermatitis in mice. *Br J Pharmacol,* 171**,** 5049-58.

KATSIMPOULAS, M., ZACHAROULIS, D., HABIB, N. & KOSTAKIS, A. 2012. Animal Models for Hydrodynamic Gene Delivery. *Chemical Biology.*

KAWANO, M., HIRANO, T., MATSUDA, T., TAGA, T., HORII, Y., IWATO, K., ASAOKU, H., TANG, B., TANABE, O., TANAKA, H. & ET AL. 1988. Autocrine generation and requirement of BSF-2/IL-6 for human multiple myelomas. *Nature,* 332**,** 83-5.

KAY, M. A., HE, C. Y. & CHEN, Z. Y. 2010. A robust system for production of minicircle DNA vectors. *Nat Biotechnol,* 28**,** 1287-9.

KIBERD, B. A. 1993. Interleukin-6 receptor blockage ameliorates murine lupus nephritis. *J Am Soc Nephrol,* 4**,** 58-61.

KIELAR, M. L., JOHN, R., BENNETT, M., RICHARDSON, J. A., SHELTON, J. M., CHEN, L., JEYARAJAH, D. R., ZHOU, X. J., ZHOU, H., CHIQUETT, B., NAGAMI, G. T. & LU, C. Y. 2005. Maladaptive role of IL-6 in ischemic acute renal failure. *J Am Soc Nephrol,* 16**,** 3315-25.

KIM, S., KIM, H. J., YANG, H. S., KIM, E., HUH, I. S. & YANG, J. M. 2011. IL-31 Serum Protein and Tissue mRNA Levels in Patients with Atopic Dermatitis. *Ann Dermatol,* 23**,** 468-73.

KIMURA, A. & KISHIMOTO, T. 2010. IL-6: regulator of Treg/Th17 balance. *Eur J Immunol,* 40**,** 1830-5.

KISHIMOTO, T., AKIRA, S., NARAZAKI, M. & TAGA, T. 1995. Interleukin-6 family of cytokines and gp130. *Blood,* 86**,** 1243-54.

KLEINER, G., MARCUZZI, A., ZANIN, V., MONASTA, L. & ZAULI, G. 2013. Cytokine levels in the serum of healthy subjects. *Mediators Inflamm,* 2013**,** 434010.

KO, G. J., GRIGORYEV, D. N., LINFERT, D., JANG, H. R., WATKINS, T., CHEADLE, C., RACUSEN, L. & RABB, H. 2010. Transcriptional analysis of kidneys during repair from AKI reveals possible roles for NGAL and KIM-1 as biomarkers of AKI-to-CKD transition. *Am J Physiol Renal Physiol,* 298**,** F1472-83.

KORN, T., BETTELLI, E., GAO, W., AWASTHI, A., JAGER, A., STROM, T. B., OUKKA, M. & KUCHROO, V. K. 2007. IL-21 initiates an alternative pathway to induce proinflammatory T(H)17 cells. *Nature,* 448**,** 484-7.

KUNSLEBEN, N., RUDRICH, U., GEHRING, M., NOVAK, N., KAPP, A. & RAAP, U. 2015. IL-31 induces Chemotaxis, Calcium Mobilization, Release of Reactive Oxygen Species and CCL26 in Eosinophils which are Capable to Release IL-31. *J Invest Dermatol.*

KUO, T. T. & AVESON, V. G. 2011. Neonatal Fc receptor and IgG-based therapeutics. *MAbs,* 3**,** 422-30.

LE SAUX, S., ROUSSEAU, F., BARBIER, F., RAVON, E., GRIMAUD, L., DANGER, Y., FROGER, J., CHEVALIER, S. & GASCAN, H. 2010. Molecular dissection of human interleukin-31-mediated signal transduction through site-directed mutagenesis. *J Biol Chem,* 285**,** 3470-7.

LEE, H. C., CHOE, J., CHI, S. G. & KIM, Y. K. 2009. Exon junction complex enhances translation of spliced mRNAs at multiple steps. *Biochem Biophys Res Commun,* 384**,** 334-40.

LIENENLUKE, B. & CHRIST, B. 2007. Impact of interleukin-6 on the glucose metabolic capacity in rat liver. *Histochem Cell Biol,* 128**,** 371-7.

LIU, F., SONG, Y. & LIU, D. 1999. Hydrodynamics-based transfection in animals by systemic administration of plasmid DNA. *Gene Ther,* 6**,** 1258-66.

LIU, Y. C., STONE, K. & VAN RHEE, F. 2014. Siltuximab for multicentric Castleman disease. *Expert Rev Hematol,* 7**,** 545-57.

LIVAK, K. J. & SCHMITTGEN, T. D. 2001. Analysis of relative gene expression data using real-time quantitative PCR and the 2(-Delta Delta C(T)) Method. *Methods,* 25**,** 402-8.

LOSER, P., JENNINGS, G. S., STRAUSS, M. & SANDIG, V. 1998. Reactivation of the previously silenced cytomegalovirus major immediate-early promoter in the mouse liver: involvement of NFkappaB. *J Virol,* 72**,** 180-90.

LOTZ, M., JIRIK, F., KABOURIDIS, P., TSOUKAS, C., HIRANO, T., KISHIMOTO, T. & CARSON, D. A. 1988. B cell stimulating factor 2/interleukin 6 is a costimulant for human thymocytes and T lymphocytes. *J Exp Med,* 167**,** 1253-8.

LUIG, M., KLUGER, M. A., GOERKE, B., MEYER, M., NOSKO, A., YAN, I., SCHELLER, J., MITTRUCKER, H. W., ROSE-JOHN, S., STAHL, R. A., PANZER, U. & STEINMETZ, O. M. 2015. Inflammation-Induced IL-6 Functions as a Natural Brake on Macrophages and Limits GN. *J Am Soc Nephrol.*

LUPARDUS, P. J., SKINIOTIS, G., RICE, A. J., THOMAS, C., FISCHER, S., WALZ, T. & GARCIA, K. C. 2011. Structural snapshots of full-length Jak1, a transmembrane gp130/IL-6/IL-6Ralpha cytokine receptor complex, and the receptor-Jak1 holocomplex. *Structure,* 19**,** 45-55.

MASON, M. R., EHLERT, E. M., EGGERS, R., POOL, C. W., HERMENING, S., HUSEINOVIC, A., TIMMERMANS, E., BLITS, B. & VERHAAGEN, J. 2010.

Comparison of AAV serotypes for gene delivery to dorsal root ganglion neurons. *Mol Ther,* 18**,** 715-24.

MAUER, J., DENSON, J. L. & BRUNING, J. C. 2015. Versatile functions for IL-6 in metabolism and cancer. *Trends Immunol,* 36**,** 92-101.

MENDOZA, C. E., ROSADO, M. F. & BERNAL, L. 2001. The role of interleukin-6 in cases of cardiac myxoma. Clinical features, immunologic abnormalities, and a possible role in recurrence. *Tex Heart Inst J,* 28**,** 3-7.

METZ, S., WIESINGER, M., VOGT, M., LAUKS, H., SCHMALZING, G., HEINRICH, P. C. & MÜLLER-NEWEN, G. 2007. Characterization of the Interleukin (IL)-6 Inhibitor IL-6-RFP: fused receptor domains act as high affinity cytokine-binding proteins. *J Biol Chem,* 282**,** 1238-48.

MIETZSCH, M., GRASSE, S., ZURAWSKI, C., WEGER, S., BENNETT, A., AGBANDJE-MCKENNA, M., MUZYCZKA, N., ZOLOTUKHIN, S. & HEILBRONN, R. 2014. OneBac: platform for scalable and high-titer production of adeno-associated virus serotype 1-12 vectors for gene therapy. *Hum Gene Ther,* 25**,** 212-22.

MINGOZZI, F. & HIGH, K. A. 2011. Therapeutic in vivo gene transfer for genetic disease using AAV: progress and challenges. *Nat Rev Genet,* 12**,** 341-55.

MUELLER, N., SCHULTE, D. M., TUERK, K., FREITAG-WOLF, S., HAMPE, J., ZEUNER, R., SCHROEDER, J. O., GOUNI-BERTHOLD, I., BERTHOLD, H. K., KRONE, W., ROSE-JOHN, S., SCHREIBER, S. & LAUDES, M. 2015. IL-6 blockade by monoclonal antibodies inhibits apolipoprotein(a) expression and lipoprotein(a) synthesis in humans. *J Lipid Res.*

MULLBERG, J., SCHOOLTINK, H., STOYAN, T., GUNTHER, M., GRAEVE, L., BUSE, G., MACKIEWICZ, A., HEINRICH, P. C. & ROSE-JOHN, S. 1993. The soluble interleukin-6 receptor is generated by shedding. *Eur J Immunol,* 23**,** 473-80.

MÜLLER-NEWEN, G., KOHNE, C., KEUL, R., HEMMANN, U., MULLER-ESTERL, W., WIJDENES, J., BRAKENHOFF, J. P., HART, M. H. & HEINRICH, P. C. 1996. Purification and characterization of the soluble interleukin-6 receptor from human plasma and identification of an isoform generated through alternative splicing. *Eur J Biochem,* 236**,** 837-42.

MÜLLER-NEWEN, G., KUSTER, A., HEMMANN, U., KEUL, R., HORSTEN, U., MARTENS, A., GRAEVE, L., WIJDENES, J. & HEINRICH, P. C. 1998. Soluble IL-6 receptor potentiates the antagonistic activity of soluble gp130 on IL-6 responses. *J Immunol,* 161**,** 6347-55.

NAGAYAMA, Y., BRAUN, G. S., JAKOBS, C. M., MARUTA, Y., VAN ROEYEN, C. R., KLINKHAMMER, B. M., BOOR, P., VILLA, L., RAFFETSEDER, U., TRAUTWEIN, C., GORTZ, D., MÜLLER-NEWEN, G., OSTENDORF, T. &

FLOEGE, J. 2014. Gp130-dependent signaling in the podocyte. *Am J Physiol Renal Physiol,* 307**,** F346-55.

NAKAMURA, S., MAEHARA, T., WATANABE, S., ISHIHARA, M. & SATO, M. 2013. Improvement of hydrodynamics-based gene transfer of nonviral DNA targeted to murine hepatocytes. *Biomed Res Int,* 2013**,** 928790.

NARAZAKI, M., YASUKAWA, K., SAITO, T., OHSUGI, Y., FUKUI, H., KOISHIHARA, Y., YANCOPOULOS, G. D., TAGA, T. & KISHIMOTO, T. 1993. Soluble forms of the interleukin-6 signal-transducing receptor component gp130 in human serum possessing a potential to inhibit signals through membrane-anchored gp130. *Blood,* 82**,** 1120-6.

NECHEMIA-ARBELY, Y., BARKAN, D., PIZOV, G., SHRIKI, A., ROSE-JOHN, S., GALUN, E. & AXELROD, J. H. 2008. IL-6/IL-6R axis plays a critical role in acute kidney injury. *J Am Soc Nephrol,* 19**,** 1106-15.

NEIS, M. M., PETERS, B., DREUW, A., WENZEL, J., BIEBER, T., MAUCH, C., KRIEG, T., STANZEL, S., HEINRICH, P. C., MERK, H. F., BOSIO, A., BARON, J. M. & HERMANNS, H. M. 2006. Enhanced expression levels of IL-31 correlate with IL-4 and IL-13 in atopic and allergic contact dermatitis. *J Allergy Clin Immunol,* 118**,** 930-7.

NEUBER, T., FRESE, K., JAEHRLING, J., JAGER, S., DAUBERT, D., FELDERER, K., LINNEMANN, M., HOHNE, A., KADEN, S., KOLLN, J., TILLER, T., BROCKS, B., OSTENDORP, R. & PABST, S. 2014. Characterization and screening of IgG binding to the neonatal Fc receptor. *MAbs,* 6**,** 928-42.

NEURATH, M. F. 2014. Cytokines in inflammatory bowel disease. *Nat Rev Immunol,* 14**,** 329-42.

NICKOLAS, T. L., BARASCH, J. & DEVARAJAN, P. 2008. Biomarkers in acute and chronic kidney disease. *Curr Opin Nephrol Hypertens,* 17**,** 127-32.

NISHIMOTO, N., KANAKURA, Y., AOZASA, K., JOHKOH, T., NAKAMURA, M., NAKANO, S., NAKANO, N., IKEDA, Y., SASAKI, T., NISHIOKA, K., HARA, M., TAGUCHI, H., KIMURA, Y., KATO, Y., ASAOKU, H., KUMAGAI, S., KODAMA, F., NAKAHARA, H., HAGIHARA, K., YOSHIZAKI, K. & KISHIMOTO, T. 2005. Humanized anti-interleukin-6 receptor antibody treatment of multicentric Castleman disease. *Blood,* 106**,** 2627-32.

NIYONSABA, F., USHIO, H., HARA, M., YOKOI, H., TOMINAGA, M., TAKAMORI, K., KAJIWARA, N., SAITO, H., NAGAOKA, I., OGAWA, H. & OKUMURA, K. 2010. Antimicrobial peptides human beta-defensins and cathelicidin LL-37 induce the secretion of a pruritogenic cytokine IL-31 by human mast cells. *J Immunol,* 184**,** 3526-34.

NORDAN, R. P. & POTTER, M. 1986. A macrophage-derived factor required by plasmacytomas for survival and proliferation in vitro. *Science,* 233**,** 566-9.

NOWELL, M. A., RICHARDS, P. J., HORIUCHI, S., YAMAMOTO, N., ROSE-JOHN, S., TOPLEY, N., WILLIAMS, A. S. & JONES, S. A. 2003. Soluble IL-6 receptor governs IL-6 activity in experimental arthritis: blockade of arthritis severity by soluble glycoprotein 130. *J Immunol,* 171**,** 3202-9.

OKADA, M., KITAHARA, M., KISHIMOTO, S., MATSUDA, T., HIRANO, T. & KISHIMOTO, T. 1988. IL-6/BSF-2 functions as a killer helper factor in the in vitro induction of cytotoxic T cells. *J Immunol,* 141**,** 1543-9.

PARK, K., PARK, J. H., YANG, W. J., LEE, J. J., SONG, M. J. & KIM, H. P. 2012. Transcriptional activation of the IL31 gene by NFAT and STAT6. *J Leukoc Biol,* 91**,** 245-57.

PATEL, N. S., CHATTERJEE, P. K., DI PAOLA, R., MAZZON, E., BRITTI, D., DE SARRO, A., CUZZOCREA, S. & THIEMERMANN, C. 2005. Endogenous interleukin-6 enhances the renal injury, dysfunction, and inflammation caused by ischemia/reperfusion. *J Pharmacol Exp Ther,* 312**,** 1170-8.

PENG, H., WANG, C., XU, X., YU, C. & WANG, Q. 2015. An intestinal Trojan horse for gene delivery. *Nanoscale,* 7**,** 4354-60.

PERRIGOUE, J. G., LI, J., ZAPH, C., GOLDSCHMIDT, M., SCOTT, P., DE SAUVAGE, F. J., PEARCE, E. J., GHILARDI, N. & ARTIS, D. 2007. IL-31-IL-31R interactions negatively regulate type 2 inflammation in the lung. *J Exp Med,* 204**,** 481-7.

PERRIGOUE, J. G., ZAPH, C., GUILD, K., DU, Y. & ARTIS, D. 2009. IL-31-IL-31R interactions limit the magnitude of Th2 cytokine-dependent immunity and inflammation following intestinal helminth infection. *J Immunol,* 182**,** 6088-94.

PETERS, M., JACOBS, S., EHLERS, M., VOLLMER, P., MULLBERG, J., WOLF, E., BREM, G., MEYER ZUM BUSCHENFELDE, K. H. & ROSE-JOHN, S. 1996. The function of the soluble interleukin 6 (IL-6) receptor in vivo: sensitization of human soluble IL-6 receptor transgenic mice towards IL-6 and prolongation of the plasma half-life of IL-6. *J Exp Med,* 183**,** 1399-406.

PFLANZ, S., TIMANS, J. C., CHEUNG, J., ROSALES, R., KANZLER, H., GILBERT, J., HIBBERT, L., CHURAKOVA, T., TRAVIS, M., VAISBERG, E., BLUMENSCHEIN, W. M., MATTSON, J. D., WAGNER, J. L., TO, W., ZURAWSKI, S., MCCLANAHAN, T. K., GORMAN, D. M., BAZAN, J. F., DE WAAL MALEFYT, R., RENNICK, D. & KASTELEIN, R. A. 2002. IL-27, a heterodimeric cytokine composed of EBI3 and p28 protein, induces proliferation of naive CD4+ T cells. *Immunity,* 16**,** 779-90.

PRESNYAK, V., ALHUSAINI, N., CHEN, Y. H., MARTIN, S., MORRIS, N., KLINE, N., OLSON, S., WEINBERG, D., BAKER, K. E., GRAVELEY, B. R. & COLLER, J. 2015. Codon optimality is a major determinant of mRNA stability. *Cell,* 160**,** 1111-24.

PUTOCZKI, T. L., THIEM, S., LOVING, A., BUSUTTIL, R. A., WILSON, N. J., ZIEGLER, P. K., NGUYEN, P. M., PREAUDET, A., FARID, R., EDWARDS, K. M., BOGLEV, Y., LUWOR, R. B., JARNICKI, A., HORST, D., BOUSSIOUTAS, A., HEATH, J. K., SIEBER, O. M., PLEINES, I., KILE, B. T., NASH, A., GRETEN, F. R., MCKENZIE, B. S. & ERNST, M. 2013. Interleukin-11 is the dominant IL-6 family cytokine during gastrointestinal tumorigenesis and can be targeted therapeutically. *Cancer Cell,* 24**,** 257-71.

RABE, B., CHALARIS, A., MAY, U., WAETZIG, G. H., SEEGERT, D., WILLIAMS, A. S., JONES, S. A., ROSE-JOHN, S. & SCHELLER, J. 2008. Transgenic blockade of interleukin 6 transsignaling abrogates inflammation. *Blood,* 111**,** 1021-8.

RATH, T., BAKER, K., DUMONT, J. A., PETERS, R. T., JIANG, H., QIAO, S. W., LENCER, W. I., PIERCE, G. F. & BLUMBERG, R. S. 2013. Fc-fusion proteins and FcRn: structural insights for longer-lasting and more effective therapeutics. *Crit Rev Biotechnol.*

REILLY, S. M., AHMADIAN, M., ZAMARRON, B. F., CHANG, L., UHM, M., POIRIER, B., PENG, X., KRAUSE, D. M., KORYTNAYA, E., NEIDERT, A., LIDDLE, C., YU, R. T., LUMENG, C. N., ORAL, E. A., DOWNES, M., EVANS, R. M. & SALTIEL, A. R. 2015. A subcutaneous adipose tissue-liver signalling axis controls hepatic gluconeogenesis. *Nat Commun,* 6**,** 6047.

RITCHIE, D. G. & FULLER, G. M. 1983. Hepatocyte-stimulating factor: a monocyte-derived acute-phase regulatory protein. *Ann N Y Acad Sci,* 408**,** 490-502.

ROOPENIAN, D. C., CHRISTIANSON, G. J. & SPROULE, T. J. 2010. Human FcRn transgenic mice for pharmacokinetic evaluation of therapeutic antibodies. *Methods Mol Biol,* 602**,** 93-104.

ROSE-JOHN, S. & HEINRICH, P. C. 1994. Soluble receptors for cytokines and growth factors: generation and biological function. *Biochem J,* 300 (Pt 2)**,** 281-90.

RUMINY, P., GANGNEUX, C., CLAEYSSENS, S., SCOTTE, M., DAVEAU, M. & SALIER, J. P. 2001. Gene transcription in hepatocytes during the acute phase of a systemic inflammation: from transcription factors to target genes. *Inflamm Res,* 50**,** 383-90.

SAITO, M., YOSHIDA, K., HIBI, M., TAGA, T. & KISHIMOTO, T. 1992. Molecular cloning of a murine IL-6 receptor-associated signal transducer, gp130, and its regulated expression in vivo. *J Immunol,* 148**,** 4066-71.

SALVADORI, M., ROSSO, G. & BERTONI, E. 2015. Update on ischemia-reperfusion injury in kidney transplantation: Pathogenesis and treatment. *World J Transplant,* 5**,** 52-67.

SANDALON, Z., BRUCKHEIMER, E. M., LUSTIG, K. H. & BURSTEIN, H. 2007. Long-term suppression of experimental arthritis following intramuscular administration of a pseudotyped AAV2/1-TNFR:Fc Vector. *Mol Ther,* 15**,** 264-9.

SATO, K., TSUCHIYA, M., SALDANHA, J., KOISHIHARA, Y., OHSUGI, Y., KISHIMOTO, T. & BENDIG, M. M. 1993. Reshaping a human antibody to inhibit the interleukin 6-dependent tumor cell growth. *Cancer Res*, 53**,** 851-6.

SCALLON, B., CAI, A., SOLOWSKI, N., ROSENBERG, A., SONG, X. Y., SHEALY, D. & WAGNER, C. 2002. Binding and functional comparisons of two types of tumor necrosis factor antagonists. *J Pharmacol Exp Ther*, 301**,** 418-26.

SCHONIG, K., SCHWENK, F., RAJEWSKY, K. & BUJARD, H. 2002. Stringent doxycycline dependent control of CRE recombinase in vivo. *Nucleic Acids Res*, 30**,** e134.

SCHROEDER, A., HERRMANN, A., CHERRYHOLMES, G., KOWOLIK, C., BUETTNER, R., PAL, S., YU, H., MÜLLER-NEWEN, G. & JOVE, R. 2014. Loss of androgen receptor expression promotes a stem-like cell phenotype in prostate cancer through STAT3 signaling. *Cancer Res*, 74**,** 1227-37.

SCHULTZ, O., OBERHAUSER, F., SAECH, J., RUBBERT-ROTH, A., HAHN, M., KRONE, W. & LAUDES, M. 2010. Effects of inhibition of interleukin-6 signalling on insulin sensitivity and lipoprotein (a) levels in human subjects with rheumatoid diseases. *PLoS One*, 5**,** e14328.

SCHWACHE, D. & MÜLLER-NEWEN, G. 2012. Receptor fusion proteins for the inhibition of cytokines. *Eur J Cell Biol*, 91**,** 428-34.

SHIGEHARA, T., ZARAGOZA, C., KITIYAKARA, C., TAKAHASHI, H., LU, H., MOELLER, M., HOLZMAN, L. B. & KOPP, J. B. 2003. Inducible podocyte-specific gene expression in transgenic mice. *J Am Soc Nephrol*, 14**,** 1998-2003.

SHIROTA, K., LEDUY, L., YUAN, S. Y. & JOTHY, S. 1990. Interleukin-6 and its receptor are expressed in human intestinal epithelial cells. *Virchows Arch B Cell Pathol Incl Mol Pathol*, 58**,** 303-8.

SIMPSON, R. J., MORITZ, R. L., RUBIRA, M. R. & VAN SNICK, J. 1988. Murine hybridoma/plasmacytoma growth factor. Complete amino-acid sequence and relation to human interleukin-6. *Eur J Biochem*, 176**,** 187-97.

SOFI, M. H., LI, W., KAPLAN, M. H. & CHANG, C. H. 2009. Elevated IL-6 expression in CD4 T cells via PKCtheta and NF-kappaB induces Th2 cytokine production. *Mol Immunol*, 46**,** 1443-50.

SONKOLY, E., MULLER, A., LAUERMA, A. I., PIVARCSI, A., SOTO, H., KEMENY, L., ALENIUS, H., DIEU-NOSJEAN, M. C., MELLER, S., RIEKER, J., STEINHOFF, M., HOFFMANN, T. K., RUZICKA, T., ZLOTNIK, A. & HOMEY, B. 2006. IL-31: a new link between T cells and pruritus in atopic skin inflammation. *J Allergy Clin Immunol*, 117**,** 411-7.

SPRANG, S. R. & FERNANDO BAZAN, J. 1993. Cytokine structural taxonomy and mechanisms of receptor engagement. *Current Opinion in Structural Biology*, 3**,** 815-827.

STEURER, W., NICKERSON, P. W., STEELE, A. W., STEIGER, J., ZHENG, X. X. & STROM, T. B. 1995. Ex vivo coating of islet cell allografts with murine CTLA4/Fc promotes graft tolerance. *J Immunol,* 155**,** 1165-74.

SUZUKI, T., ISHII-WATABE, A., TADA, M., KOBAYASHI, T., KANAYASU-TOYODA, T., KAWANISHI, T. & YAMAGUCHI, T. 2010. Importance of neonatal FcR in regulating the serum half-life of therapeutic proteins containing the Fc domain of human IgG1: a comparative study of the affinity of monoclonal antibodies and Fc-fusion proteins to human neonatal FcR. *J Immunol,* 184**,** 1968-76.

TAGA, T., HIBI, M., HIRATA, Y., YAMASAKI, K., YASUKAWA, K., MATSUDA, T., HIRANO, T. & KISHIMOTO, T. 1989. Interleukin-6 triggers the association of its receptor with a possible signal transducer, gp130. *Cell,* 58**,** 573-81.

TAKAOKA, A., ARAI, I., SUGIMOTO, M., YAMAGUCHI, A., TANAKA, M. & NAKAIKE, S. 2005. Expression of IL-31 gene transcripts in NC/Nga mice with atopic dermatitis. *Eur J Pharmacol,* 516**,** 180-1.

TAM, S. H., MCCARTHY, S. G., BROSNAN, K., GOLDBERG, K. M. & SCALLON, B. J. 2013. Correlations between pharmacokinetics of IgG antibodies in primates vs. FcRn-transgenic mice reveal a rodent model with predictive capabilities. *MAbs,* 5**,** 397-405.

TANAKA, T., NARAZAKI, M. & KISHIMOTO, T. 2012. Therapeutic targeting of the interleukin-6 receptor. *Annu Rev Pharmacol Toxicol,* 52**,** 199-219.

TANAKA, T., NARAZAKI, M. & KISHIMOTO, T. 2014. IL-6 in inflammation, immunity, and disease. *Cold Spring Harb Perspect Biol,* 6**,** a016295.

TANAKA, T., OGATA, A. & NARAZAKI, M. 2013. Tocilizumab: An Updated Review of Its Use in the Treatment of Rheumatoid Arthritis and Its Application for Other Immune-Mediated Diseases. *Clinical Medicine Insights: Therapeutics***,** 33-52.

TENTEN, V., MENZEL, S., KUNTER, U., SICKING, E. M., VAN ROEYEN, C. R., SANDEN, S. K., KALDENBACH, M., BOOR, P., FUSS, A., UHLIG, S., LANZMICH, R., WILLEMSEN, B., DIJKMAN, H., GREPL, M., WILD, K., KRIZ, W., SMEETS, B., FLOEGE, J. & MOELLER, M. J. 2013. Albumin is recycled from the primary urine by tubular transcytosis. *J Am Soc Nephrol,* 24**,** 1966-80.

URLINGER, S., BARON, U., THELLMANN, M., HASAN, M. T., BUJARD, H. & HILLEN, W. 2000. Exploring the sequence space for tetracycline-dependent transcriptional activators: novel mutations yield expanded range and sensitivity. *Proc Natl Acad Sci U S A,* 97**,** 7963-8.

VACCARO, C., ZHOU, J., OBER, R. J. & WARD, E. S. 2005. Engineering the Fc region of immunoglobulin G to modulate in vivo antibody levels. *Nat Biotechnol,* 23**,** 1283-8.

VAN DE LOO, F. A., DE HOOGE, A. S., SMEETS, R. L., BAKKER, A. C., BENNINK, M. B., ARNTZ, O. J., JOOSTEN, L. A., VAN BEUNINGEN, H. M., VAN DER KRAAN, P. K., VARLEY, A. W. & VAN DEN BERG, W. B. 2004. An inflammation-inducible adenoviral expression system for local treatment of the arthritic joint. *Gene Ther,* 11**,** 581-90.

VAN RHEE, F., FAYAD, L., VOORHEES, P., FURMAN, R., LONIAL, S., BORGHAEI, H., SOKOL, L., CRAWFORD, J., CORNFELD, M., QI, M., QIN, X., HERRING, J., CASPER, C. & KURZROCK, R. 2010. Siltuximab, a novel anti-interleukin-6 monoclonal antibody, for Castleman's disease. *J Clin Oncol,* 28**,** 3701-8.

VAN SNICK, J., VINK, A., CAYPHAS, S. & UYTTENHOVE, C. 1987. Interleukin-HP1, a T cell-derived hybridoma growth factor that supports the in vitro growth of murine plasmacytomas. *J Exp Med,* 165**,** 641-9.

VENEREAU, E., DIVEU, C., GRIMAUD, L., RAVON, E., FROGER, J., PREISSER, L., DANGER, Y., MAILLASSON, M., GARRIGUE-ANTAR, L., JACQUES, Y., CHEVALIER, S. & GASCAN, H. 2010. Definition and characterization of an inhibitor for interleukin-31. *J Biol Chem,* 285**,** 14955-63.

VIGNALI, D. A. & KUCHROO, V. K. 2012. IL-12 family cytokines: immunological playmakers. *Nat Immunol,* 13**,** 722-8.

WALDNER, M. J., FOERSCH, S. & NEURATH, M. F. 2012. Interleukin-6--a key regulator of colorectal cancer development. *Int J Biol Sci,* 8**,** 1248-53.

WALLENIUS, V., WALLENIUS, K., AHREN, B., RUDLING, M., CARLSTEN, H., DICKSON, S. L., OHLSSON, C. & JANSSON, J. O. 2002. Interleukin-6-deficient mice develop mature-onset obesity. *Nat Med,* 8**,** 75-9.

WEGENKA, U. M., LUTTICKEN, C., BUSCHMANN, J., YUAN, J., LOTTSPEICH, F., MULLER-ESTERL, W., SCHINDLER, C., ROEB, E., HEINRICH, P. C. & HORN, F. 1994. The interleukin-6-activated acute-phase response factor is antigenically and functionally related to members of the signal transducer and activator of transcription (STAT) family. *Mol Cell Biol,* 14**,** 3186-96.

WEI, Q. & DONG, Z. 2012. Mouse model of ischemic acute kidney injury: technical notes and tricks. *Am J Physiol Renal Physiol,* 303**,** F1487-94.

WEISSENBACH, J., CHERNAJOVSKY, Y., ZEEVI, M., SHULMAN, L., SOREQ, H., NIR, U., WALLACH, D., PERRICAUDET, M., TIOLLAIS, P. & REVEL, M. 1980. Two interferon mRNAs in human fibroblasts: in vitro translation and Escherichia coli cloning studies. *Proc Natl Acad Sci U S A,* 77**,** 7152-6.

WELLS, J. A. & DE VOS, A. M. 1996. Hematopoietic receptor complexes. *Annu Rev Biochem,* 65**,** 609-34.

WIESINGER, M. 2008. *Development and characterization of an IL-6 inhibitor based on functional analysis of murine IL-6R alpha.* PhD PhD Thesis, RWTH Aachen University.

WIESINGER, M. Y., HAAN, S., WULLER, S., KAUFFMANN, M. E., RECKER, T., KUSTER, A., HEINRICH, P. C. & MÜLLER-NEWEN, G. 2009. Development of an IL-6 inhibitor based on the functional analysis of murine IL-6Ralpha(1). *Chem Biol,* 16**,** 783-94.

WONG, P. K., CAMPBELL, I. K., EGAN, P. J., ERNST, M. & WICKS, I. P. 2003. The role of the interleukin-6 family of cytokines in inflammatory arthritis and bone turnover. *Arthritis Rheum,* 48**,** 1177-89.

YAMASAKI, K., TAGA, T., HIRATA, Y., YAWATA, H., KAWANISHI, Y., SEED, B., TANIGUCHI, T., HIRANO, T. & KISHIMOTO, T. 1988. Cloning and expression of the human interleukin-6 (BSF-2/IFN beta 2) receptor. *Science,* 241**,** 825-8.

YI, H., KIM, Y., KIM, J., JUNG, H., RIM, Y. A., JUNG, S. M., PARK, S. H. & JU, J. H. 2014. A new strategy to deliver synthetic protein drugs: self-reproducible biologics using minicircles. *Sci Rep,* 4**,** 5961.

YOKOTA, S., TANAKA, T. & KISHIMOTO, T. 2012. Efficacy, safety and tolerability of tocilizumab in patients with systemic juvenile idiopathic arthritis. *Ther Adv Musculoskelet Dis,* 4**,** 387-97.

YOSHITAKE, F., ITOH, S., NARITA, H., ISHIHARA, K. & EBISU, S. 2008. Interleukin-6 directly inhibits osteoclast differentiation by suppressing receptor activator of NF-kappaB signaling pathways. *J Biol Chem,* 283**,** 11535-40.

YOSHIZAKI, K., MATSUDA, T., NISHIMOTO, N., KURITANI, T., TAEHO, L., AOZASA, K., NAKAHATA, T., KAWAI, H., TAGOH, H., KOMORI, T. & ET AL. 1989. Pathogenic significance of interleukin-6 (IL-6/BSF-2) in Castleman's disease. *Blood,* 74**,** 1360-7.

ZHENG, X. X., STEELE, A. W., HANCOCK, W. W., KAWAMOTO, K., LI, X. C., NICKERSON, P. W., LI, Y., TIAN, Y. & STROM, T. B. 1999. IL-2 receptor-targeted cytolytic IL-2/Fc fusion protein treatment blocks diabetogenic autoimmunity in nonobese diabetic mice. *J Immunol,* 163**,** 4041-8.

ZHOU, L., IVANOV, II, SPOLSKI, R., MIN, R., SHENDEROV, K., EGAWA, T., LEVY, D. E., LEONARD, W. J. & LITTMAN, D. R. 2007. IL-6 programs T(H)-17 cell differentiation by promoting sequential engagement of the IL-21 and IL-23 pathways. *Nat Immunol,* 8**,** 967-74.

8   Supplementary Figures

```
CLUSTAL O(1.2.1) multiple sequence alignment

mgp130  MSAPRIWLAQALLFFLTTESIGQLLEPCGYIYPEFPVVQRGSNFTAICVLKEACLQHYYV 60
mIL-31R ------------------------------------------------------------

mgp130  NASYIVWKTNHAAVPREQVTVINRTTSSVTFTDVVLPSVQLTCNILSFGQIEQNVYGVTM 120
mIL-31R ---------------------------------MNPLGVNAGIMWTLALWAFSFLCKF 25

                    D2
mgp130  LSGFPPDKPTNLTCIVNEGKNMLCQWDPGRETYLETNYTLKS--EWATEKFPDCQSK--- 175
mIL-31R SLAVLPTKPENISCVFYFDRNLTCTWRPEKETNDT-SYIVTLTYSYGKSNYSDNATEASY 84
                    D1                                    D2    D3
mgp130  -HGTSCMVSYMPTYYVNIEVWVEAENALGKVSSESINFDPVDKVKPTPPYNLSVTNSEEL 234
mIL-31R SFPRSCA---MPPDIC--SVEVQAQNGDGKVKSDITYWHLISIAKTEPPIILSVNP--IC 137
                                                         D1    D2
mgp130  SSILKLSWVSSGLGGLLDLKSDIQYRTKDASTWIQVPLEDTMSPRTSFTVQDLKPFTEYV 294
mIL-31R NRMFQIQWKPREKTRGFPLVCMLRFRTVNSSHWTEVNFENCKQ---VCNLTGLQAFTEYV 194
                   D3
mgp130  FRIRSIKDSGKGYWSDWSEEASGTTYEDRPSRPPSFWYKTNPSHGQEYRSVRLIWKALPL 354
mIL-31R LALRF-RFNDSRYWSKWSKEETRVTMEEVPH-VLDLWRILEPADMNGDRKVRLLWKKARG 252
                   D2
mgp130  SEANGKILDYEVILTQSKS--VSQTYTVTGTELTVNLTNDRYVASLAARNKVGKSAAAVL 412
mIL-31R APVLEKTFGYHIQYFAENSTNLTEINNITTQQYELLLMSQAHSVSVTSFNSLGKSQEAIL 312

mgp130  TIPSPHVTAAYSVVNLKAFPKDNLLWVEWTPPPKPVSKYILEWCVLSENAP-CVEDWQQE 471
mIL-31R RIPDVHEKTFQYIKSMKAYIAEPLLVVNWQSSIPAVDTWIVEWLPEAAMSKFPALSWESV 372

mgp130  DATVNRTHLRGRLLESKCYQITVTPVFATGPGGSESLKAYLKQAAPARGPTVRTKKVGKN 531
mIL-31R SQVTNWTIEQDKLKPFTCYNISVYPVLGHRVGEPYSIQAYAKEGTPLKGPETRVENIGLR 432

mgp130  EAVLAWDQIPVDDQNGFIRNYSISYRTSVGKEMVVHVDSSHTE--YTLSSLSSDTLYMVR 589
mIL-31R TATITWKEIPKSARNGFINNYTVFYQAEGGKELSKTVNSHSPQVYYALTAAKSRNSRNLQ 492

mgp130  MAAYTDEGGKDGPEFTFTTPKFAQGEIEAIVVPVCLAFLLTTLLGVLFCFNKRDLIKKHI 649
mIL-31R ------------------------------------------------------------

mgp130  WPNVPDPSKSHIAQWSPHTPPRHNFNSKDQMYSDGNFTDVSVVEIEANNKKPCPDDLKSV 709
mIL-31R ------------------------------------------------------------

mgp130  DLFKKEKVSTEGHSSGIGGSSCMSSSRPSISSNEENESAQSTASTVQYSTVVHSGYRHQV 769
mIL-31R ------------------------------------------------------------

mgp130  PSVQVFSRSESTQPLLDSEERPEDLQLVDSVDGGDEILPRQPYFKQNCSQPEACPEISHF 829
mIL-31R ------------------------------------------------------------

mgp130  ERSNQVLSGNEEDFVRLKQQQVSDHISQPYGSEQRRLFQEGSTADALGTGADGQMERFES 889
mIL-31R ------------------------------------------------------------

mgp130  VGMETTIDEEIPKSYLPQTVRQGGYMPQ 917
mIL-31R ----------------------------
```

Supplementary Figure 1: Alignment of murine IL-31R and murine gp130 amino acid sequence

Curriculum Vitae

Personal Information

Dieter (Schwache) Görtz

Born on May 10th, 1980 in Heinsberg, Germany

Married

One daughter (3 years) and one son (1 year)

Higher Education

11/2009 - 12/2015	**PhD Student** in the Group of Prof. Dr. Müller-Newen at the Institute of Biochemistry and Molecular Biology, Uniklinik RWTH Aachen
10/2008 - 11/2009	**Diploma Student** in the Group of Prof. Dr. Fred Schaper at the Institute of Biochemistry and Molecular Biology, Uniklinik RWTH Aachen Thesis title "Quantitative Analysis of IL-6 Signal Transduction"
10/2001 - 11/2009	**Biology (Degree: Diploma / Master of Science)** Major: Molecular and Cellular Biology Minors: Immunology, Molecular Medicine, General Biotechnology RWTH Aachen University
10/2000 - 09/2001	**Mechanical Engineering** RWTH Aachen University

Military Service

11/1999 - 06/2000	Infrastructure Division, DDO/DtA NATO E-3A Component, Geilenkirchen-Teveren
09/1999 - 11/1999	Basic military training, 19./LwAusbRgt 1, Schönewalde-Holzdorf

Education

1999	Higher Education Entrance qualification Kreisgymnasium Heinsberg

Danksagung

Zuallerst möchte ich Herrn Prof. Dr. Gerhard Müller-Newen für die Aufnahme in seine Arbeitsgruppe danken. Neben der angenehmen Arbeitsatmosphäre, schätze ich die weitestgehend freie Gestaltung des eigenen Forschungsprojektes. Weiterhin möchte ich mich für schöne Sommer-Grillpartys in Deinem Garten, sowie nette gemeinsame Besuche des Aachener Weihnachtsmarktes bedanken. Ganz besonders möchte ich mich für die Unterstützung bei der Durchführung dieser Arbeit und der Vereinbarkeit von Familie und Wissenschaft bedanken.

Herrn Univ.-Prof. Dr. Bernhard Lüscher danke ich für die freundliche Übernahme des Koreferats.

Den Mitarbeitern der Medizinischen Klinik II danke ich sehr, da sie in wesentlichen Teilen zu dieser Arbeit beigetragen haben. Ganz besonders möchte ich dabei Herrn Dr. med. Gerald Braun für die hervorragende Kooperation, die nephrologische Expertise, und seinem persönlichen Engagement im mIL-6-RFP-Projekt danken.

Allen Mitarbeitern des Instituts für Biochemie und Molekularbiologie danke ich für ihre Hilfs- und Diskussionsbereitschaft. Ich danke besonders dem Flur 42 der Etage 3 für die angenehme Arbeitsatmosphäre und auch für schöne Zeiten ausserhalb des Labors.

Dank gilt weiterhin allen alten und aktuellen Weggefährten des Labor 13: Anne Mohr, Antons Martincuks, Corina Zimmermann, Liv Brolund, Michael Vogt, Natalie Rinis, Sara Zafarnia, Tamas Domoszlai und Tobias Recker.

Eidesstattliche Versicherung

Name: Görtz Vorname: Dieter

Matrikel-Nr.: 229584 Studiengang: Biologie, Promotion

Hiermit erkläre ich, Dieter Görtz, an Eides statt, dass ich die Dissertation mit dem Titel „Development and optimization of receptor fusion protein for the inihibtion of IL-6 type cytokines *in vivo*" selbständig verfasst und keine anderen als die angegebenen Quellen und Hilfsmittel benutzt habe.

_____   _____

Ort, Datum   Unterschrift